

**Enhancement of cross-linking efficiency of hyaluronic acid-based hydrogels cross-linked with 1, 4-butanediol diglycidyl ether**

**“A comparative evaluation of different method conditions”**

Dissertation

zur Erlangung des akademischen Grades  
doctor rerum naturalium (Dr. rer. nat.)

der  
Naturwissenschaftlichen Fakultät I  
Biowissenschaften  
der Martin-Luther-Universität Halle-Wittenberg

vorgelegt

von  
**Mohammed Abdullah Al-Sibani**  
geb. am 28. Juni 1971 in Oman

Gutachter /in

1. Prof. Dr. Reinhard Neubert
2. Prof. Dr. Dagmar Fischer
3. Prof. Dr. Ahmed AL-Harrasi

**Tag der Verteidigung: Halle (Saale), 17.05.2017**

# TABLE OF CONTENT

TABLE OF CONTENT.....	2
LIST OF FIGURES .....	4
LIST OF TABLES.....	6
LIST OF ABBREVIATION.....	7
ABSTRAKT .....	9
ABSTRACT .....	10
AIMS OF STUDY.....	11
<b>CHAPTER 1.....</b>	<b>15</b>
1. Theoretical background .....	15
1.1 Introduction to hyaluronic acid (HA).....	15
1.3 HA cross-linking .....	20
1.4 Cross-linking efficiency .....	24
<b>CHAPTER 2.....</b>	<b>25</b>
2. Cross-linking hyaluronic acid with BDDE .....	25
2.1 Introduction.....	25
2.2 Preparation of cross-linked BDDE-HA hydrogel .....	25
2.3 Comparison between native and cross-linked HA .....	27
2.4 Conclusion .....	36
<b>CHAPTER 3.....</b>	<b>37</b>
3. Evaluation of <i>in-vitro</i> degradation rate of cross-linked BDDE-HA hydrogel. ....	37
3.1 Introduction.....	37
3.2 Development of (chromatographic, colorimetric and gravimetric) methods.....	38
3.4 Conclusion .....	49
<b>CHAPTER 4.....</b>	<b>50</b>
4. Reaction time, pH and temperature.....	50
4.1 Introduction.....	50
4.2 Reaction time .....	50
4.3 pH.....	55
4.4 Temperature. ....	58

TABLE OF CONTENT

4.4.1 Materials .....	58
4.5 Conclusion .....	62
<b>CHAPTER 5</b> .....	63
5. HA initial concentration.....	63
5.1 Introduction.....	63
5.2 HA initial concentration.....	63
5.3 Conclusion .....	73
<b>CHAPTER 6</b> .....	74
6. HA molecular weight.....	74
6.1 Introduction.....	74
6.2 HA molecular weight.....	74
6.3 Conclusion .....	81
<b>CHAPTER 7</b> .....	82
7. Mixing approach .....	82
7.1 Introduction.....	82
7.2 Mixing approach .....	82
7.3 Conclusion .....	96
<b>SUMMARY AND OUTLOOK</b> .....	98
<b>ACKNOWLEDGMENT</b> .....	100
<b>REFERENCES</b> .....	101
<b>APPENDICES</b> .....	111
Appendix 1: Introduction to the analytical instruments employed for HA characterization .....	111
Appendix 2: ESI-Mass spectrometry analysis .....	118
Appendix 3: The relation between degree of modification and BDDE concentration. ....	138
Appendix 4: Chromatographic analysis.....	142
Appendix 5: Colorimetric analysis .....	160
Appendix 6: Results of the <i>in-vitro</i> degradation rate.....	164
Appendix 7: Results of the swelling ratio measurements .....	166
Appendix 8: Excel data for the rheological measurements.....	168
Appendix 9: Images for different hydrogel samples obtained in our work .....	174
<b>ERKLÄRUNG/ DECLARATION</b> .....	178
<b>PUBLICATIONS</b> .....	179
<b>CURRICULUM VITAE</b> .....	180

## LIST OF FIGURES

Figure 1. 1 Structure of the disaccharide repeating unit in HA .....	15
Figure 1. 2 Esterification using alkyl halide and the reaction of HA with glycidyl methacrylate .....	22
Figure 1. 3 Ether formation by crosslinking two HA chain with BDDE .....	22
Figure 1. 4 Complex coacervation between a polyanion and a polycation .....	23
Figure 2. 1 Hydrated BDDE-HA hydrogel (A), Lyophilized BDDE-HA hydrogel (B).....	26
Figure 2. 2 FTIR spectra of lyophilized native HA .....	29
Figure 2. 3 FTIR spectra of cross-linked HA .....	29
Figure 2. 4 CE electropherogram of native HA fragments .....	30
Figure 2. 5 CE electropherogram of cross-linked BDDE-HA fragments .....	31
Figure 2. 6 The ESI-MS profiles of native HA .....	32
Figure 2. 7 The ESI-MS profiles of cross-linked HA-BDDE hydrogel .....	32
Figure 2. 8 NMR spectra of lyophilized native HA digested fragments .....	35
Figure 2. 9 NMR spectra of lyophilized BDDE- HA digested fragments .....	35
Figure 3. 1 Chromatograms of (NAG) for X <sub>1</sub> A and X <sub>1</sub> B .....	42
Figure 3. 2 Chromatograms of standard solutions and the calibration curve .....	43
Figure 3. 3 The violet color developed by Ehrlich's reagent in samples X <sub>4</sub> A and X <sub>4</sub> B .....	45
Figure 3. 4 Color gradient of standards developed by Ehrlich's reagent .....	45
Figure 3. 5 Average degradation rates obtained from the three analytical methods .....	47
Figure 4. 1 Degradation profiles of BDDE-HA hydrogels prepared at different reaction time .....	53
Figure 4. 2 Swelling ratios of hydrogels prepared at different reaction times .....	54
Figure 4. 3 Degradation profiles of BDDE-HA hydrogels prepared at different pH number.....	57
Figure 4. 4 Swelling ratios of hydrogels prepared at different pH number .....	58
Figure 4. 5 Degradation profiles of BDDE-HA hydrogels prepared at different temperature.....	60
Figure 4. 6 Swlling ratios of hydrogels prepared at different temperature. ....	61
Figure 5. 1 Degradation profiles of hydrogels prepared at different HA concentrations .....	65
Figure 5. 2 Swelling ratios of hydrogels prepared at different HA concentration .....	67
Figure 5. 3 SEM image for hydrogel prepared at 7.0 % HA initial concentration .....	68
Figure 5. 4 SEM image for hydrogel prepared at 8.0 % HA initial concentration .....	68

LIST OF FIGURES

Figure 5. 5 SEM image for hydrogel prepared at 9.0 % HA initial concentration ..... 69

Figure 5. 6 SEM image for hydrogel prepared at 10.0 % HA initial concentration ..... 69

Figure 5. 7 SEM image for hydrogel prepared at 11.0 % HA initial concentration ..... 69

Figure 5. 8 SEM image for hydrogel prepared at 12.0 % HA initial concentration ..... 70

Figure 5. 9 SEM image for hydrogel prepared at 13.0 % HA initial concentration ..... 70

Figure 5. 10 SEM image for hydrogel prepared at 14.0 % HA initial concentration..... 70

Figure 6. 1 Degradation profiles of hydrogels prepared at different HA molecular weight. .... 76

Figure 6. 2 Swelling ratio of hydrogels prepared at different HA molecular weight..... 78

Figure 6. 3 Storage modulus  $G'$  and Loss modulus  $G''$  (Pa) for native HA ..... 78

Figure 6. 4 Storage modulus  $G'$  and Loss modulus  $G''$  (Pa) for hydrogel with 100,000 Da HA ..... 79

Figure 6. 5 Storage modulus  $G'$  and Loss modulus  $G''$  (Pa) for hydrogel with 1000,000 Da HA ..... 79

Figure 6. 6 Storage modulus  $G'$  and Loss modulus  $G''$  (Pa) for hydrogel with 2000,000 Da HA ..... 79

Figure 6. 7 Measurements of dynamic viscosity for native HA and cross-linked hydrogels..... 81

Figure 7. 1 Degradation profiles of native HA and hydrogels 1 and 2 ..... 85

Figure 7. 2 Swelling ratios of hydrogels 1 and 2 ..... 87

Figure 7. 3 Morphological structure of native HA and hydrogels 1 and 2 ..... 91

Figure 7. 4 Storage modulus  $G'$  and Loss modulus  $G''$  (Pa) for hydrogel 1 ..... 92

Figure 7. 5 Storage modulus  $G'$  and Loss modulus  $G''$  (Pa) for hydrogel 2 ..... 92

Figure 7. 6 FTIR and  $^1\text{H}$  NMR spectra for native HA and hydrogels 1 and 2 ..... 95

## LIST OF TABLES

Table 2. 1 Possible oligomers of native HA hydrogel .	34
Table 2. 2 Possible oligomers of cross-linked BDDE-HA hydrogel	34
Table 3. 1 Degradation rates of samples ( $X_1$ , $X_2$ , and $X_3$ ) obtained from HPLC method.	44
Table 3. 2 Degradation rates of samples $X_4$ , $X_5$ , and $X_6$ obtained from the colorimetric method.	46
Table 3. 3 Degradation rates of samples $X_7$ , $X_8$ , and $X_9$ obtained from the weight loss method.	46
Table 4. 1 BDDE-HA hydrogels prepared at various reaction time	51
Table 4. 2 BDDE-HA hydrogels prepared at various pH number	55
Table 4. 3 BDDE-HA hydrogels prepared at various temperature	58

## LIST OF ABBREVIATION

HA	Hyaluronic acid
BDDE	1, 4-butanedioldiglycidyl ether
NAG	<i>N</i> - acetyl glucosamine
M <sub>w</sub>	Molecular weight
ECM	Extracellular matrix
PEG	Polyethylene glycol
DVS	Divinyl sulfone
PEGDGE	poly (ethylene glycol) diglycidyl ether
COOH	Carboxylic group
OH	Hydroxyl group
3D	Three-dimensional
FTIR	Fourier-transformed infrared
μm	Micrometer
NMR	Nuclear magnetic resonance spectroscopy
D <sub>2</sub> O	Deuterium oxide
HPLC	High performance liquid chromatography
UV	Ultra-violet
nm	Nano-meter
M	Molarity
CE	Capillary electrophoreses
GAGs	Glycosaminoglycans

## LIST OF ABBREVIATION

SEM	Scanning electron microscope
G'	Storage modulus
G''	Loss modulus
SAOS	Small amplitude oscillatory strain
LVR	Linear viscoelastic region
$\gamma$	Sinusoidal deformation
$\delta$	Phase shift
NaOH	Sodium hydroxide
pKa	Expression number for weak acids acidity
pH	Potential of hydrogen (acidity number)
HCl	Hydrochloric acid
U	Enzyme activity
PBS	Phosphate buffer saline
BTH	Bovine testicular hyaluronidase
EOF	Electro-osmotic flow
GlcNAc	<i>N</i> -acetyl-D-glucosamine
GlcA	Glucuronic acid
$\Delta$ UA	Unsaturated uronic acid
ANOVA	Analysis of variance
ESI -MS	Electro-spray ionization mass spectrometry
SEI	Secondary electron imaging
m/z	Mass to charge ratio



## ABSTRAKT

Unabhängig von verschiedenen Vernetzungsstrategien suchen aktuelle Studien alternative Lösungen für die Vernetzung von Hyaluronsäure mit einem niedrigeren Niveau der chemischen Vernetzer um Komplikationen und Zelltoxizität zu vermeiden. In dieser Studie war es unser Ziel, die Vernetzungseffizienz von HA-basierten Hydrogelen, vernetzt mit 1, 4-Butandiol diglycidyl ether (BDDE) durch verschiedener Verfahrensbedingungen, einschließlich der Reaktionszeit, pH, Temperatur, HA-Konzentration, HA Molekular Gewicht und Mischansatz zu überprüfen. Die Studie ergab, dass die Verfahrensbedingungen mit wenigen Ausnahmen spürbare Auswirkungen auf Vernetzungseffizienz von BDDE-HA-Hydrogelen mit wenigen Ausnahmen hatte. Ergebnisse von Hydrogelen 'Eigenschaften wie in vitro-Abbauraten, Quellfähigkeit, morphologische und rheologische Verhalten bestätigt diese Erweiterung. Für vier Tage mit Hyaluronidase inkubiert, wird die in vitro Abbaugeschwindigkeit um nahezu 11,7% verringert, 18,3%, 18,2%, 18,0%, bezogen auf den 1., 2., 3., 4. Tag nach Beginn der neuen Verfahrensbedingungen während der chemischen Quervernetzer angenommen werden BDDE konstant gehalten wurde. Das Quellverhältnis in destilliertem Wasser zeigte auch eine dramatische Abnahme von  $145 \pm 4,9$  (g / g) auf  $130 \pm 3,8$  (g / g), aber war die Abnahme war nicht stabil. Allerdings hat die Schwellung in PBS gezeigt dass es keinen signifikanten Rückgang gibt, nur etwa 1,0 g aus der gequollenen Masse war reduziert worden, denn von den ersten bis zu den letzten Messungen wurde nur 1,9 g aus der gequollenen Masse reduziert. Die Verringerung der Porengrößenverteilung liegt im Bereich zwischen 10 & mgr; m bis weniger als 50 & mgr; m im Vergleich zum ersten mikroskopischen Scan zu verengen, die Zusammenbruch zeigte und viel größeren Porengrößenverteilung. Dynamische Moduli; der Speichermodul ( $G'$ ) und der Verlustmodul ( $G''$ ) erhöht wurden und zeigten viskoelastische Verhalten mit geringer Frequenzabhängigkeit. Schließlich bestätigen diese Ergebnisse, dass die verschiedenen Verfahren relativ Stimuli die Vernetzungseffizienz ohne Ausnutzung übermäßige Menge des chemischen Quervernetzer BDDE-HA Hydrogele verbessern könnte.

## ABSTRACT

Regardless of various cross-linking strategies, current studies seek alternative solutions for cross-linking hyaluronic acid with a lower level of chemical cross-linker to avoid complications and cell toxicity. In this study, we aimed to enhance the cross-linking efficiency of HA-based hydrogels cross-linked with 1, 4-butanediol diglycidyl ether (BDDE) via studying the effect of various method conditions such as reaction time, pH, temperature, HA concentration, HA molecular weight and mixing approach. The study revealed that the method conditions had noticeable effects on BDDE-HA properties with few exceptions. For four days incubating with hyaluronidase, the *in-vitro* degradation rate decreased by almost 11.7 %, 18.3 %, 18.2 %, 18.0 % on the 1<sup>st</sup>, 2<sup>nd</sup>, 3<sup>rd</sup>, 4<sup>th</sup> day respectively after employing the optimum method conditions. The swelling ratio in distilled water showed also a dramatic decrease from  $145 \pm 4.9$  (g/g) to  $130 \pm 3.8$  (g/g). However, the swelling in PBS did not show a significant decline, about 1.0 g only had been reduced from the swollen mass when moved from the initial measurements to the final measurements. The pore-size distribution decreased to narrower ranges between 10  $\mu\text{m}$  to less than 50  $\mu\text{m}$  compared to the first microscopic scan which showed collapse and much wider pore-size distribution. Dynamic moduli; the storage modulus ( $G'$ ) and the loss modulus ( $G''$ ) were increased and showed viscoelastic behavior with less frequency-dependence. Finally, these findings confirmed that the method conditions could relatively enhance the cross-linking efficiency of BDDE-HA hydrogels without exploiting excessive amount of the chemical cross-linker.

## AIMS OF STUDY

Hyaluronic acid (HA) is a high-molecular weight, poly-anionic polymer with many applications in human medicine ([Šimkovic et al., 2000](#)). Naturally, it is found in human skin, extra-cellular matrix (ECM) and synovial fluid of vertebrates ([Zawko et al., 2009](#)). The HA functions are to create volume and provide lubricants to tissues, consequently preventing cell damages induced through various physical stresses ([Romagnoli & Belmontesi, 2008](#)). HA is biocompatible, biodegradable and hydrophilic, so it allows the influx and retention of large amounts of water due to the abundant hydrophilic carboxyl groups ([Allemann & Baumann, 2008](#)).

Due to the unique biological properties of HA which are very similar of that in human tissues, it has gained great attention and interest over the years. These properties have allowed HA to be used in different biomedical applications such as wound-healing, osteoarthritis ([Liu et al., 2007](#)) and tissue-augmentation ([Kenne et al., 2013](#)). However, native HA has very limited applications due to its poor mechanical properties and *in vivo* rapid degradation ([Liu et al., 2007](#); [Jeon et al., 2007](#); [Pitarresi et al., 2007](#) ; [Verpaele & Strand, 2006](#)). It has been reported that the half-life of HA after injection into the skin or joints is no longer than 1 day ([Brown et al., 1991](#)). Consequently, it is not a suitable material for therapeutic action, particularly for the dermatological applications.

To overcome these drawbacks, HA should be stabilized via chemical modification processes to ensure a longer residence time within the soft tissue after administration into the body. These processes involve cross-linking of different HA chains by covalent bonds using chemical cross-linkers ([Luo et al, 2000](#)). Various methods have been developed for the production of cross-linked HA, the result of each method is a cross-linked HA hydrogel with a three-dimensional network structure that retains water within its cross-linked network upon the hydration in an aqueous environment ([Berkó et al, 2013](#) ; [Masters et al, 2005](#) ; [Kim, Mauck & Burdick, 2011](#); [Yamanlar et al, 2011](#)) .

The cross-linked hydrogel is more resistant than native HA towards enzymatic degradation due to the formation of bridges and intermolecular bonds between the HA chains and the cross-linker. A number of chemical cross-linkers have been addressed for HA cross-linking including methacrylamide (Segura et al., 2005), hydrazide (Prestwich et al., 1998), carbodiimide (Lai, 2012), divinyl sulfone (DVS), 1, 4-butanediol diglycidyl ether (BDDE) and poly (ethylene glycol) diglycidyl ether (PEGDGE) (Gatta et al, 2013 ; Schanté et al, 2011). Several studies showed that by increasing the cross-linker content or concentration, the degree of cross-linking is increased (Caillard et al, 2008 ; Wong, Ashton & Dodou, 2015 ; Schanté et al, 2011), subsequently, slower degradation rate towards enzyme is exhibited. In cosmetic, patients commonly prefer HA hydrogels with higher degrees of cross-linking to exhibit longevity and mechanical strength. Hydrogels prepared with a higher degree of cross-linking become stiffer and exhibit greater resistance against enzymatic degradation. Stronger HA-filler can also provide adequate force to lift the tissues and resist subsequent deformation.

However, from a health perspective, incorporation of high contents of chemical cross-linkers in HA modification is not feasible. The excessive amounts of cross-linkers are often toxic and can give unwanted reactions with the bioactive substances present in the hydrogel matrix (Hennink, and van Nostrum, 2012 ; Boogaard et al., 2000). They affect the integrity of the substances to be entrapped such as drugs or proteins. Treating patients with excessive amounts of cross-linker is not a healthy practice and may be associated with undesirable effects, particularly if the dose contains residues of un-reacted cross-linker. The chemical cross-linkers are considered the major obstacles in the use of injectable polymer scaffolds due to their toxicity to the cells (Sung et al, 1998 ; Ferretti et al, 2006 ; Tan et al, 2009).

Many studies have reported various complications and side-effects correlated with the chemical cross-linkers used in HA modification, particularly for the HA fillers treated with excessive amounts of cross-linkers (Sung et al, 1998 ; ; Ferretti et al, 2006 ; Tan et al, 2009 ; Alijotas-Reig & García-Giménez, 2008 ; Micheels, 2001 ; Loewe et al, 2001 ; John & Price, 2009 ; Clark, 2007 ; Hennink & Nostrum, 2012 ; Boogaard, Denneman, & Van Sittert, 2000). Any side effects or allergic reactions produced by HA-based fillers are thought to be caused by the cross-linkers (Clark, 2007; Carpintero, Candelas & Ruiz-Rodríguez).

Some complications such as hypersensitivity reactions, nodules, induration, facial edema and localized cutaneous reaction have been widely reported in humans when treated with HA fillers (Alijotas & García, 2008; Micheels, 2001; Loewe, et al., 2001). In practical, the injectable filler should be safe, biocompatible and non-immunogenic (Kablik et al, 2009), non-allergenic, non-carcinogenic, adverse-effect free and not associated with migration and excessive inflammatory response following its application (Iannitti, Bingol, Rottigni & Palmieri, 2013 ; John & price, 2009).

Currently, the cross-linking strategies take into account reduction of the toxic agents, so there has been an increasing demand for HA-based hydrogels that offer advantages of lower chemical cross-linkers. However, when an amount of a cross-linker is reduced, it is not easy to obtain a stiff cross-linked hydrogel. In fact, preparing a cross-linked HA hydrogel with both a low amount of chemical cross-linker and a high degree of cross-linking is difficult. This field of study is currently receiving considerable attention, and has become one of the major challenging issues in hydrogels manufacturing. Therefore, the main objective of our study was to enhance the HA cross-linking efficiency while maintaining a constant level of the chemical cross-linker. The cross-linking efficiency is a theoretical term introduced in this study to describe the total strength of formed hydrogels. It represents the chemical cross-linking raised from the formation of covalent bonds between HA chains and the cross-linker and the physical cross-links raised from the polymer entanglements or conformation. We selected 1, 4-butanediol diglycidyl ether (BDDE) as the chemical cross-linker, because it is currently used in the majority of market-leading HA hydrogels. Such studies would provide alternative solutions for the enhancement of cross-linking efficiency without exploiting excessive quantities of BDDE. The cross-linking efficiency in each formed hydrogel was evaluated by measuring hydrogel's properties such as *in-vitro* degradation rate, swelling ability, morphological and rheological behavior.

This dissertation is organized into seven chapters; **Chapter 1** presents a theoretical background of relevant information for hyaluronic acid and its application in cosmetic and medical treatments. **Chapter 2** describes the synthesis process applied for producing the HA hydrogel cross-linked with 1, 4-butanediol diglycidyl ether. It also confirms the occurrence of chemical modification by comparing the resulting BDDE-HA hydrogel with a native HA solution. **Chapter 3** compares three different analytical methods (chromatography, colorimetry and gravimetry) for measuring the *in-vitro* degradation rate of cross-linked hydrogels.

**Chapter 4** investigates the influence of reaction time, pH and temperature on cross-linking efficiency of BDDE-HA hydrogels. **Chapters 5 & 6** study the effect of HA initial concentration and HA molecular weight on BDDE-HA cross-linking efficiency. In **Chapter 7**, the mixing approach of HA with the reagent (BDDE) solution was described. Each chapter starts with an introduction and ends with a conclusion describing the most essential results. The chapters were subdivided after introduction as following: materials, synthesis, measurements, results and discussion. If much data (numbers, tables or graphs) were extracted from the experiments, the results and discussion were separated. Finally, the dissertation was ended with a summary describing the presented work and references. Appendices were provided for additional information.

# CHAPTER 1

## 1. Theoretical background

### 1.1 Introduction to hyaluronic acid (HA)

Hyaluronic acid (HA) also known as hyaluronan (Fig.1.1) is a high-molecular weight, naturally occurring biodegradable polymer. HA is a linear (unbranched) and non-sulphated glycosaminoglycans (GAG). It is composed of repeating disaccharide units of *N*-acetyl-D-glucosamine and D-glucuronic acid chemically linked by alternating glycosidic bonds  $\beta$  - (1, 4) and  $\beta$ - (1, 3) (Schanté, Zuber, Herlin, & Vandamme, 2011; Šimkovic et al., 2000 ; Fan, et al, 2006).

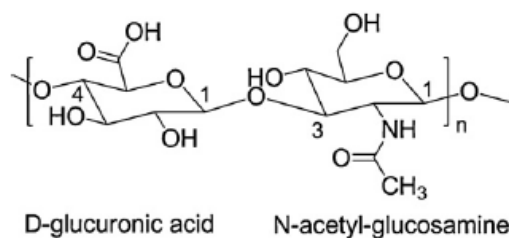


**Figure 1. 1** Structure of the disaccharide repeating unit in HA

The name of " hyaluronic acid " was derived from two terms: the term "hyalos" which means glass in the Greek language and the uronic acid. HA is a highly charged polyanion polymer and it binds with water extensively due to the abundant hydrophilic carboxyl groups (Allemann & Baumann, 2008; Kablik et al, 2009). Based on X-ray diffraction and NMR, the molecular structure of HA can be found in different helical conformations depending on different conditions such as pH, humidity, water content and temperature. The most common forms are fully extended helix, three-fold helix and four-fold helix stabilized by hydrogen bonds (Kaufmann, Mohle, Hofmann & Arnold, 1997).

In physiological solutions, the HA backbone forms a twisted ribbon structure called “coiled structure” due to the interactions of hydrogen bonds with the solvent where the axial hydrogen atoms relatively form a non-polar face whereas the equatorial side forms the polar face (Fakhari & Berkland, 2013). The molecular weight of HA depends on the number of disaccharide units present in the chain which is proportional to the HA molecular weight. The commercial HA is usually supplied as a sodium salt with a molecular weight 401 Da for its basic unit (Kablik et al, 2009). HA is widely distributed throughout the human body and it forms a major element in the extracellular matrix, ECM (Scott,1995; Rhodes, 2007, Zhu, 2010;). It is present in almost all biological fluids including synovial fluid and the vitreous humor of the eye (Zawko, Suri, Truong, & Schmidt, 2009). The mean concentration of HA in human body is about 200 mg/kg, so that a body weighing 60 kg contains about 12.0 g of hyaluronic acid (Romagnoli & Belmontesi, 2008). The larger amount of HA is found in the skin and it approximately contains more than 50 % of the total content within the body (Kablik et al, 2009). In normal state, HA is present as a free polymer, however in some tissues, it is linked to different glycoproteins or specific cell receptors (Romagnoli & Belmontesi, 2008). The main function of HA is to create volume and provide lubricants to tissues, consequently preventing cell damages induced through various physical stresses (Romagnoli & Belmontesi, 2008). HA shows also inhibitory effects against a range of bacterial and fungal species as well as antiviral activity (Iannittia, Bingölc, Rottignib & Palmierib, 2013). Moreover, HA is responsible for the regulation of cell adhesion, cell migration and cell proliferation (Fakhari & Berkland, 2013). It plays also an important role in cartilage matrix stabilization (Pitarresi et al, 2007). HA was first isolated by an American scientist Karl Meyer and his assistant in 1934 from the vitreous body of cows’ eyes (Fakhari & Berkland, 2013 ; Simoni et al, 2002) and Later, it was extracted from bovine vitreous humor. The current source of HA powder is extracted from rooster comb or by bacterial bio-fermentation. Efforts have been focused on producing high yields of HA from genetically modified bacteria (Streptococcus) with low costly methods (Schanté, Zuber, Herlin, & Vandammea, 2011).



## 1.2 Applications of HA

As reported, commercial HA is biocompatible and it possesses properties similar of that in human tissues. These properties have allowed HA to be used in different biomedical applications. In 1942, Endre Balazes was the first man who used HA in a commercial purpose as a substitute for egg white in bakery products (Fakhari & Berkland, 2013). However, over last two decades, HA has become a material of great importance in modern medicine and it has been widely employed in tissue engineering and cosmetic surgery (Liu et al., 2007 ; Kenne et al., 20). Here, we describe the most common applications of HA in medicine and cosmetic fields.

### 1.2.1.1 Medicine

HA-based hydrogels have been widely used in tissue engineering because they provide three-dimensional scaffolds which allow nutrients and cellular waste to be diffused through it (Hoffman,2002). Treatment of osteoarthritis is a major biomedical application of HA, where the viscoelastic properties of synovial fluid decrease as a result of reduced HA molecular weight and concentration caused by aging (Arrich et al, 2005). After aging or damage, synovial fluid cannot provide the required viscoelastic response to various external stimuli allowing the development of cartilages contact and increasing wear of joint surface, so HA has been accepted as a common therapy for reducing this pain (Fakhari & Berkland, 2013). On the other hand, Hyaluronic acid has been studied as an ophthalmic material in eye surgery including corneal transplantation, glaucoma, cataract surgery and surgery to repair retinal detachment (Ruckmani et al, 2013 ; Limberg, McCaa, Kissling, & Kaufman, 1987) . HA could promote corneal epithelial, and improve function and integrity of superficial corneal cells (Yokoi, Komuro, Nishida & Kinoshita, 1997 ). HA is widely used as an eye lubricant and a viscoelastic to raise intraocular pressure (Holzer, 2001). Based on HA properties in the intraocular lens and water swelling, Beek, Jones and Sheardown suggested in their study that HA containing materials may have significant potential for use in contact lens applications (Beek, Jones & Sheardown, 2007).

Recently, the HA-based hydrogels have been used in drug delivery (Eenschooten et al., 2012). The HA drug carriers overcome the limitation of other polymeric carriers which are not biodegradable or do not have potential drug loading. The drugs can be easily loaded into the matrices of HA-based hydrogels and then released at a rate dependent on hydrogel properties and *in vivo* degradation rate. The HA-based hydrogels can also be tailored to control the release profile of the entrapped therapeutic macromolecules.

### 1.1.3.2 Cosmetic

In cosmetic, the HA-based hydrogels have been increasingly used as anti-aging products. We mentioned in the “ aims of study “ that most of complications associated with the application of HA-based hydrogels are thought to be caused by the chemical cross-linkers. It is known that as early as the third decade of life, the soft tissue structures of the face start gradually to weaken and skin loses its elasticity associated with wrinkles and thinning of subcutaneous fat (Sadick, Karcher & Palmisano, 2009). The swelling properties of hyaluronic acid make it an effective agent for use as injectable fillers to compensate loss of soft-tissues volume. The HA fillers have become very popular in correcting facial folds and producing a younger facial appearance. They achieve a substantial tissue augmentation into the affected skin and remain swollen in tissue for longer time (Robinson & Aasi, 2011). HA fillers with different types and various cross-linking efficiency are currently available in the market. Physicians select the most suitable one for skin treatment and in some cases, more than one type can be injected in layers to achieve substantial results, better elevating and skin visualization. Lips, cheek and oral region are the most requested areas for tissue augmentation due to their observable effect by aging process (Sadick, Karcher, & Palmisano, 2009). Full lips, cheek and perioral region are esthetic features of the younger face and have symbolized glamour, especially in women. So, elevating these areas by HA fillers, will have a significant rejuvenation effect (Johl & Burgett, 2006).

Several aspects should be considered when dealing with HA-based dermal fillers such as: source of HA, HA initial concentration, swelling capacity, stiffness, inclusion of an anesthetic agent and whether the hydrogel is monophasic (soft continuous matrix) or

biphasic (particles suspended in physiological solution) (Wollina and Goldman, 2013). The clinical performance of HA filler is largely affected by the aforementioned factors. HA-hydrogel particles are ranged in diameters from 1 micron to 1000 microns and are usually mixed with native or free HA solution to provide an easy injection (Allemann & Baumann, 2008; Beasley et al., 2009). The normal range of total HA concentration (modified + free HA) used in today HA fillers is between 18 mg/ml and 24 mg/ml. Higher total HA concentration requires larger needle and greater force for injection.

It is worth noting here, that the physicians should consider the needle and depth at which the material is implanted in order to achieve a good outcome with the HA fillers (Cirillo et al, 2008 ; Carruthers et al, 2008). Injection procedure is crucial for obtaining good results, a number of injection have been reported with two common procedures; linear threading and serial puncture. The linear threading requires the needle to be injected along the length of wrinkle line or fold, and a thread containing the HA filler is introduced as the needle is removed. In the serial puncture, multiple injections of fillers are administered close together followed by a massage to ensure equal distribution of the gel throughout the affected area (Sánchez-Carpintero, Candelas & Ruiz-Rodríguez, 2010). Several HA fillers have been approved by the US Food and Drug administration (FDA) for the correction of facial wrinkles and folds that include *Restylane* (Medicis; Scottsdale, Arizona), *Hylaform* (INAMED Aesthetics) and *Juvéderm* (INAMED Aesthetics) (Raghu & Athre, 2007). The *Restylane* and *Juvéderm* are bacteria-derived fillers, however the *Hylaform* is derived from rooster combs (Narins & Bowman, 2005). Since the approval of these fillers, the cosmetic market for hyaluronic acid HA-based dermal fillers is in continuous and rapid growth. *Restylane* and *Perlane* are particulate-based fillers where the particles are formed during the sizing process. These fillers are widely used for mid -to - deep dermal injection. In contrast, *Juvéderm* is a non-particulate and more homogenous filler (Baumann, 2004). It is more indicated for superficial fine lines and wrinkles.

## 1.3 HA cross-linking

HA has been used in various medical and cosmetic application, however, most of these applications are not addressed with native HA. As stated before, the native HA has very limited applications, because it does not remain in human body for prolonged periods due to its *in vivo* rapid degradation and poor mechanical properties (Liu et al., 2007; Jeon et al., 2007 ; Pitarresi et al., 2007). As reported, the half-life of native HA in the skin is longer than 24 hours (Brown, Laurent, & Fraser, 1991). HA is degraded into monosaccharide by an enzyme called hyaluronidase (Hyal) (Zhong et al, 1994 ; Lepperdinger, Fehrer, & Reitingner, 2004 ; Coleman & Grover, 2006). This enzyme cleaves the internal  $\beta$ -*N*-acetyl glucosaminidic linkages yielding fragments with *N*- acetyl –glucosamine at the reducing terminus and glucuronic acid at the non-reducing end (Zhong et al, 1994). HA can also be degraded in the organism by CD44 cell surface receptors and the reactive oxygen species (ROS) (Schante, Zuber, Herlin, & Vandamme, 2011). In fact, HA stability forms a crucial part to its utilization in the clinical application (Serben, Yang, & Prestwish, 2008). Therefore, HA should be stabilized via cross-linking methods to ensure a longer residence time within the soft tissue after administration into the body. These methods are of two main parts: chemical and physical cross-linking.

### 1.3.1 Chemical cross-linking

Chemical cross-linking is a common method used to improve HA mechanical behavior and prolong its duration. It involves cross-linking different HA chains by covalent bonds using a chemical cross-linker. The number of cross-linker molecules that form double links (reacts with HA at both ends) to the number of HA disaccharides units is expressed by the degree of cross-linking (Edsman et al., 2012). The degree of cross-linking plays an important role in commercializing HA products particularly in the industry of cosmetic. It is essential to evaluate the degree of cross-linking prior to the clinical administration. A product with a high degree of cross-linking shows slower degradation rate, good mechanical properties and higher restoration and correction.

The degree of cross-linking is sometime used interchangeably with the degree of modification. However, this is technically incorrect. The degree of modification is the ratio of cross-linker molecules that form mono- and double links to the number of HA disaccharides (Kenne et al., 2013). The mono-linked molecules do not form covalent bonds because they are reacted with the HA chains at one end leaving the other end pendants. These pendants do not contribute in hydrogel's strength or resistance against enzymatic de-polymerization process. The result of chemical cross-linking is a three-dimensional HA-hydrogel which could retain water within its cross-linked network, but does not dissolve in water. Chemically or covalently cross-linked hydrogels are stable materials and show much higher resistant against enzymatic degradation than native HA due to the formation of bridges and intermolecular bonds between the HA chains and the cross-linker. As stated before, various chemical cross-linkers have been employed for HA cross-linking such as carbodiimide, divinyl sulfone (DVS) and 1,4-butanediol diglycidyl ether (BDDE). The chemical cross-linking usually targets the carboxylic group (-COOH) or the hydroxyl group (-OH) of the HA chain structure.

### 1.3.1.1 (-COOH)

The -COOH group of HA can be modified to form ester bond via alkylation or reaction with epoxides. Esterification by alkylation (Fig. 1.2 A) uses alkyl halides such as alkyl bromides or iodides. This reaction was described by (Della Valle & Romeo, 1986), and it was performed at 30 °C for 12h. Later, (Pelletier et al, 2000) described similar method but with longer reaction time. Alkylation is performed in DMSO which means that the native HA has to be first converted into its TBA salt. Epoxide is a cyclic ether with a three-atom ring. It undergoes a ring-opening reaction and forms ester with HA polymer through the carboxylic group. A one example of this reaction; the reaction of HA with glycidyl methacrylate to form methacrylated HA as shown in (Fig. 1.2 B) (Bencherif et al., 2008 ; Leach, Bivens, Patrick & Schmidt, 2003 ; Pata, Barth, Bencherif & Washburn, 2010 ; Weng, Gouldstone, We & Chen, 2008). This reaction is performed in water in the presence of excess triethylamine as a catalyst (Schante, Zuber, Herlin, & Vandamme, 2011).

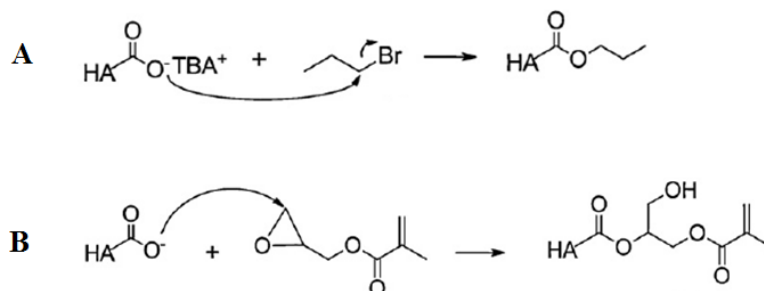


**Figure 1. 2** Esterification using alkyl halide (A), the reaction of HA with glycidyl methacrylate to form methacrylated HA (B) (Schante, Zuber, Herlin, & Vandamme, 2011)

### 1.3.1.2 (-OH)

Modification targeting (-OH) group in the HA chains is widely employed, particularly for the development of HA fillers, because it preserves the polyanionic nature of HA (Allemann & Baumann, 2008 ; Andre, 2004 ; Beasley, Weiss & Weiss, 2009 ; Falcon & Berg, 2008 ; Gatta et al., 2013; Chug et al., 2011 ; Hwang et al., 2012 ; Ibrahim et al., 2010 ; Kang et al., 2009 ; Kim et al., 2007 ; Segura et al., 2005 ; Yoon et al., 2011 & Gatta et al., 2013). The chemical reaction between HA and 1,4-butanediol diglycidyl ether BDDE was first described by (Malson & Lindqvist, 1986), the HA solution was mixed with BDDE under alkaline conditions and an ether linkage was formed (Fig 1.3). This reaction involves “epoxide ring opening” process and it is performed in a basic medium, where the epoxide ring reacts preferentially with the hydroxyl group to form ether bonds

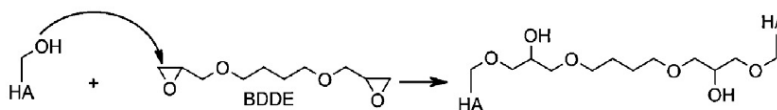


**Figure 1. 3** Ether formation by crosslinking two HA chain with BDDE (Schante, Zuber, Herlin, & Vandamme, 2011)

### 1.3.2 Physical cross-linking

Currently, there has been an increasing interest on physical cross-linking due to the ease of synthesis and advantage of not using a chemical cross-linker. Physical cross-linking is carried out via various physical methods including formation of complex coacervation and polymer conformations (Hennink & Nostrum, 2002 ; Gulrez, Al-Assaf & Phillips, 2011). Complex coacervation can be obtained by binding of two oppositely charged polymer (polyanion + polycation) driven by electrostatic interactions and form soluble and insoluble complexes (Fig. 1.4). One example of this binding is coacervating hyaluronic acid with lysozyme (Water et al., 2014) and also binding of polyanionic xanthan with polycationic chitosan (Esteban & Severian, 2000). Physical cross-linking can also be obtained through polymer conformations and entanglements. By increasing chains entanglements of a soluble polymer, the polymer solubility decreases and a 3 D network composite is formed with an elastic property. Cross-linked hydrogels may also be prepared in the presence of a strong acid to induce hydrogen bonds, this involves replacing the sodium in the polymer with the hydrogen in the acid. An example of hydrogen bonding, is the intermolecular bonding between polyacrylic acid and polyethylene oxide (Hoffman, 2002 ; Gulrez, Al-Assaf & Phillips, 2011).

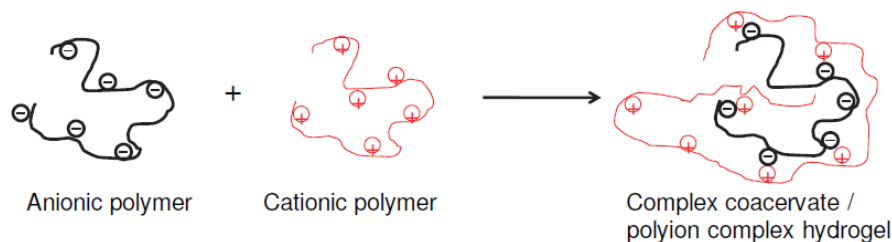


**Figure 1. 4** Complex coacervation between a polyanion and a polycation (Gulrez, Al-Assaf & Phillips, 2011)

Despite the advantages of physical cross-linking, this method alone is not enough for the formation of stiff cross-linked hydrogel. The network interactions of physically cross-linked hydrogels are reversible and can be disrupted by stress or change in physical conditions (Rosiak & Yoshii, 1999). They do not show a high resistance against enzymatic degradation and even they do not retain their 3D network for longer time particularly when they come in contact with aqueous fluids (Amargier et al., 2006).

## 1.4 Cross-linking efficiency

As we stated earlier, the main goal of this work was to enhance cross-linking efficiency of BDDE-HA hydrogel without increasing BDDE concentration. The cross-linking efficiency describes the total hydrogel's strength which includes the chemical and physical cross-linking occurred within the hydrogel's network. To achieve this goal, our hypothesis was set on changing method conditions that yielded less pendants formation, more covalent bonds between HA and BDDE and more HA entanglements. Evaluation of cross-linking efficiency requires analysis of hydrogel's properties including degradation rate, swelling capacity, surface morphology and rheological behavior. Several analytical instruments were employed to study these properties such as digital balance, high performance liquid chromatography (HPLC), UV-Visible spectrophotometer, scanning electron microscopy (SEM) and rheometer . Other instruments such as Fourier transform infrared (FTIR), capillary electrophoresis (CE), electro-spray ionization mass spectrometry (ESI-MS) and nuclear magnetic resonance spectroscopy (NMR) are more eligible for the confirmation of the occurrence of chemical modification. The *Appendix 1* displays an introduction to some analytical instruments employed in this study for the characterization of HA hydrogels.



## CHAPTER 2

## 2. Cross-linking hyaluronic acid with BDDE

### 2.1 Introduction

HA cross-linking refers to a process in which HA chains are chemically bound with a chemical cross-linker through one of the HA functional groups including (- OH, - COOH, - NHCOCH<sub>3</sub>), in order to improve HA's mechanical properties and prolong its residence after administration into the body. Due to the importance of cross-linked hydrogel versus linear or native HA in biomedical application, researchers have developed several synthetic routes based on various characteristics sought, to obtain hydrogels with more desired effect. In our work, we modified a reported method described by (Malson & Lindqvist, 1986) and later improved by (Piron & Tholin, 2002), for cross-linking HA chains with 1, 4-butanediol diglycidyl ether BDDE. The reaction was carried out in strong alkaline conditions to form stable ether bonds (De Boulle et al., 2013). The epoxide groups of BDDE preferentially react with the hydroxyl groups of HA, because at high pH range, the deprotonated hydroxyls are more predominant than both anionic carboxylic group and the amide (Kenne et al., 2013).

### 2.2 Preparation of cross-linked BDDE-HA hydrogel

#### 2.2.1 Materials

The sodium salt of hyaluronic acid was obtained from Vivatis Pharma (Hamburg, Germany), with an average molecular weight 1,000,000 Da. For synthesis and de-polymerization: 1, 4-butanediol diglycidyl ether (BDDE) and hyaluronidase powder (3000 U/ mg) were purchased from Sigma-Aldrich Co (St. Louis, Missouri, USA). All other chemicals were of analytical grade, unless otherwise stated.

### 2.2.2 Synthesis

A 2.0 % (v/v) cross-linking reagent solution was prepared by adding 200  $\mu\text{l}$  of BDDE into 9.80 ml of 0.25M NaOH . About 1.20 g of hyaluronic acid HA powder was added to the mixture and allowed to mix thoroughly at room temperature for 60 min (pH 13), so the HA concentration was 12 % (w/v). The epoxide ring in BDDE opened to form ether bonds with the HA hydroxyl groups as described in Fig. 1.3. After the reaction is complete, the mixture was neutralized by adding an equivalent amount of 0.1M HCl to a pH of approximately 7.0 and then dialyzed against distilled water for 3 days to remove un-reacted HA fragments and BDDE residue. The resulting product was a transparent gel (Fig. 2.1 A). The cross-linked hydrogel was then lyophilized using (Labtech freeze-dryer LFD 5518 model, Daihan Labtech Co); the sample was first frozen at  $-80\text{ }^{\circ}\text{C}$  in an ultra-low temperature freezer (MDF-U3386S, SANYO Electric Co. Japan) for 4 h to ensure complete freezing and then sublimed at  $-50\text{ }^{\circ}\text{C}$  for 24 h under a vacuum of 5 mTorr. When all free ice was removed, the temperature was raised to  $25\text{ }^{\circ}\text{C}$  and the sample was left for 2 h to remove excess water bound to it (Fig. 2.1 B). Finally, the product was stored at  $8\text{ }^{\circ}\text{C}$  until the characterization studies were carried out. The cross-linked hydrogel was compared with a native HA polymer to confirm the occurrence of cross-linking process.

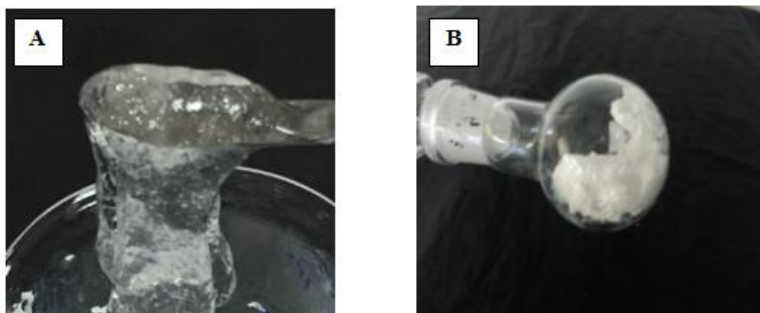


**Figure 2. 1** Hydrated BDDE-HA hydrogel (A), Lyophilized BDDE-HA hydrogel (B).

## 2.3 Comparison between native and cross-linked HA

### 2.3.1 Materials

Samples of native HA and cross-linked BDDE-HA hydrogel, enzyme hyaluronidase (solid powder) with 3000 U/mg. Ehrlich's reagent, phosphate buffer saline (PBS) and alkaline solution.

### 2.3.2 Measurements

The resulting cross-linked hydrogel was compared with the native HA solution to confirm the occurrence of modification process using four analytical techniques.

#### 2.3.2.1 Fourier-transformed infrared (FT-IR) analysis

Portions from native HA solution and cross-linked BDDE-HA hydrogel were obtained and characterized using Bruker Tensor 37; Fourier Transform Infrared Spectroscopy (FT-IR) (Ettlingen, Germany). All spectra were recorded between 4000 and 400  $\text{cm}^{-1}$  with a resolution of 4  $\text{cm}^{-1}$  and the data was manipulated using OPUS software.

#### 2.3.2.2 Capillary electrophoresis (CE)

Equivalent portions from native HA solution and cross-linked BDDE-HA hydrogel were obtained and dissolved in BTH solution separately. The two extracts were filtered, degassed and then moved into capillary electrophoresis vials. The analysis was performed using a Hewlett-Packard CE system (Waldbronn, Germany) at 50 mbar pressure and 22 kV separation potential for 10 min. Analysis was performed in normal polarity mode with hydrodynamic injection and the analytes were detected by direct ultraviolet (UV) absorbance at 194 nm. A buffer solution at 50 mM concentration was prepared by dissolving 5.0 g sodium tetraborate  $\text{Na}_2\text{B}_4\text{O}_7$  (Mw= 201.22 g/mole) in distilled water and filled up to 500 ml. The pH was adjusted to 7.4 and measured by a pH meter.

### 2.3.2.3 Electro-spray ionization mass spectrometry ESI-MS

Known amounts of native HA and cross-linked hydrogel were obtained and treated with hyaluronidase for 4 h digestion. The resulting solutions were centrifuged and the supernatant in each container was collected and then diluted 1: 50 in purified water. Electro-spray ionization mass spectrometry (ESI-MS) measurements were carried out using the Quattro Premier XE mass spectrometer instrument Q-MS (Waters Corporation, Manchester, UK). The hydrogels extracts were introduced into the instrument through direct infusion using a syringe pump and the experimental conditions were set as follow: capillary voltage 4.0 kV, cone voltage (voltage of sampling cone to ionize and direct ions to the mass analyzer) 30 V, desolvation temperature 150 °C and source temperature 100 °C. The full scan mass spectra from m/z 200-2000 were acquired in negative ionization mode with a scan speed of 1 s per scan.

### 2.3.2.4 Nuclear magnetic resonance spectroscopy (NMR)

Portions from lyophilized native HA and the cross-linked hydrogel were taken and digested with hyaluronidase solution placed in separate containers. The extracts were filtered via 45 µm Watmaan paper and then centrifuged at 2000 rpm for 2 min. The supernatants were removed then re-lyophilized to afford white foam. The <sup>1</sup>H NMR spectra were recorded on a Bruker 600 MHz (Zurich, Switzerland) operating at a frequency of 600 MHz.

## 2.3.3 Results and discussion

### 2.3.3.1 FTIR

The FTIR spectra (Figures 2.2 & 2.3) revealed three characteristic peaks that confirmed the successful modification of the native HA ; peak 1 at 3343 cm<sup>-1</sup> observed in native HA and cross-linked hydrogel, peak 2 at 2900 cm<sup>-1</sup> observed in cross-linked hydrogel and relatively in native HA. Peak 3 at 1300 cm<sup>-1</sup> observed in the cross-linked hydrogel. Peak 1 was assigned to the hydroxyl group whereas peaks 2 and 3 represented the C- H stretching and ether linkage respectively. As stated, at high pH values or above the pKa value of the hydroxyl groups, the hydroxyl groups become almost deprotonated.

The deprotonated hydroxyl groups are stronger nucleophiles than both the carboxylic group and the amide. Hence, the epoxide groups of BDDE react preferentially with the hydroxyl groups of HA to form stable ether bonds (Schanté et al. 2011). Theoretically, there are two epoxide groups in BDDE and four alcohols reactive sites per unit of HA. The relative preference of epoxide group to react with hydroxyl groups depends on reaction conditions. Under alkaline conditions, the BDDE molecules target the reactive hydroxyl groups in native HA to form ether bonds. When two (-OH) groups in two adjacent HA chains are covalently blocked with BDDE epoxides, the total -OH will decrease. This means that the total (-OH) amount decreases when HA is subject to a chemical modification reaction, subsequently appears with a smaller downward peak than non-modified HA.

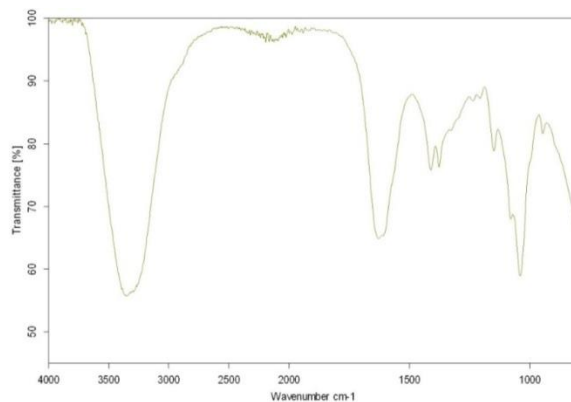


**Figure 2. 2** FTIR spectra of lyophilized native HA obtained at 25 °C. The spectra demonstrates large - OH downward peak at 3343 cm<sup>-1</sup>.

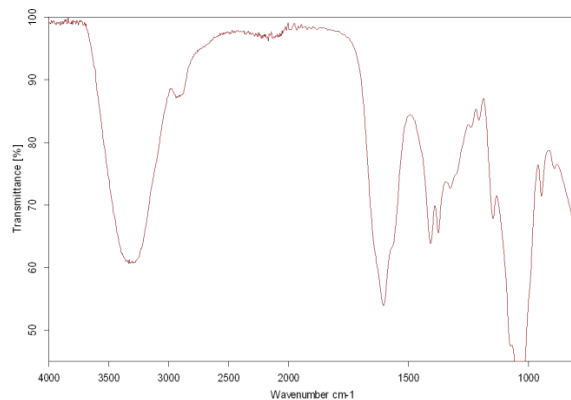


**Figure 2. 3** FTIR spectra of cross-linked HA obtained at 25 °C. The spectra demonstrates smaller - OH downward peak at 3343 cm<sup>-1</sup> and a distinct peak at 2900 cm<sup>-1</sup>

Finally, the FTIR data confirmed the occurrence of chemical modification with the BDDE molecules. The hydroxyl band group of native HA was larger than its counterpart in the cross-linked hydrogel.

### 2.3.3.2 Capillary electrophoresis (CE)

Based on CE results, the hyaluronic acid showed negative electrophoretic mobility in the direction of cathode. However, due to the hydrodynamic sizes or the (*charge to mass*) ratios of HA fragments, their separation under CE conditions became difficult. The electrophoretic mobility of HA fragments yielded a single broad peak or a group of overlapping peaks at 5.788 min as shown in figure 2.4 . The method conditions including viscosity, electro-osmotic flow (EOF), voltage across the capillary, temperature, fragments concentrations, phosphate buffer and the pH of buffer; all have a significant impact on CE separation.

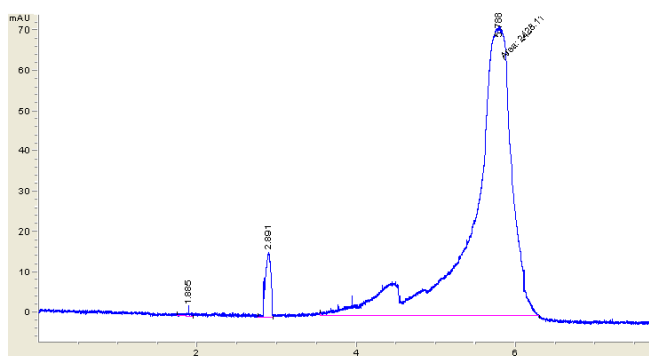


**Figure 2. 4** CE electropherogram of native HA fragments obtained by enzymatic digestion

In contrast, the fragments of BDDE-HA hydrogel, had more chance to be separated by CE than native HA. The electropherogram of cross-linked hydrogel (Fig 2.5) revealed several small peaks that were not found in native HA. The enzymatic digestion is likely to break down the BDDE-HA network into fragments with different hydrodynamics sizes which produced different masses and migrated at different rates. These data confirmed the occurrence of modification process and so, they proved that HA chains had been chemically modified with BDDE molecules.

The CE is a powerful technique to separate glycosaminoglycan-derived oligosaccharides, however, for the quantification of cross-linked HA fragments, it requires an extensive preparation procedure.

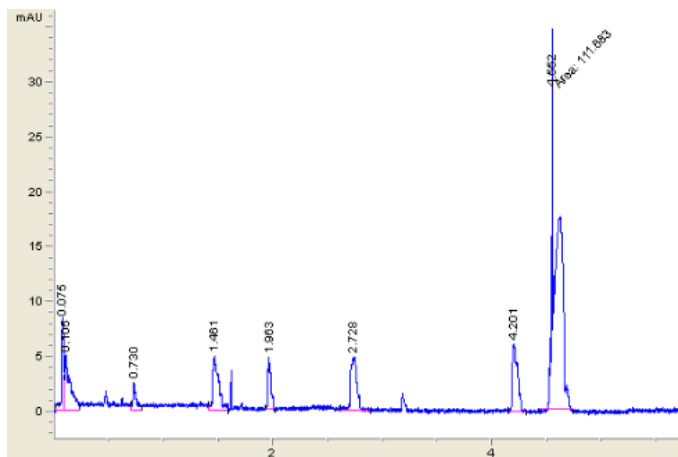


**Figure 2. 5** CE electropherogram of cross-linked BDDE-HA fragments obtained by enzymatic digestion

### 2.3.3.3 ESI-MS

The bovine testicular hyaluronidase was used to digest known quantities of native HA and cross-linked BDDE-HA hydrogel. Extracts were qualitatively analyzed by electro-spray ionization mass spectrometry ESI-MS using direct infusion. Fig. 2.6 displays MS spectra of native HA oligomers generated by the enzymatic digestion, whereas Fig. 2.7 displays the MS spectra of cross-linked BDDE-HA hydrogel generated under similar conditions. The ESI-MS technique could clearly distinguish the native HA and cross-linked ion species and relatively exhibited different mapping spectra. The MS spectrum of cross-linked hydrogel showed no identical peaks with its counterpart spectrum of HA. The oligosaccharides of cross-linked hydrogel exhibited a different charge state distribution profile suggesting that the BDDE-HA had undergone a successful modification. The results showed various oligosaccharide fragments with different relative intensities and chain length ranged from the basic unit of hyaluronic acid to a greater than 16-mers. In general, the ions observed in native HA and cross-linked hydrogel were singly and multiply charged ions corresponding to the disaccharide oligomer of hyaluronic acid.

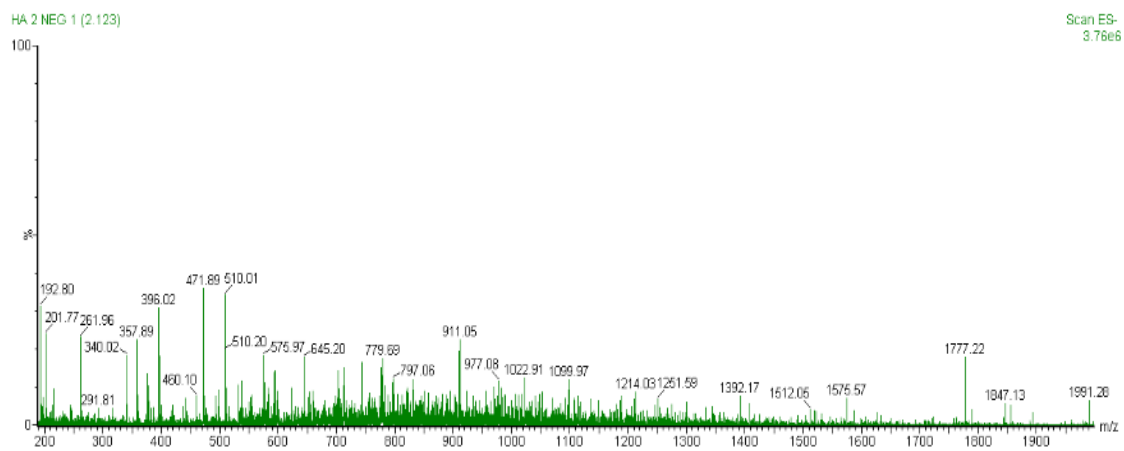


Figure 2. 6 The ESI-MS profiles of native HA obtained by direct infusion at 4.0 kV capillary voltage

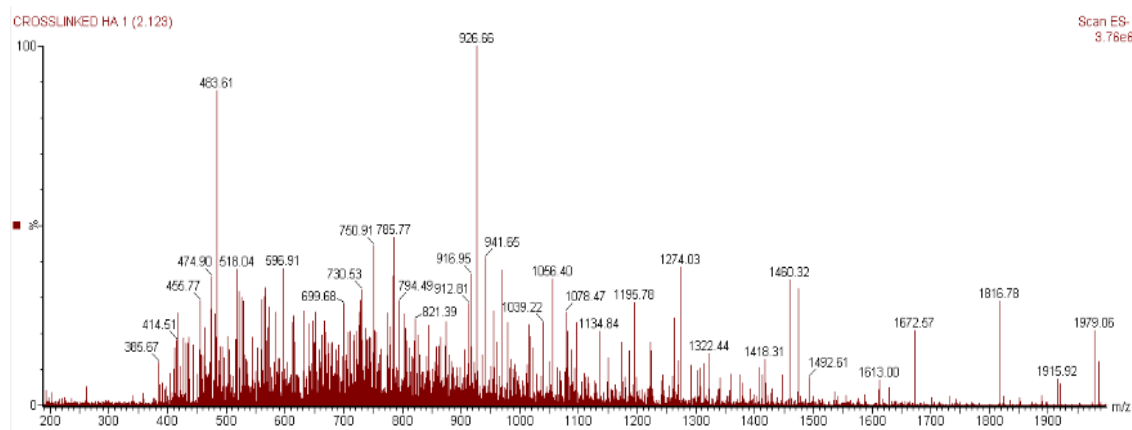


Figure 2. 7 The ESI-MS profiles of cross-linked HA-BDDE hydrogel obtained by direct infusion at 4.0 kV capillary voltage

According to the data, some small and large peaks that commonly represent the disaccharide unit of hyaluronic acid are clearly observed in native HA, but not in the cross-linked hydrogel, particularly at the lower range of MS spectrum. These peaks confirmed the occurrence of chemical modification. For instance, The mass peak observed at  $m/z$  396 in native HA spectra is attributed to the disaccharide unit and a water molecule ( $[\text{GlcUA} - \text{GlcNAc}] + \text{H}_2\text{O}$ ). Also, the peak at  $m/z$  192.8 which further showed a fragment at  $m/z$  176 after losing a water molecule and the peak at  $m/z$  201.89 appeared in native HA were assigned for glucuronic acid (GlcA) and *N*-acetyl-D-glucosamine ( $\text{GlcNAc} - \text{H}_2\text{O}$ ) respectively.



On the other hand, the triply charged peak  $[M-3H]^{2-}$  at  $m/z$  510.01 and the doubly charged peak at  $m/z$  575.97 were also observed in native HA but not in the cross-linked hydrogel. In our experiment, some oligosaccharides were easily defined and they were in good agreement with the theoretical ion species of HA degradation products. However, some oligosaccharides were difficult to be assigned due to the fragmentation and collisional activation which are usually seen during the ESI-MS analysis. The enzyme cleaves the 1,4-linkages between *N*-acetyl-D-glucosamine (GlcNAc) and glucuronic acid (GlcA) yielding oligomers with *N*-acetyl-D-glucosamine at the reducing terminal and unsaturated uronic acid ( $\Delta$ UA) at the non-reducing terminal (even-numbered oligosaccharides) and fragments with uronic acid UA at both the reducing and non-reducing terminal (odd-numbered oligosaccharides). Table 2.1 displays fragmentation pattern of even and odd-numbered oligomers obtained from native HA, while table 2.2 displays fragmentation pattern of even and odd-numbered oligomers obtained from the cross-linked hydrogels.

Based on the results, most of native HA oligomers were observed at lower mass range and became more abundant at  $m/z$  below 900. This was due to high degradation rate of native HA which had a very low resistance toward enzymatic digestion. In contrast, the cross-linked oligomers generally appeared to have higher mass ranges where BDDE can slow down the enzymatic degradation. However, detailed analysis of cross-linked oligosaccharides or estimating the total degree of modification by ESI-MS is still challenging due to the viscoelastic properties and complex mixture of larger oligosaccharides generated by hyaluronidase . (Kenne et al., 2013). Additionally, we observed in our method, that the resulting oligomers were greatly influenced by method conditions and mass spectrometric parameters. For example, any change in cone voltage or dissolution temperature produces different fragmentation pattern. The (*appendix 2*) demonstrates the MS spectrum of disaccharide unite and the extended range of native and cross-linked hydrogel up to 2000  $m/z$  .

**Table 2. 1** Possible oligomers of native HA hydrogel formed after 4h digestion with hyaluronidase and detected by direct infusion, ESI-MS at 30 v con voltage .

Observed m/z	Charge	Possible oligomer
192.80	-1	GlcA
201.89	-1	GlcNAc
378.04	-1	2 mer
396.02	-1	2 mer + H2O
471.89	-4	10 mer
510.01	-3	8 mer + H2O
575.97	-2	6 mer + H2O
1135.9	-1	6 mer
1894	-1	10 mer

**Table 2. 2** Possible oligomers of cross-linked BDDE-HA hydrogel formed after 4h digestion with hyaluronidase and detected by direct infusion, ESI-MS at 30 v con voltage .BDDE = mono-linked, BDDE\* = cross-linked

Observed m/z	Charge	Possible oligomer
571.7	-3	8-mer-BDDE*
651.53	-3	8-mer-2BDDE
668.27	-2	6-mer-BDDE*
703.95	-3	10-mer-BDDE
717.49	-4	14-mer-BDDE
960	-2	8-mer-2BDDE*
1010.31	-3	16-mer-BDDE
1018.08	-3	14-mer-2BDDE*
1077.21	-3	16-mer-BDDE*
1197	-1	4-mer-2BDDE
1223.87	-2	13-mer
1338	-1	6-mer-BDDE*
1338.9	-2	12-mer-2BDDE*
1428	-2	14-mer-BDDE*
1515.25	-2	16-mer-BDDE
1527.48	-2	14-mer-2BDDE*
1919.9	-1	8-mer-2BDDE*

### 2.3.3.4 NMR

According to the NMR spectra, two interesting peaks were considered; peak (1) represented the acetyl glucosamine N-CH<sub>3</sub> at about 1.9 ppm in native HA and cross-linked hydrogel.

Peak (2) represented the – (CH<sub>2</sub>) for BDDE at about 1.5 ppm in the cross-linked hydrogel which suggested chemical modification in HA polymer. Fig. 2.8 shows the NMR spectra of HA native, while Fig 2.9 represents the spectra of cross-linked hydrogel.

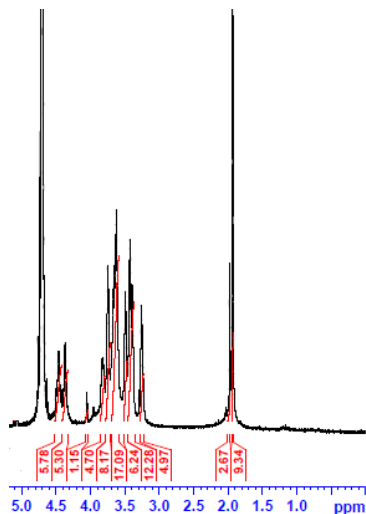


Figure 2. 8 NMR spectra of lyophilized native HA digested fragments obtained at 25 °C.

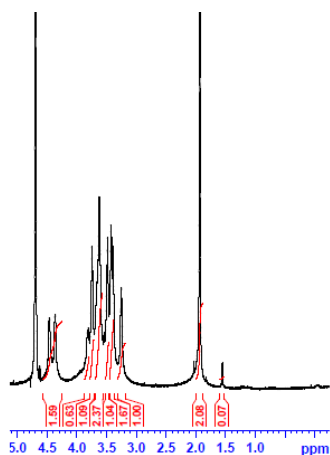


Figure 2. 9 NMR spectra of lyophilized BDDE- HA digested fragments obtained at 25 °C

Integration of the signal at 1.5 ppm (BDDE) with respect to the signal at 1.9 ppm (N-CH<sub>3</sub>) gives an approximation of the total degree of modification occurred within HA chains. The degree of modification was found to be 3.4%, this value corresponded to the amount of BDDE linked with HA.

In fact, this degree of modification was far less than the theoretical degree of modification which was supposed to equal 30 % based on molar ratio. This explained that the amount of BDDE mixed with HA was not completely consumed in the chemical reaction. NMR is a powerful technique for studying the relationship between the cross-linker concentration and the degree of modification. It is widely employed to confirm the occurrence of chemical modification or estimate the total degree of modification. In a separate work, we validated this relationship by preparing four HA hydrogels cross-linked with different BDDE concentrations: 0.25%, 0.50%, 0.75% and 1.0% (v/v). The (*appendix 3*) concludes the results and show how the degree of modification was increased with the increase of BDDE concentration.

## 2.4 Conclusion

In this chapter, a cross-linked BDDE-HA hydrogel was prepared according to a reported method with a little modification. The cross-linking reaction was performed in a strong alkaline medium and allowed to stand for 60 min at pH 13 and 25 °C. The cross-linked hydrogel was compared with a native HA solution using FTIR, CE, ESI-MS and NMR, the result confirmed the occurrence of cross-linking process. The FTIR proved that the total amount of (–OH) in the cross-linked hydrogel was less than in native HA. The native HA had a slight different migration time from the cross-linked hydrogel with less separated fragments than the cross-linked hydrogel. The ESI-MS could relatively discriminate the native HA spectrum from the cross-linked HA spectrum. NMR was more characteristic for confirmation of the modification process by showing a distinctive peak at 1.5 ppm for BDDE. Furthermore, integration of BDDE signal to the (N-CH<sub>3</sub>) signal in the NMR spectra allowed the estimation of the total degree of modification.

## CHAPTER 3

### 3. Evaluation of *in-vitro* degradation rate of cross-linked BDDE-HA hydrogel.

#### 3.1 Introduction

Evaluation of the degradation rates of cross-linked hydrogels has become one of most important considerations in the market and forms a key factor to the cross-linking efficiency. Durability or resistance toward enzymatic reaction can make the hydrogel a unique material. So, the development of reliable analytical methods for assessing such ability is fundamental. Although most currently available commercial HA fillers are cross-linked with BDDE, there are a few of analytical methods described in literature to follow-up the *in-vitro* degradation rate. The majority of reported methods included change in viscosity, change in water content, and colorimetric assay (carbazol reaction) for the liberated glucuronic acid (Sall & Fe´rard, 2007). These methods are time-consuming, less accurate and all of them are substantially employed to test the sensitivity of native HA to the reaction of hyaluronidase. Therefore, prior to working on method conditions, we dedicated this chapter to compare three different analytical methods (chromatographic, colorimetric and gravimetric) for the evaluation of *in-vitro* degradation rate of HA-based hydrogels.

## 3.2 Development of (chromatographic, colorimetric and gravimetric) methods to quantify the *in-vitro* degradation rate

### 3.2.1 Material

Sodium salt of HA was donated from Vivatis Pharma. BDDE reagent and hyaluronidase powder (3000 U/ mg) were purchased from Sigma-Aldrich. Ehrlich's reagent, phosphate buffer saline (PBS) and alkaline solutions were prepared in the laboratory.

### 3.2.2 Synthesis

Nine hydrogels X<sub>1</sub>- X<sub>9</sub> were synthesized according to (Malson & Lindqvist, 1986; Piron & Tholin, 2002) using 1, 4-butanediol diglycidyl ether (BDDE) as a chemical cross-linker. All cross-linked hydrogels were lyophilized and kept in the fridge until the *in-vitro* degradation tests were performed. The hydrogels X<sub>1</sub>, X<sub>2</sub> and X<sub>3</sub> were assigned for HPLC method, X<sub>4</sub>, X<sub>5</sub> and X<sub>6</sub> for UV-Visible spectroscopy method and X<sub>7</sub>, X<sub>8</sub> and X<sub>9</sub> for weight loss method.

### 3.2.3 Measurements

#### 3.2.3.1 Chromatographic method

The lyophilized hydrogels X<sub>1</sub>, X<sub>2</sub> and X<sub>3</sub> were swollen in distilled water and left overnight to reach their equilibrium states. Three samples X<sub>1</sub>A, X<sub>2</sub>A, and X<sub>3</sub>A equivalent in weight (5.0 g per each) were cut from the swollen hydrogels and placed in separate containers. Each sample was mixed with 500µl of hyaluronidase BTH solution (specific activity of 300 units per milliliter) and incubated at 37 °C. After 24h, the reactions were stopped by boiling for 10 min and then centrifuged at 2000 rpm for 2 min to separate the extract from the solid part. The three extracts were then diluted with purified water up to the mark in 100 ml volumetric flasks. Another three samples X<sub>1</sub>B, X<sub>2</sub>B, and X<sub>3</sub>B equivalent in weight (5.0 g per each) were cut from the swollen hydrogels and kept with hyaluronidase (BTH) under same conditions until complete digestion had occurred.

The contents of NAG in liquid extracts of all samples X<sub>1</sub>A, X<sub>2</sub>A, X<sub>3</sub>A, X<sub>1</sub>B, X<sub>2</sub>B, and X<sub>3</sub>B were quantified by HPLC (Agilent 1220 infinity, Waldbronn, Germany) equipped with a built-in auto-sampler and diode-array detector. The stationary phase was C18 end-capped column (100cm x 2mm) with 5 µm particle size from (Knauer, Berlin, Germany). Different compositions of mobile phase were initially tested to obtain best signals and robust method. Finally the mobile phase composed of two solutions A: 96% (water 96% + acetonitrile 4%), B: methanol 4%.

The column was first equilibrated with the mobile phase and the analysis was performed in isocratic mode with an injection volume of 2 µl and a flow rate of 0.4 ml/min. The wavelength was set up at 195 nm and the run time of the method was 10 min. Quantification was carried out against series of standard solutions prepared by enzymatic digestion of non-cross-linked hyaluronic acid and treated in the same manner of cross-linked hydrogels. The concentrations of standards ranged between 20 and 300 µg/ml and they were all prepared in 100 ml volumetric flasks. The degradation rates of the three hydrogels X<sub>1</sub>, X<sub>2</sub> and X<sub>3</sub> were then evaluated by calculating the relative difference (%) of NAG found in the extracts released after one day enzymatic digestion (samples A) to the total amount of NAG found in the extracts released after complete digestion (sample B). Finally, an average degradation rate of the three hydrogels was obtained with 95% confidence interval.

### **3.2.3.2 Colorimetric method**

A colorimetric method for the quantification of NAG in sugars was developed by (Morgan & Elson, 1934) who described that the heated medium of NAG could produce reddish-purple color after addition of acetic acid and *p*-dimethyl amino- benzaldehyde acidified with hydrochloric acid (Ehrlich's reagent). They showed that under certain conditions the NAG found in the extract can be converted into oxazole derivative which are condensed by Ehrlich's reagent giving the perceptible color. In our work, the greatest color intensity per 1 ml of NAG solution was achieved when the reaction was carried out in a solution containing 0.25M Na<sub>2</sub>CO<sub>3</sub> and boiled for 1 min. Boiling for more than 1 min led to the destruction of glucosamine and produced less color intensity.

Regarding the glacial acetic acid, the final color intensity could be developed if the volume of this solvent was approximately six-fold larger than the volume of NAG solution. By using this proportion, the method was sensitive and the amount of NAG as small as 0.001g found in the extract was possible to be detected. The lyophilized hydrogels X<sub>4</sub>, X<sub>5</sub> and X<sub>6</sub> were swollen in distilled water until reached their equilibrium states. In analogy to the HPLC method, two samples A and B equivalent in weight (5.0 g per each) were cut from each hydrogel and placed in separate test tubes. Each sample was treated with 500µl of bovine testicular hyaluronidase BTH (activity of 300 U/ml) at 37C<sup>0</sup>. The reactions of samples A were stopped after 24 h, while the reactions of samples B were left until complete digestion. All liquid extracts were further purified through centrifugation and then transferred into 10 ml volumetric flasks and diluted up to the mark.

Nine standard solutions ranging from 20 µg /ml to 400 µg/ml were prepared by enzymatic digestion of native HA and kept also in 10 ml volumetric flasks. For UV spectroscopy analysis, 1.0 ml from each standard solution and samples X<sub>4</sub>A, X<sub>5</sub>A, X<sub>6</sub>A, X<sub>4</sub>B, X<sub>5</sub>B, and X<sub>6</sub>B was withdrawn and mixed with 0.1 ml of 0.25 M sodium carbonate. Each mixture was boiled for 1 min in a water bath to produce the oxazole derivative. Approximately 6.0 ml of glacial acetic acid was then added to each mixture followed by 1.0 ml of Ehrlich's reagent. All mixtures were then stirred on a vortex mixer and then allowed to cool until a violet color developed in each container. The most of colors reached their maximum intensity in 16-20 min. A plank sample was prepared with the glacial acetic acid and Ehrlich's reagent.

The content of NAG was then quantified in each sample by a single beam UV-Visible spectrophotometer (Spekol 1500, Analytik, jena, Germany) and the absorbance was recorded at 585 nm. Similarly, the degradation rates of the hydrogels X<sub>4</sub>, X<sub>5</sub> and X<sub>6</sub> were evaluated by calculating the relative difference (%) of NAG found in samples A extracts to the total amount of NAG found in samples B extracts. Finally, an average degradation rate of the three hydrogels was obtained with 95% confidence interval.



### 3.2.3.3 Gravimetric method

The commonly reported method (*weight loss method*) was employed in our study to evaluate the degradation rates of the hydrogels X<sub>7</sub>, X<sub>8</sub> and X<sub>9</sub>. The lyophilized hydrogels X<sub>7</sub>, X<sub>8</sub> and X<sub>9</sub> were swollen in distilled water until reached their equilibrium states. A sample weighed 5.0 g was cut from each swollen hydrogel and incubated with hyaluronidase BTH (activity of 300 U/ml) at 37 °C for 24 h. The degradation rate of each hydrogel was evaluated due to the change in hydrogel weight before and after enzymatic incubation and calculated in accordance with the following equation:

$$\text{Weight loss \%} = \frac{(W_0 - W_r)}{W_0} \times 100\% \quad \dots\dots\dots \text{e.q. 3.1}$$

Where W<sub>0</sub> is the original weight of the swollen hydrogel at equilibrium state and W<sub>r</sub> is the remaining weight after one day enzymatic digestion. An average degradation rate of the three hydrogels was obtained with 95% confidence interval.

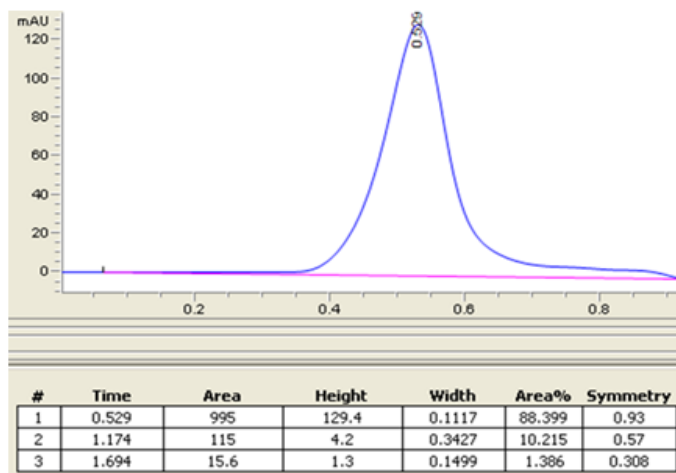
### 3.2.4 Statistics

Statistical analysis for significance between the three methods (HPLC, UV-Visible, and Wight loss) was performed by means of Student's t-test, assuming unequal variance and one-way ANOVA. Value of P < 0.05 was statistically considered significant.

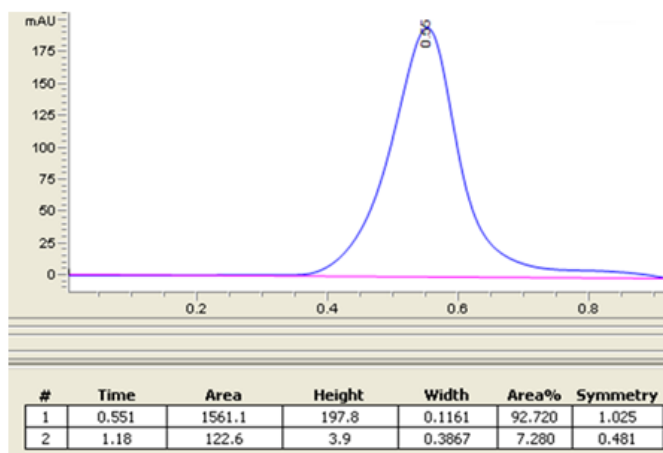
### 3.2.5 Results

#### 3.2.5.1 High performance liquid chromatography (HPLC)

The HPLC measurements showed broad peaks for all standard solutions and samples A and B of the three hydrogels X<sub>1</sub>, X<sub>2</sub> and X<sub>3</sub>. Fig.3.1 displays representative chromatograms of NAG for two samples extracts; X<sub>1</sub>A after one-day enzymatic digestion and X<sub>1</sub>B after complete digestion, (*all HPLC results are shown in appendix 4*). The chromatograms of standards solutions and the calibration curve are demonstrated in Fig. 3.2 a & b.

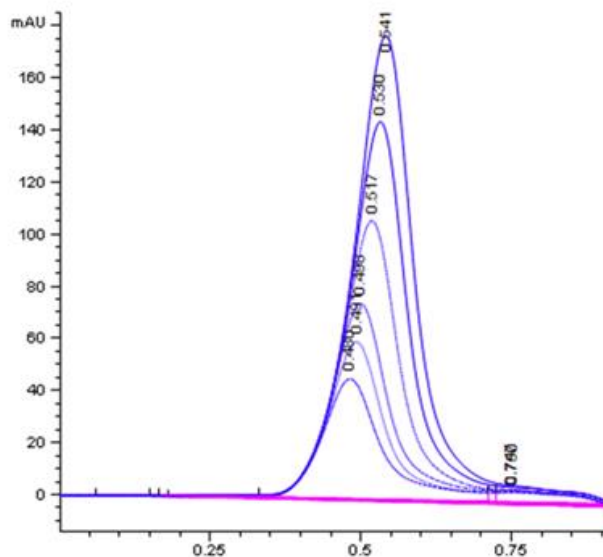


(a)

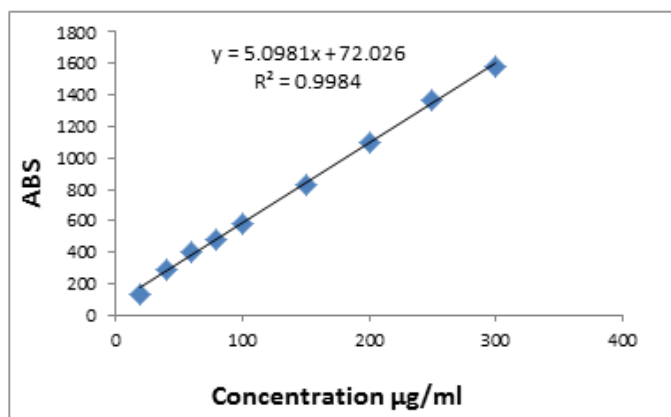


(b)

**Figure 3. 1** Chromatograms of (NAG) for: X<sub>1</sub> A after one-day enzymatic digestion (a) and X<sub>1</sub> B after complete digestion (b)



(a)



(b)

**Figure 3. 2** Chromatograms of standard solutions at 195 nm (a) and the calibration curve of series standard solutions at 195 nm (b)

The linear equation  $y = 5.0981x + 72.026$  was obtained from the calibration curve where  $y$  was the measured absorption and  $x$  was the concentration of HA ( $\mu\text{g}/\text{ml}$ ). The correlation coefficient  $R^2$  was 0.9984. The equation was employed to quantify the amounts of *N*-acetyl glucosamine NAG in samples A and samples B of  $X_1$ ,  $X_2$ , and  $X_3$ .

Differences between the amounts of NAG found in samples A and samples B were relatively used to evaluate the number of cleavages of glycosidic bonds per unit time which corresponds to the degradation rates of the three hydrogels per one day. The degradation rates of the three hydrogels X<sub>1</sub>, X<sub>2</sub>, and X<sub>3</sub> are demonstrated in table 3.1.

**Table 3. 1** Degradation rates of samples (X<sub>1</sub>, X<sub>2</sub>, and X<sub>3</sub>) obtained from HPLC method. The average degradation rate with 95% confidence interval equaled to 62.6% ±12.3 (w/w)

Sample	Amount of (NAG) in samples (A) extracts.	Amount of (NAG) in samples (B) extracts	Degradation rate (A /B) X 100
X <sub>1</sub>	18.5 mg	29.8 mg	62%
X <sub>2</sub>	14.7 mg	25.4 mg	57.9%
X <sub>3</sub>	20.0 mg	29.5 mg	67.8%

The limit of detection (LOD) was estimated as the three times the standard deviation of y-residuals divided by the slope of the regression line, and found as 6.4 µg/ ml. Recovery was identified as the ratio of the content of the total NAG measured after complete enzymatic digestion to the theoretical content found in original sample weight (5.0g) of swollen hydrogel. The HPLC achieved recoveries of 91.0 %, 73.2% and 82.2% for hydrogels X<sub>1</sub>, X<sub>2</sub> and X<sub>3</sub> respectively.

### 3.2.5.2 UV-Vis spectrophotometer

The colorimetric method was performed for samples A and B of hydrogels X<sub>4</sub>, X<sub>5</sub> and X<sub>6</sub> by the UV-Visible spectrophotometer at 585 nm. The analysis was carried out when the violet color reached its maximum intensity and confirmed that no more violet color was produced by addition of Ehrlich's reagent. Fig.3.3 illustrates the violet color developed by Ehrlich's reagent in the extract of samples X<sub>4</sub>A and X<sub>4</sub>B. The color gradient of standard solutions developed by Ehrlich's reagent and the calibration curve are illustrated in Fig.3.4 a & b. *(For more details about colorimetric method, refer to appendix 5)*

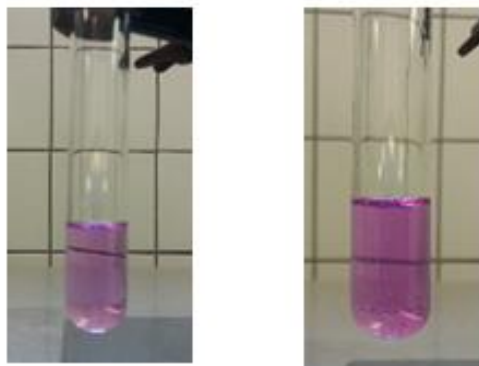
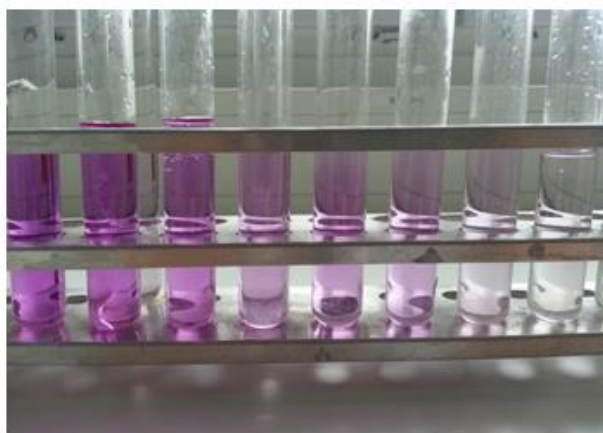
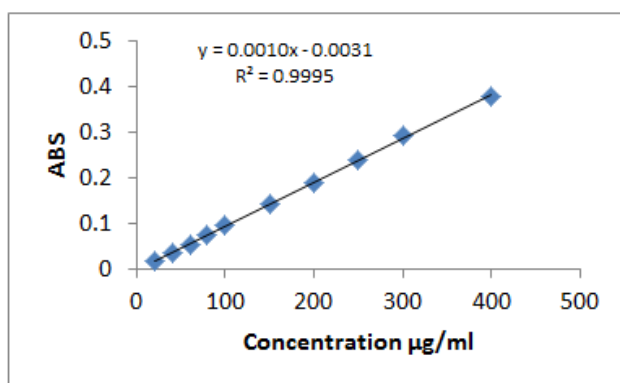


**Figure 3. 3** The violet color developed by Ehrlich's reagent in samples: X<sub>4</sub> A after one-day enzymatic digestion (left) and X<sub>4</sub> B after complete enzymatic digestion (right)



(a)



(b)

**Figure 3. 4** Color gradient of standards developed by Ehrlich's reagent (a) and the calibration curve of standards solutions prepared under similar treatment of digestion (b).

A linear equation  $y= 0.001 x-0.0031$  was also obtained from the calibration curve with a correlation coefficient  $R^2$  of 0.9995. The linear equation was employed to quantify the amounts of NAG produced after one-day enzymatic digestion in samples A and after complete digestion in samples B. The degradation rates of the three hydrogels  $X_4$ ,  $X_5$  and  $X_6$  were then evaluated by calculating the percentage of NAG in samples A to the total amounts of NAG in samples B. Table 3.2 demonstrates the degradation rates of  $X_4$ ,  $X_5$  and  $X_6$  and their average value:

**Table 3. 2** Degradation rates of samples  $X_4$ ,  $X_5$ , and  $X_6$  obtained from the colorimetric method. The average degradation rate with 95% confidence interval equaled to  $63..3\% \pm 13.9$  (w/w)

Sample	Amount of (NAG) in samples (A) extracts.	Amount of (NAG) in samples (B) extracts	Degradation rate (A/B) X 100
$X_4$	17.8 mg	27.3 mg	65.2 %
$X_5$	16.4 mg	28.7 mg	57.0 %
$X_6$	17.4mg	25.7 mg	67.7 %

The limit of detection was also evaluated in accordance with y-residuals of the regression line and found to be  $5.4 \mu\text{g}/\text{ml}$ . The method recovery was varied at 75.4% for  $X_4$ , 94.2% for  $X_5$ , and 79.7 % for  $X_6$ .

### 3.2.5.3 Weight loss

The degradation rates of hydrogels  $X_7$ ,  $X_8$ , and  $X_9$  were calculated in term of the percentage of weight loss over one-day enzymatic digestion by hyaluronidase. The results are shown in table 3.3.

**Table 3. 3** Degradation rates of samples  $X_7$ ,  $X_8$ , and  $X_9$  obtained from the weight loss method. The average degradation rate with 95% confidence interval =  $73..4\% \pm 5.7$  (w/w)

Sample	Initial weight	Remaining weight after one-day enzymatic digestion	Weight lost	Degradation rate = (weight lost)/(Initial weight) x 100%
$X_7$	5.0 g	1.2 g	3.8 g	76%
$X_8$	5.0 g	1.37 g	3.63 g	72.6%
$X_9$	5.0 g	1.42 g	3.58 g	71.6%

### 3.2.6 Discussion

The chromatographic measurements showed only a single large peak which is possibly attributed to the variation in hydrodynamic radius of HA fragments. However, the HPLC method proved its reliability and reproducibility for quantification of the total amount of *N*-acetyl glucosamine NAG in cross-linked hydrogels. A nine-point calibration curve was constructed by plotting peak areas vs. concentrations of standards having correlation coefficient  $R^2$  of 0.998. A linear response was obtained for injections between 20 $\mu$ g/ml to 300  $\mu$ g/ml. The average degradation rates obtained from the HPLC method was 62.6%  $\pm$ 12.3 w/w. Similarly, the colorimetric method was as reproducible as HPLC method. It could quantify the total amount of *N*-acetyl glucosamine in the cross-linked hydrogels with an average degradation rate of 63.3 $\pm$ 13.9 w/w. The colorimetric method showed also a good linearity  $R^2=0.9995$  within a wide range concentrations of hyaluronic acid (20  $\mu$ g/ml to 400 $\mu$ g/ml). On other hand, the weight loss method showed a higher degradation rate and a lower confidence interval 73.4%  $\pm$  5.7 w/w. This high rate was probably due to some error associated when sample quantity and balance were considered. A portion of remaining solid could also be lost during sample treatment process (e.g. digestion, filtration or drying steps) and that led to a higher degradation rate value. Fig.3.5 shows a column chart with error bars of the average degradation rates obtained from the three analytical methods:

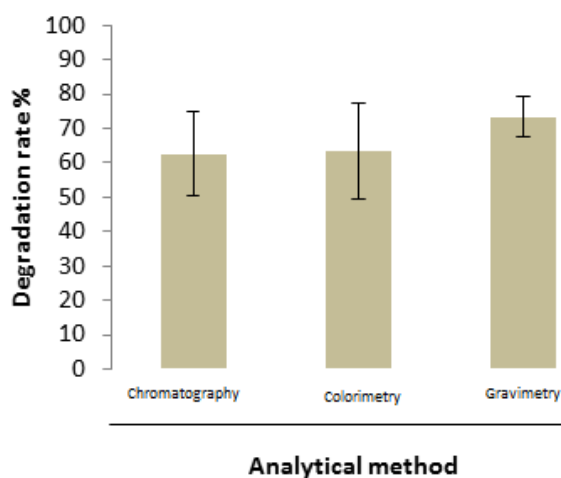


**Figure 3. 5** Average degradation rates obtained from the three analytical methods with the 95% confidence interval

In general, the 95% confidence intervals around the average degradation rates of the three methods were large and showed high uncertainty. These results could be due to the insufficient sample size ( $n=3$ ) used for each method or to the spatial inhomogeneity of the network in each hydrogel. Despite the controlled parameters over the course of synthesis and purification, hydrogels can be subjected to various environmental conditions or any external stimuli and they always exhibit an inhomogeneous cross-link density distribution. The irregular distribution of cross-linking density throughout the hydrogel explains the existence of some regions with more or less rich in cross-linking density. This factor can dramatically affect the hydrogel strength and its degradation rate. This behavior is probably interpreted as some samples were cut from a higher polymer concentration (densely cross-linked region) and some from a lower polymer concentration (loosely cross-linked region). According to the analysis of one-way ANOVA test, the degradation rate obtained from the conventional gravimetric method was significantly different from the degradation rates obtained from the chromatographic and colorimetric methods ( $P < 0.05$ ,  $n=3$ ). Although the colorimetric method does appear to have a slightly higher average degradation rate than the chromatographic method and even lower detection limit, a t-test was applied and showed that there was no significant difference between the rates of the two methods. The large confidence interval of chromatographic method %R.S.D = 7.27 and colorimetric method % R.S.D of 8.84 compared to the gravimetric method % R.S.D of 3.13 could be explained to the higher sensitivity of HPLC and UV-Visible spectrophotometer for detecting the NAG groups. The significant advantage of the HPLC and colorimetric methods developed in our work was that the two methods worked efficiently with all HA-BDDE fragments generated by hyaluronidase regardless their sizes or molecular weights. The two methods were also able to detect very low amount of HA-BDDE fragments obtained after one-day enzymatic digestion with hyaluronidase. Finally, although that RP-HPLC method proved its reliability and reproducibility for quantification of NAG in BDDE-HA hydrogels, the application of chromatographic method in the evaluation of the degradation rate of hydrogels with various degrees of cross-linking becomes tedious and more challenging, particularly, if the degradation test is held in different days or intervals.



The physicochemical properties of HA and the digestion process could also affect resolution, separation and retention time. If the stationary phase becomes saturated or blocked over the course of analysis, that will lead to a variation in the retention time. The retention time also experiences a drift with increased HA content. As the amount of HA fragments increases, they stay longer in the column and thus, has a slower retention time. Due to the silanol groups found in silica or the chemical interaction between the polar mobile phase and non-polar stationary phase, the native HA and cross-linked HA are mostly eluted with peak tailing. The strongly acidic silanol groups work as cation-exchange sites for ionized bases of HA fragments. Chromatograms of this phenomenon are demonstrated in detail in the (*appendix 4*). In contrast, the colorimetric method exhibits simplicity and less time-consuming. In term of cost, the colorimetric method was also less expensive and did not introduce chemicals with the exception of Ehrlich's reagent. Therefore, we selected the colorimetric method in our work for the quantification of the amount of NAG content in the non-digested fraction of all prepared hydrogels. The results of colorimetric method, standard solutions and recovery are all demonstrated in (*appendix 5*).

### **3.4 Conclusion**

Evaluation of HA-BDDE degradation rate becomes a criterion for an appropriate expression for the extent of cross-linking efficiency. In this chapter, three analytical methods were developed for the evaluation of HA degradation: HPLC, UV-Visible spectroscopy and weight loss. The results showed that the chromatographic and colorimetric methods exhibited good linearity and reproducibility with correlation coefficients  $R^2$  of 0.998 and 0.9995 respectively. Recoveries were estimated as an average of the three measurements which yielded 81.0% for HPLC and 83.1% for UV-Visible spectroscopy. They also showed good detection limits of 6.4 $\mu$ g/ml for HPLC and 5.4  $\mu$ g/ml for UV-Visible respectively. To sum up, the chromatographic and colorimetric methods were both reliable for quantification of NAG content. However due to simplicity and sensitivity of the colorimetric method, we selected the colorimetric method for the evaluation of *in-vitro* degradation for all prepared BDDE-HA hydrogels in our study.

## CHAPTER 4

### 4. Reaction time, pH and temperature

#### 4.1 Introduction

Due to the chemical and physical structure of HA, it was hypothesized that the experimental parameters such as reaction time, pH, and temperature, HA initial concentration, HA molecular and mixing approach might have potential impacts on increasing chemical and physical interaction (cross-linking efficiency) between HA and BDDE. Study of the effect of each experimental factor is very important in order to determine the most influencing factor on cross-linking efficiency. Enhancement of cross-linking efficiency of HA hydrogel without exploiting further quantities of BDDE needs sequential studies. The optimum conditions obtained from the former studies are incorporated in the method conditions of the following studies. In this chapter, we studied the effect of three significant factors that have a significant correlation with chemical reaction ; reaction time, pH and temperature.

#### 4.2 Reaction time

##### 4.2.1 Materials

Sodium salt of hyaluronic acid with an average molecular weight 1,000,000 Da. BDDE, hyaluronidase (solid powder with an activity of 3000 U/mg). Ehrlich's reagent, phosphate buffer saline (PBS) and alkaline solution.

##### 4.2.2 Synthesis

A total of six BDDE-HA hydrogels were prepared by mixing 1.2 g HA with 200  $\mu$ l BDDE in 10 ml basic solution (pH 13). The solutions were allowed to mix at room temperature for different reaction times as shown in table 4.1.

When cross-linking process was complete, the solutions were neutralized with 0.1M HCl. As previously described in section 2.2.2, all hydrogels were then purified by dialysis tubes, lyophilized and then kept at 8 °C until measurements and characterization. The cross-linking efficiency of each formed hydrogel was estimated by measuring the *in-vitro* degradation rate using the colorimetric method and the swelling ratio.

**Table 4. 1** BDDE-HA hydrogels prepared at various reaction time

Hydrogel	BDDE con	HA con	pH	Tem	Time
1	2.0 % (v/v)	12 % (w/v)	13	25 °C	30 min
2	2.0 % (v/v)	12 % (w/v)	13	25 °C	1 h
3	2.0 % (v/v)	12 % (w/v)	13	25 °C	2 h
4	2.0 % (v/v)	12 % (w/v)	13	25 °C	4 h
5	2.0 % (v/v)	12 % (w/v)	13	25 °C	8 h
6	2.0 % (v/v)	12 % (w/v)	13	25 °C	24 h

## 4.2.3 Measurements

### 4.2.3.1 *In-vitro* degradation rate

Five equivalent samples A, B, C, D and E from each prepared hydrogel were cut and placed in separate test tubes (the total was 30 samples). Each sample was mixed with 500 µl of hyaluronidase (BTH) with an activity of 300 units /ml in 10 ml phosphate buffer saline (PBS) solution. Samples “A” were kept for one day of treatment whereas samples “ B, C and D ” were treated for 2, 3 and 4 days respectively. Samples “E” were left with hyaluronidase until complete digestion. The enzymatic reaction was then stopped by heating each test tube in boiling water for 5 min. The resulting extracts were centrifuged and the supernatants were transferred into 10 ml volumetric flasks and diluted up to the mark. Approximately 1.0 ml from each filtrate was mixed with 0.1 ml of 0.25 M sodium carbonate and then boiled for 1 min in a water bath. Amounts 6:1 of glacial acetic acid and Ehrlich's reagent were added to the filtrates and left until the violet color was produced and reached its maximum intensity. The *in-vitro* degradation rate for each sample was expressed as the % NAG remaining in the non-digested fraction according to the following equation:

$$\text{Remaining NAG} = (C_{\text{NAG}} - P_{\text{NAG}}) / C_{\text{NAG}} \times 100\% \dots\dots\dots \text{Eq. 4.1}$$

Where  $C_{\text{NAG}}$  represents NAG content after complete degradation while  $P_{\text{NAG}}$  represents NAG content after first, second, third and fourth day of treatment.

#### 4.2.3.2 Swelling ratio

Swelling measurements were carried out through gravimetric method using 4-decimal point analytical balance from Adam Equipment Inc. (USA). Equivalent aliquots from cross-linked hydrogels were cut and immersed in distilled water and phosphate buffer saline (PBS). The samples were allowed to swell until equilibrium state and then removed, excess of water was removed by absorption paper. The samples were then re-weighed and the equilibrium weight swelling ratio was calculated as following:

$$\text{Swelling ratio (g/g)} = W_s / W_d \dots\dots\dots \text{Eq.4.2}$$

Where  $W_s$  is the weight of swollen-sample at equilibrium state and  $W_d$  is the weight of initial lyophilized sample.

#### 4.2.4 Statistics

Each analysis was carried out at least three times and the results were analyzed by ANOVA single factor and Student's t-test. Significance was accepted with  $P < 0.05$ . The results were expressed as mean  $\pm$  95% confidence interval.

#### 4.2.5 Results and discussion

##### 4.2.5.1 *In-vitro* degradation rate

The (*appendix 6.1*) summarizes the amount of NAG remaining in the solid parts of the cross-linked hydrogels after incubating with hyaluronidase for four consecutive days. The results revealed that the reaction time had a noticeable effect on the degradation rate of hydrogels prepared at duration less than 2 h. However, hydrogels prepared at reaction times longer than 2 h showed no significant difference ( $P > 0.05$ ,  $N=3$ ).

This meant that, the chemical modification lasting for more than 2 h did not enhance cross-linking efficiency, and so generated hydrogels with similar resistance toward enzymatic digestion. Based on these data, we could hypothesize that the cross-linking reaction between HA chains and BDDE molecules was completed at a time equaled approximately 2 h. The fast degradation rate observed with the hydrogels prepared in 30 min and 1 h, particularly on the first two days indicated that their reaction times were not long enough to construct effective cross-linked networks. Fig. 4.1 shows the degradation profiles of hydrogels prepared at different reaction times.

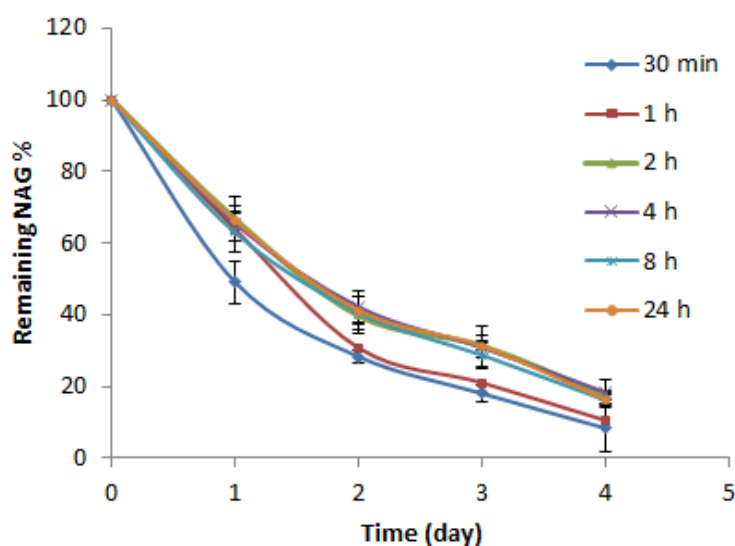


**Figure 4. 1** Degradation profiles of BDDE-HA hydrogels prepared at different reaction time, plotted as a function of time with the 95% confidence interval

#### 4.2.5.2 Swelling ratio

Swelling ratio is a fundamental feature characterizing cross-linked HA hydrogel where it forms one of the most important factor for the biomaterials used in medical application. The water-absorption ability forms a basic requirement in soft tissue augmentation and dermal fillers. Regardless of reaction duration, all hydrogels showed a remarkable affinity towards water. The (*appendix 7.1*) lists swelling ratios of all cross-linked hydrogels in distilled water and phosphate buffer saline (PBS). The amount of water contents absorbed by hydrogels prepared at reaction time (2h, 4h, 8h and 24h) in distilled water were statistically not different (ANOVA test,  $P= 0.30$ ,  $N=3$ ).

The average swelling ratios of hydrogel with 30 min ( $154 \pm 15.5$  g/g) and hydrogel with 1h ( $145 \pm 4.9$  g/g) differed significantly from the average swelling ratio of hydrogel with 2h ( $136 \pm 8.0$ ),  $P= 0.006$ . It was evident that with short periods of reaction, a low densely cross-linked network was formed. The 30 min and 1 h reaction times were not enough to allow BDDE molecules to diffuse during chemical reaction or mix thoroughly with HA chains, so they yielded hydrogels with larger pores than did the longer reaction times. In fact, lower cross-linking means more water is absorbed into the hydrogel network, subsequently higher swelling ratio is obtained. On the other hand, the swelling ratios of BDDE-HA hydrogels in PBS were lower than their swelling in distilled water pointing out to the influence of ionic strength of buffer. The values of swelling ratios in PBS appeared also with no significant difference among each other, except the hydrogel with 30 min reaction time which showed a higher swelling value at  $135 \pm 8.6$  g/g than all hydrogels. In general, the results of swelling ratios were in good agreement with the results of *in-vitro* degradation rates. Both measurements suggested that modifying HA (12.0 % w/v) with BDDE (2.0 % v/v) produced less efficient cross-linked hydrogel if it was proceeded in less than 2 h. Fig. 4.2 represents a bar graph of swelling ratios of cross-linked hydrogels in distilled water and PBS.

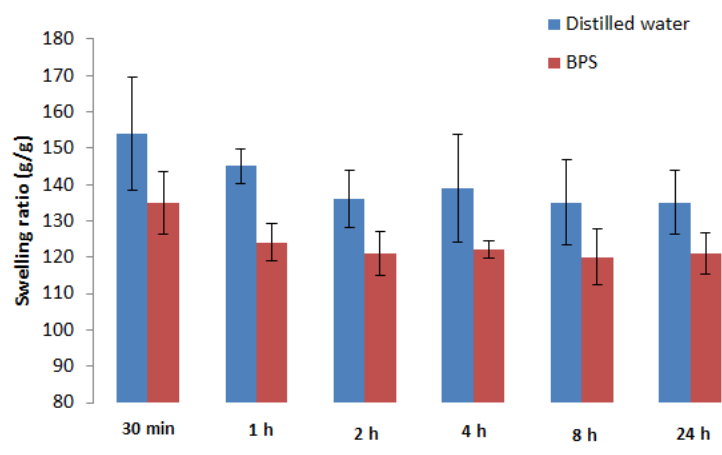


**Figure 4. 2** A bar graph represents swelling ratios (g/g) of BDDE-HA hydrogels with 95% confidence intervals prepared at different reaction times .

## 4.3 pH

### 4.3.1 Materials

{As stated in section 4.2.1}

### 4.3.2 Synthesis

Four BDDE-HA hydrogels were prepared by mixing 1.2 g HA with 200  $\mu$ l BDDE solution. The hydrogels were prepared at different pH range; three of them in basic medium and one in acidic medium as illustrated in table 4.2. The solutions were allowed to mix at room temperature for 2 h. As previously described, all hydrogels were then neutralized, purified by dialysis tubes, lyophilized and then kept at 8  $^{\circ}$ C until measurements and characterization. The cross-linking efficiency of each formed hydrogel was estimated by measuring the *in-vitro* degradation rate using the colorimetric method and the swelling ratio.

**Table 4. 2** BDDE-HA hydrogels prepared at various pH number

Hydrogel	BDDE con	HA con	pH	Tem	Time
1	2.0 % (v/v)	12 % (w/v)	13	25 $^{\circ}$ C	2 h
2	2.0 % (v/v)	12 % (w/v)	11	25 $^{\circ}$ C	2 h
3	2.0 % (v/v)	12 % (w/v)	9	25 $^{\circ}$ C	2 h
4	2.0 % (v/v)	12 % (w/v)	3	25 $^{\circ}$ C	2 h

### 4.3.3 Measurements

#### 4.3.3.1 *In-vitro* degradation rate

Equivalent portions from cross-linked hydrogels were cut and incubated with hyaluronidase in PBS solution for different intervals: 1, 2, 3 and 4 days. The enzymatic reactions were then stopped by heating each solution in boiling water for 5 min. The amount of *N*-acetyl glucosamine (NAG) found in each extract was quantified using the colorimetric method. The degradation rates of all samples were plotted as a function of time using the equation 4.1 described in section 4.2.3.1

#### 4.3.3.2 Swelling ratio

Equivalent portions from cross-linked hydrogels were immersed in distilled water and phosphate buffer saline (PBS) until equilibrium state. Measurements were carried out as described in section 4.2.3.2.

#### 4.3.4 Statistics

{As stated in section 4.2.4 }

#### 4.3.5 Results and discussion

##### 4.3.5.1 *In-vitro* degradation rate

The average amounts of NAG remained in the non-digested parts of cross-linked hydrogels prepared at different pH numbers are shown in the (*appendix 6.2*). According to the results, hydrogel degradability was increased with the decrease of pH with the exception of hydrogel 4 (pH 3) that showed a higher resistance against enzymatic digestion than hydrogel 2 (pH 11) or hydrogel 3 (pH 9). The reason beyond this could be referred to the reactive groups involved in the chemical reaction. At very strong basic conditions, the cross-linked BDDE-HA hydrogel worked as an inhibitor for the enzyme attack, because most of hydroxyls or the reactive groups are chemically blocked, thus the testicular hyaluronidase failed to cleave the ether linkage. On the other hand, the carboxylic group of glucuronic acid in the HA backbone acts as an activation centre for hyaluronidase attack. However, this centre could be blocked, if modification reaction was performed in acedic condition due to the formation of ester bonds between HA chains and BDDE molecules. Fig. 4.3 displays the degradation profiles of BDDE-HA hydrogels prepared at different pH medium.



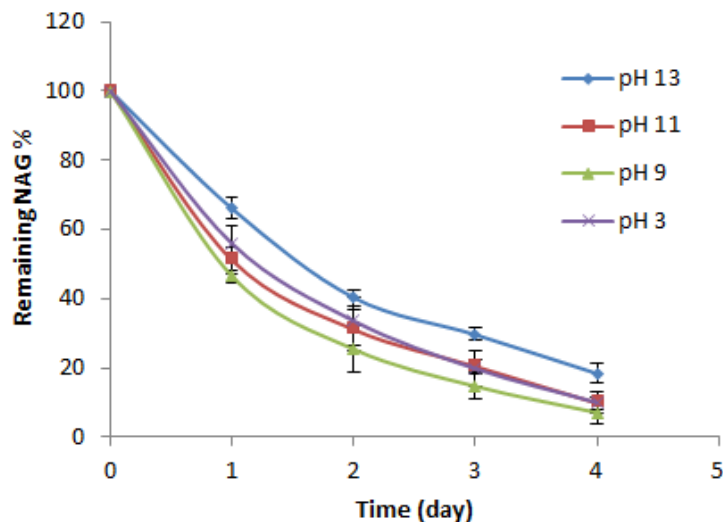


**Figure 4. 3** Degradation profiles of BDDE-HA hydrogels prepared at different pH number, plotted as a function of time with the 95% confidence interval

#### 4.3.5.2 Swelling ratio

The (*appendix 7.2*) demonstrates the swelling ratios of formed hydrogels prepared at different pH (13, 11, 9 & 3). Based on the results, the pH medium had also a noticeable influence on swelling ratios of the cross-linked hydrogels. It was shown that the hydrogel prepared at a very strong basic medium produced a high efficient cross-linked network, subsequently absorbed less water than those prepared at lower range. However, the chemical modification occurred at low pH or acidic reaction medium (pH 3) increased the formation of cross-linked network and relatively exhibited a lower swelling ability than the chemical modifications occurred at pH 9 or pH 11 reaction medium. Swelling of hydrogels in PBS provided a further evidence for the influence of pH in the cross-linking efficiency. Due to the effect of ionic strength, the hydrogels absorbed lower amounts of water and each hydrogel expanded to a lower extent than its expansion in distilled water. These data clearly supported the data of *in-vitro* degradation rates, the cross-linking efficiency was decreased with the decrease of pH number in the basic range. Fig 4.4 shows a bar graph for the swelling ratios of formed hydrogels in distilled water and PBS.

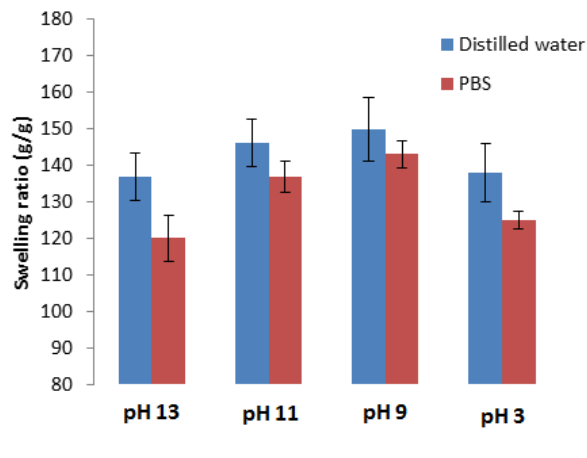


**Figure 4. 4** A bar graph represents swelling ratios (g/g) of BDDE-HA hydrogels with 95% confidence intervals prepared at different pH number .

## 4.4 Temperature.

### 4.4.1 Materials

{As stated in section 4.2.1 }

### 4.4.2 Synthesis

Six BDDE-HA hydrogels were prepared by mixing 1.2 g HA with 200  $\mu$ l BDDE in 10 ml basic solutions (pH 13). The solutions were allowed to mix for 2 h at different temperatures as demonstrated in table 4.3. As previously described, all hydrogels were then neutralized, purified by dialysis tubes, lyophilized and then kept at 8  $^{\circ}$ C until measurements and characterization. The cross-linking efficiency was also evaluated by measuring the *in-vitro* degradation and swelling ratio.

**Table 4. 3** BDDE-HA hydrogels prepared at various temperature

Hydrogel	BDDE con	HA con	pH	Tem	Time
1	2.0 % (v/v)	12 % (w/v)	13	25 $^{\circ}$ C	2 h
2	2.0 % (v/v)	12 % (w/v)	13	30 $^{\circ}$ C	2 h
3	2.0 % (v/v)	12 % (w/v)	13	35 $^{\circ}$ C	2 h
4	2.0 % (v/v)	12 % (w/v)	13	40 $^{\circ}$ C	2 h
5	2.0 % (v/v)	12 % (w/v)	13	45 $^{\circ}$ C	2 h
6	2.0 % (v/v)	12 % (w/v)	13	50 $^{\circ}$ C	2 h

### 4.4.3 Measurements

#### 4.4.3.1 *In-vitro* degradation rate

Equivalent portions from cross-linked hydrogels were cut and incubated with hyaluronidase solution for different intervals: 1, 2, 3 and 4 days. The enzymatic reactions were then stopped by heating each solution in boiling water for 5 min. The amount of *N*-acetyl glucosamine (NAG) found in each extract was quantified using the colorimetric method. The degradation rates of all samples were plotted as a function of time using the equation 4.1 described in section 4.2.3.1

#### 4.4.3.2 Swelling ratio

Equivalent portions from cross-linked hydrogels were immersed in distilled water and phosphate buffer saline (PBS) until equilibrium state. Measurements were carried out as described in section 4.2.3.2.

### 4.4.4 Statistics

{As stated in section 4.2.4 }

### 4.4.5 Results and discussion

#### 4.4.5.1 *In-vitro* degradation rate

The effect of temperature on hydrogel's resistance against enzymatic decomposition was investigated. Within the entire range of tested temperatures, none of cross-linked hydrogels showed complete degradation. Generally, the results showed that the degradation rate was decreased with the increase of temperature from 25 °C to 40 °C and then increased at 45 °C with no significant difference. The hydrogel prepared at temperature above 45 °C exhibited lower resistance towards hyaluronidase and appeared to degrade much faster than hydrogels prepared at lower temperature. The slowest degradation rate was observed for hydrogel prepared at 40 °C with an average remaining NAG at 65.9 % ± 4.6 on the first day of incubation followed by the hydrogel prepared at 35 °C which showed an average remaining NAG at 65.2 % ± 4.7.

It was noted that the NAG content in the non-digested fraction was increased by almost 1- 4 % for every 5 °C increase in the temperature from hydrogel 1 to hydrogel 4. Possible reason for this: by increasing the temperature, the HA chains move faster and entangle more frequently, subsequently more conformation and entanglements are formed. The effect of increased temperature may also lead to a more collision between HA chains and BDDE molecules that enhance the occurrence of chemical modification. However, this theory does not apply at all reactions, reactions exposed to a very high temperature (e.g. 45 °C and 50 °C) could form mass agglomerate or lead to irregular distribution of cross-linking density. The hydrogel scaffold will then show less restriction towards hyaluronidase invasion. Fig. 4.5 displays a graph showing the degradation profiles of the hydrogels prepared at different temperature. The (*appendix 6.3*) illustrates the remaining NAG amounts of all these hydrogels.

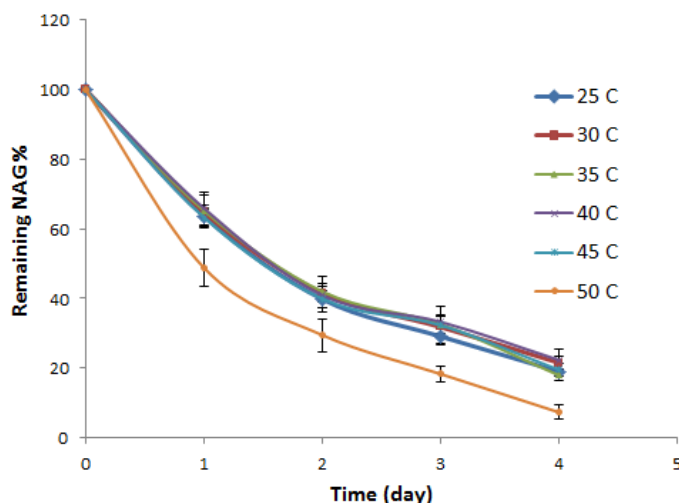


**Figure 4. 5** Degradation profiles of BDDE-HA hydrogels prepared at different temperature, plotted as a function of time with the 95% confidence interval

#### 4.4.5.2 Swelling ratio

The swelling capacity of formed hydrogels was slightly decreased with the increase of reaction temperature from 25 °C to 45 °C and then showed a rapid decrease at 50 °C. All hydrogels showed a lower water absorption ability in PBS than in distilled water with more effective ionic strength on hydrogel prepared at 50 °C.

In general, the swelling ratios were ranged from a maximum value observed at  $139 \pm 4.9$  g/g in water and  $128 \pm 3.8$  g/g in PBS for the hydrogel 1 and a minimum value observed at  $120 \pm 11.7$  g/g in water and  $112 \pm 7.5$  g/g in PBS for the hydrogel 6. Excluding the swelling ratios of hydrogels 5 and 6, the results of swelling ratios were consistent with the results of degradation rates and confirmed that the cross-linking efficiency was increasing with the increase of temperature, and thus higher tightness and strength (lower degradation rate and swelling) were exhibited. As illustrated in the (*appendix 7.3*), the swelling ability was decreased by almost 2.0 % corresponding to the 5.0 % increase in the temperature of reaction medium. Moreover, the inconsistent values observed between the swelling ratio and degradation rate of hydrogels 5 and 6 were not correlated to the cross-linking efficiency rather than the network collapse or loss of hydration that probably hardened the polymer matrix. Therefore despite their rapid degradation, particularly the hydrogel with 50 °C, they showed lower ability of swelling. Furthermore, the 95% confidence intervals observed around the average swelling ratio of hydrogel 6 was very large compared to the other hydrogel, this high uncertainty level reflected some inhomogeneity or rigidity occurred within hydrogel matrix during the chemical modification. Fig.4.6 demonstrates a bar graph of the swelling ratios of cross-linked BDDE-HA hydrogels prepared at different temperature.

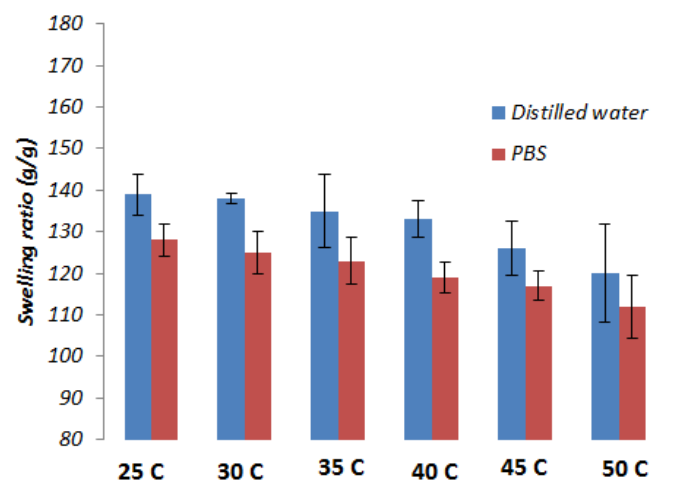


**Figure 4. 6** A bar graph represents swelling ratios (g/g) of BDDE-HA hydrogels with 95% confidence intervals prepared at different temperature.

## 4.5 Conclusion

A series of HA hydrogels cross-linked with BDDE were prepared at different reaction time, pH and temperature. The *in-vitro* degradation profile and swelling ratio were measured to evaluate the cross-linking efficiency of each cross-linked hydrogel. The results revealed that by increasing the reaction time from 30 min to 2 h, the cross-linking efficiency increased (slower degradation rate and lower swelling ability). The chemical reaction lasted more than 2 h, produced hydrogels with no significant effect on hydrogel degradation or swelling capacity. The hydrogels prepared at different pH showed also different cross-linking efficiency. By decreasing the pH from 13 to 9, the cross-linking efficiency declined. However if the chemical reaction was performed in acidic medium (pH 3), a more efficient cross-linked network than those obtained with pH 9 and pH 11 was observed. The temperature had also a noticeable effect on cross-linking efficiency of BDDE-HA hydrogels. Roughly the temperature ranged between 25 °C and 45 °C formed an ideal heated medium for cross-linking reaction, the 40 °C was probably the most ideal. Based on above conclusion, we adopted the following method conditions on our subsequent works: reaction time 2h, pH > 12 and temperature 40 °C.

## CHAPTER 5

### 5. HA initial concentration

#### 5.1 Introduction

As we stated earlier, there has been an increasing demand for HA-based hydrogels that offer advantages of lower chemical cross-linker. However, synthesis of hydrogels utilizing both low amount of chemical cross-linker and high efficient cross-link is complicated and challenging. So in this chapter we aimed to explore the effect of HA initial concentration on cross-linking efficiency of BDDE-HA hydrogel. HA initial concentration is different from the total HA concentration expressed by the manufacturers. The total HA concentration usually includes the initial HA concentration bound with the cross-linker and free HA solution which is added after chemical modification to facilitate the extrusion through fine-bore needles (Kablik et al. 2009). This free HA is easily metabolized and does not remain within hydrogel's matrix. The HA initial concentration represents the starting amount of HA powder involved in the gel formation process.

#### 5.2 HA initial concentration

##### 5.2.1 Materials

{As stated in section 4.2.1}

##### 5.2.2 Synthesis

A total of eight cross-linked BDDE-HA hydrogels were prepared by mixing 0.7, 0.8, 0.9, 1.0, 1.1, 1.2, 1.3, and 1.4 g of HA powder with 10 ml basic solution (0.25M NaOH) containing 200  $\mu$ l (2.0 % v/v) of BDDE.

So, the added quantities of HA formed various initial concentrations equaled to 7.0 %, 8.0 %, 9.0 %, 10.0 %, 11.0 %, 12.0 %, 13.0 %, and 14.0 % (w/v) respectively. Each mixture was allowed to mix thoroughly for 2h at 40 °C and then neutralized by adding equivalent amounts of 0.1M HCl to a pH of approximately 7.0. As previously described, all hydrogels were then purified by dialysis tubes, lyophilized and then kept at 8 °C until measurements and characterization. The cross-linking efficiencies of formed hydrogels were estimated by measuring the *in-vitro* degradation rate using the colorimetric method, the swelling ratio using gravimetric balance, surface morphology using scanning electron microscope (SEM).

### **5.2.3 Measurements**

#### **5.2.3.1 *In-vitro* degradation rate**

Equivalent portions from cross-linked hydrogels were cut and incubated with hyaluronidase in PBS solution for different intervals: 1, 2, 3 and 4 days. The enzymatic reactions were then stopped by heating each solution in boiling water for 5 min. The amount of *N*-acetyl glucosamine (NAG) found in each extract was quantified using the colorimetric method. The degradation rates of all samples were plotted as a function of time using the equation 4.1 described in section 4.2.3.1.

#### **5.2.3.2 Swelling ratio.**

Equivalent portions from cross-linked hydrogels were obtained and immersed in distilled water and phosphate buffer saline (PBS, pH = 7.4). The samples were left to reach their equilibrium states and then removed, excess water was gently dried by absorption paper. Measurements were carried out as described in section 4.2.3.2.

#### **5.2.3.3 Scanning electron microscope (SEM)**

The morphologies of cross-linked hydrogels were investigated by scanning electron microscope (SEM) from JEOL (Tokyo, Japan). Initially, the lyophilized samples were coated with platinum using an ion sputter prior to visualization process. The SEM was adjusted to obtain images in the Secondary Electron Imaging (SEI) mode with a voltage of 10 kV. All images were captured at similar conditions and magnification.



## 5.2.4 Statistics

{As stated in section 4.2.4 }

## 5.2.5 Results

### 5.2.5.1 *In-vitro* degradation tests

The (Appendix 6.4) displays the values of the *in-vitro* degradation rates of formed hydrogels with 95% confidence interval for four days incubating with hyaluronidase. Fig. 5.1 shows a graph comparing their degradation profiles over the period of treatment.

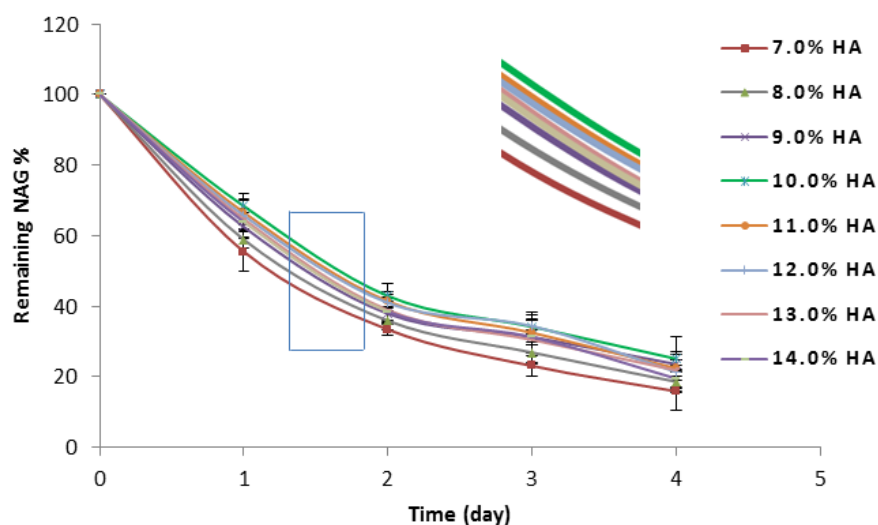


**Figure 5. 1** Degradation profiles of BDDE-HA hydrogels prepared at different HA concentrations, plotted as a function of time with the 95% confidence interval

The results verified that HA initial concentration had a substantial effect on hydrogel degradation during enzymatic incubation. A noticeable decline in the degradation rate was observed with the increasing of HA concentration from BDDE-HA hydrogel prepared at 7.0 % HA initial concentration to the hydrogel prepared at 10.0 % HA initial concentration. A slight increase in the degradation rate was then observed from the 10.0 % HA hydrogel to the hydrogel prepared at 14.0 % HA initial concentration. According to these data, the degradation rate was inversely proportional to the HA initial concentration to a certain level which was 10.0 % w/v in our experiments, and then showed a relatively opposite effect.

This meant, that the 10.0 % HA exhibited an ideal level of HA initial concentration corresponding to 2.0 % (v/v) BDDE solution. Statistically, the degradation rates of hydrogels containing low HA concentration (7.0 % 8.0 %) and high HA concentration (13.0 % and 14.0 %) showed a significant difference ( $p < 0.05$ ,  $n=3$ , ANOVA test) from the degradation rate of the 10.0 % HA hydrogel for four days incubating with hyaluronidase. However, the degradation rates of hydrogels prepared at moderate HA initial concentration (9.0 %, 11.0 % and 12.0 % ) did not differ significantly from the degradation rate of 10.0 % HA hydrogel except on last day for the 11.0 % and 12.0 % HA hydrogels and on the first two days for the 9.0 % HA hydrogel. As a comparison, the 10.0 % HA hydrogel exhibited much higher resistance against the action of enzyme than did hydrogels prepared at the lowest (7.0 %) or the highest (14.0 %) HA initial concentration, particularly on the first day of treatment. Approximately two-third of the 10.0 % HA hydrogel original NAG content ( $68.4\% \pm 1.8$ ) remained unreleased in the dry mass after one day compared to the 7.0 % or 14.0 % HA hydrogels which showed NAG remaining percentages of approximately ( $55.5 \pm 5.7$ ) and ( $63.9 \pm 2.0$ ) respectively. Furthermore, the 7.0 % and 14.0 % HA hydrogels appeared to have lost more than 80 % of their NAG contents within the whole period of treatment in comparison to the 10.0 % HA hydrogel which lost approximately 75 % after similar period.

#### **5.2.5.2 Swelling ratio**

The results of welling ratios are shown in (*appendix 7.4*) with the 95 % confidence interval, a bar graph is displayed in Fig 5.2 comparing the swelling ratios of formed hydrogels in distilled water and phosphate buffer saline (PBS). The results of the swelling ratios were in good agreement with the results of the *in-vitro* degradation tests and the 10.0 % HA-based hydrogel proved the most stable hydrogel. The results confirmed that the swelling ratios of tested hydrogels in distilled water and PBS were inversely correlated with the HA initial concentration from the 7.0 % HA hydrogel to the 10.0 % HA hydrogel. Pattern was then changed and the swelling ratio was steadily increased with the increase of HA concentration until the 14.0 % HA hydrogel.

The hydrogels prepared at low (7.0 % and 8.0 %) and high (13.0 % and 14.0 %) HA initial concentration differed significantly from the 10.0 % HA hydrogel. The hydrogels with moderate HA: 9.0 %, 11.0 % and 12.0 % HA swelled to extents close to that reached by 10.0 % HA hydrogel in distilled water, however, in phosphate buffer saline (PBS), they showed different water-absorption ability. Generally, the data of swelling ratios were ranged from maximum values at  $137 \pm 7.4$  g/g in distilled water and  $127 \pm 6.2$  g/g in PBS reached by the 14.0 % HA hydrogel to minimum values at  $129 \pm 3.2$  g/g in distilled water and  $116 \pm 2.4$  g/g in PBS reached by the 10.0 % HA hydrogel.

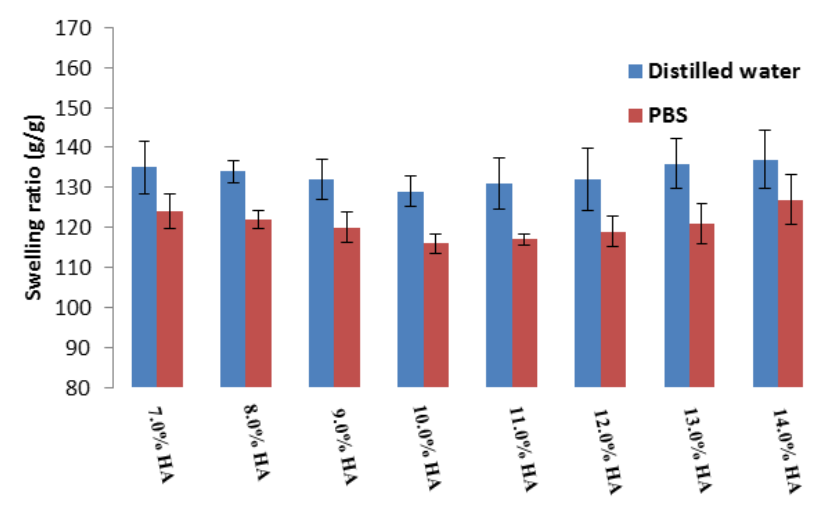


**Figure 5. 2** A bar graph represents swelling ratios (g/g) of BDDE-HA hydrogels with 95% confidence intervals prepared at different HA concentration

### 5.2.5.3 Scanning electron microscope (SEM)

The SEM images of the tested hydrogels showed different morphologies and pores-size distribution. Hydrogels with moderate HA initial concentration exhibited better network interconnection than hydrogels with low or high HA initial concentrations. The hydrogels with moderate HA initial concentration appeared with dense surface structures. In contrast, the low and high HA hydrogels showed less cross-linking density and appeared with some collapses occurred probably during the freeze-drying process. The hydrogels with moderate HA had also narrower pores-size distribution.

For instance, the 10.0 % HA hydrogel showed a pores-size distribution ranged in diameter from less than 50  $\mu\text{m}$  to approximately 300  $\mu\text{m}$  compared to the low or high HA hydrogels which showed much wider distribution ranges. Furthermore, the hydrogels with moderate HA were more homogenous and showed more regular porous networks. Fig.5.3 illustrates SEM surface images of lyophilized hydrogels captured at similar (x100) magnification parameter using the Secondary Electron Imaging (SEI).

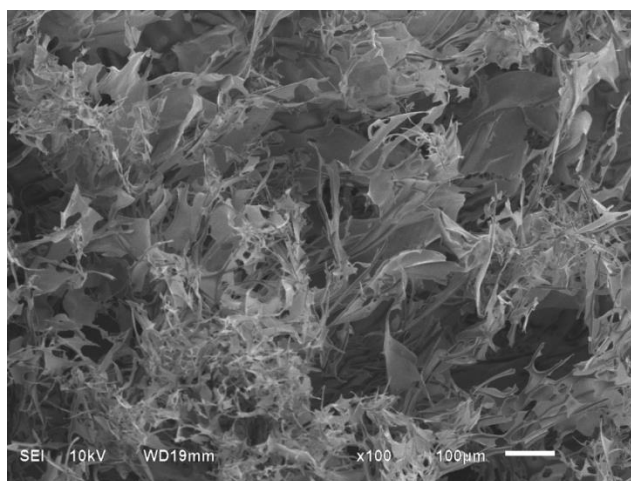


**Figure 5. 3** SEM image for lyophilized BDDE-HA hydrogel prepared at 7.0 % HA initial concentration

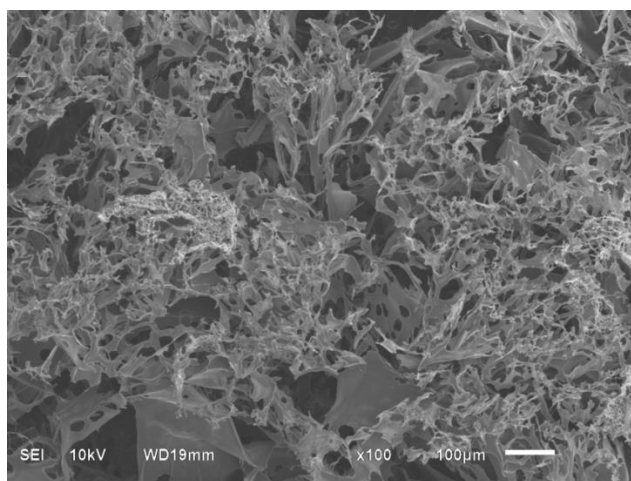


**Figure 5. 4** SEM image for lyophilized BDDE-HA hydrogel prepared at 8.0 % HA initial concentration

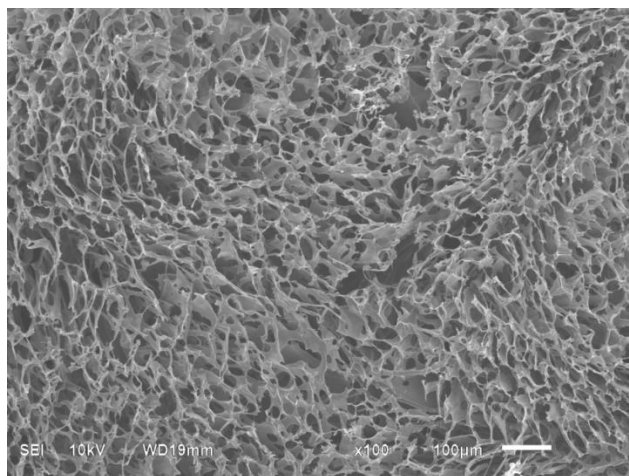


**Figure 5. 5** SEM image for lyophilized BDDE-HA hydrogel prepared at 9.0 % HA initial concentration

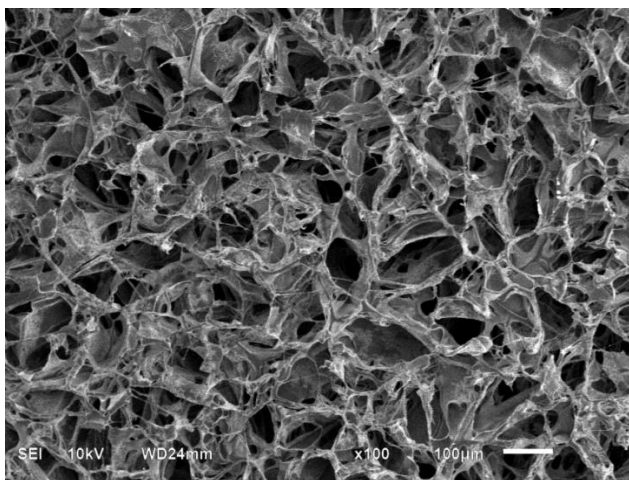


**Figure 5. 6** SEM image for lyophilized BDDE-HA hydrogel prepared at 10.0 % HA initial concentration

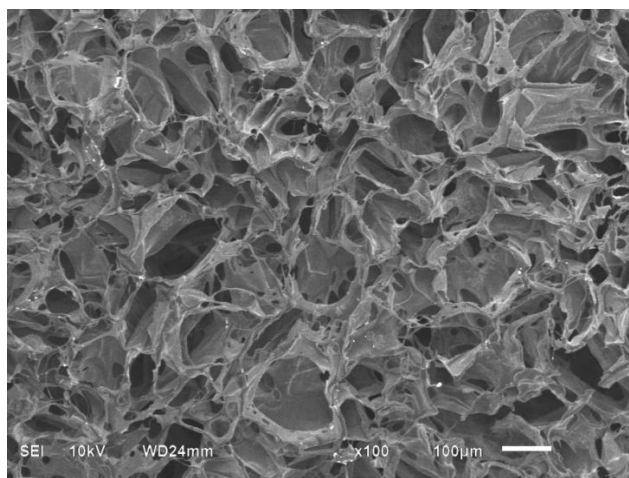


**Figure 5. 7** SEM image for lyophilized BDDE-HA hydrogel prepared at 11.0 % HA initial concentration

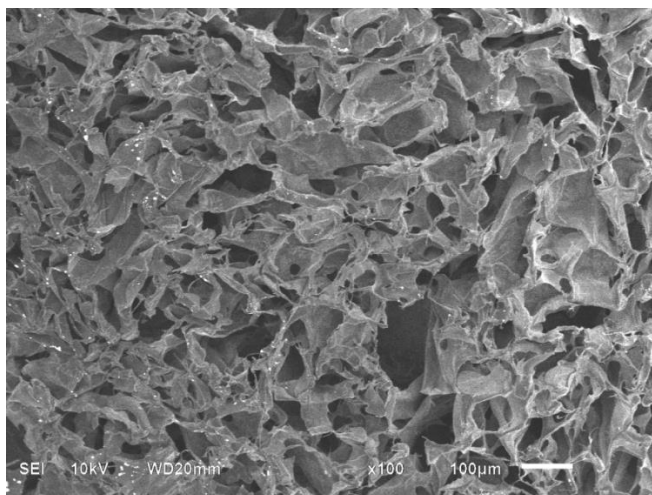


**Figure 5. 8** SEM image for lyophilized BDDE-HA hydrogel prepared at 12.0 % HA initial concentration

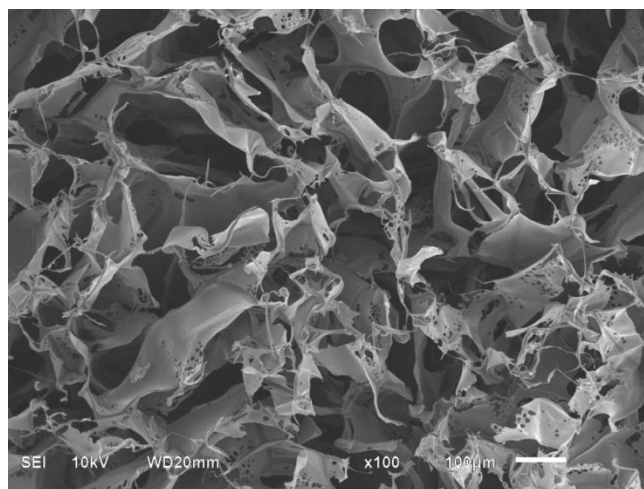


**Figure 5. 9** SEM image for lyophilized BDDE-HA hydrogel prepared at 13.0 % HA initial concentration

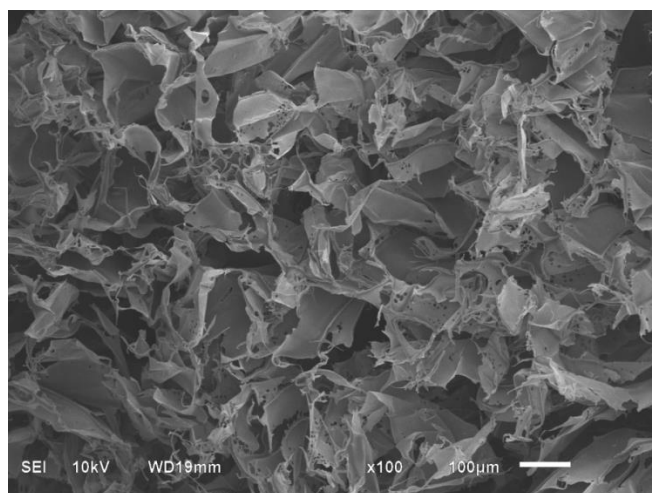


**Figure 5. 10** SEM image for lyophilized BDDE-HA hydrogel prepared at 14.0 % HA initial concentration

### 5.2.6 Discussion

As mentioned earlier, HA cross-linking is crucial for providing a chemical shield against decomposition acted by hyaluronidase and producing HA-based hydrogels with longer residence. The faster release of NAG fragments (low cross-linking efficiency) observed with the hydrogels of low HA initial concentration was more likely attributed to the insufficient quantity of HA to form covalent bridges with BDDE molecules. In contrast, the slower release of NAG fragments (high cross-linking efficiency) with the moderate HA hydrogels was resulted from an adequate abundance of HA chains within their network matrices. It was evident, that incorporation of a larger HA content in the reaction medium resulted in a more exposure of HA chains to BDDE molecules, thus more covalently ether bonds were formed. The bovine testicular hyaluronidase failed then to cleave such linkages. By increasing HA concentration, the distance between HA chains become even shorter and the probability of BDDE molecules to bind with HA chains becomes larger. This phenomenon could also be assigned to the physical cross-linking occurred between polymer chains as a resultant of increased HA contents. As stated, HA is a linear polymer, however, in solution it shows extensive intermolecular hydrogen bonding that induce distinctive secondary (helical) and tertiary (coiled coil) interactions (Prestwish et al. 1998; Scott et al. 1989). At high HA concentration, the chains show greater entanglements and self-association of HA random coils in solution which relatively work as an enzyme-attack inhibitor. The larger HA concentration, the larger quantity of HA “monomer unit” available in the reaction medium, subsequently higher tendency of HA chains to entangle. Furthermore, studies suggest that the hydrogel stiffness may be affected by the HA viscoelasticity; a rheological characteristic depending also on HA concentration and chains cross-linking (measurements were not carried out in this chapter). The hydrogen bonding between adjacent chains occur electrostatic repulsion between the carboxylic groups, subsequently the HA network is stiffened (Fakhari and Berklund 2013; Necas et al. 2008; Vejlens 1971). Although the occurrence of physical cross-linking as opposed to the chemical cross-linking is not entirely clear during the synthetic method, the HA concentration is postulated to play a significant role in the HA-HA polymer interconnection.

However, if HA initial concentration has exceeded moderate level, the cross-linking efficiency weakens and the hydrogels start to degrade faster. Possible reason for this; the excess amount of HA in reaction medium will lack the BDDE molecules and form viscous aggregates. High HA concentration may restrict reaction movement or prevent HA powder to disperse thoroughly within the reagent solution. In addition, it may lead to inhomogeneity or irregular distribution of cross-linking density throughout hydrogel matrix, subsequently, different densely regions are generated. In our experiments, the solutions exposed to high HA content (13.0 % and 14.0 % HA) were more viscous and had slower gelation reaction than those mixed with moderate HA content. The results of swelling ratios supported the results of *in-vitro* degradation rates. All tested hydrogels showed remarkable affinities towards water and swelled to various extents depending on their cross-linking efficiencies. Due to the effect of ionic strength, the hydrogels in PBS expanded to lower extents than their expansions in distilled water. Generally, it has been described that, the increase of cross-linking results in decrease water content ([Cardoso et al. 2014](#)). The cross-linking efficiency usually determines the overall swelling of cross-linked hydrogel and penetration depth of water into hydrogel matrix, so it has a significant influence on the equilibrium state between extension and retraction forces. Comparing to the swelling ratios of low and high HA hydrogels, the hydrogels prepared at moderate HA initial concentration (9.0 % - 12.0 %) showed a limitation on the extent to which they could swell due to the large formation of chemical cross-linkages between HA chains and BDDE molecules, subsequently they could not preserve a good water up-take ability. Moreover, the larger HA-HA entanglements occurred in the moderate HA hydrogels were proposed to contribute on the elastic network retraction force that oppose additional swelling and thus show less swelling capacity. As shown in SEM images, the moderate HA hydrogels appeared more rigid and cohesive throughout their surface sections. They showed continuous network structures with pores being very small and more regularly distributed, these small pores allowed the polymer matrix to swell to lower ranges.



The hydrogels with low or high HA initial concentration did not show good morphology and appeared with softer surface microstructures, particularly the low HA hydrogels. They had weak scaffolds and large pores allowing more water to be absorbed into the hydrogels matrices, subsequently higher swelling ratios were obtained. Furthermore, the low and high HA hydrogels were less homogenous and their cross-linking densities were irregularly distributed, such inhomogeneity weakens the network structure of cross-linked hydrogel and contributes in the rise of swelling capacity. The high uncertainty level or wider 95% confidence intervals observed around the average swelling ratios of the 7.0 % , 13.0 % and 14.0 % HA hydrogels verified this conclusion. In fact, hydrogels with moderate initial HA concentration were more homogenous and more thoroughly mixed during gelation process.

### **5.3 Conclusion**

This chapter was aimed to study the potential effect of (HA) initial concentration on cross-linking efficiency of BDDE-HA hydrogel. The results revealed that the BDDE-HA hydrogels prepared at moderate-HA initial concentrations (9.0 – 12.0 %) exhibited higher resistance against enzymatic digestion and lower swelling ratios than those prepared at either low (7.0 % , 8.0%) or high (13.0% and 14.0 %) HA concentrations. For four days incubating with hyaluronidase, the 10.0 % HA hydrogel showed the slowest degradation rate with a significant difference ( $P < 0.05$ , t-test) to the degradation rates of 11.0 % and 12.0 % HA hydrogels on the fourth day and to the degradation rate of 9.0 % HA hydrogel on the first two days. The swelling ratio of 10.0 % HA hydrogel was significantly different with the swelling ratios of 9.0 % , 11.0 % and 12.0 % HA hydrogels in phosphate buffer saline PBS. The SEM images showed different morphologies and pore-size distribution within the entire range of tested HA concentrations. The moderate-HA hydrogels, however, were more homogeneous and appeared with narrower pore-size distribution compared to the low and high-HA hydrogels. The effect of HA initial concentration was further investigated by FTIR which confirmed that the moderate-HA hydrogels showed greater chemical modifications. In conclusion, the 10.0 % (1.0g ) HA initial concentration proved to be the idlest concentration level corresponding to the 2.0 % v/v BDDE and it was selected for the up-coming studies.

## CHAPTER 6

### 6. HA molecular weight

#### 6.1 Introduction

The HA molecular weight (Mw) is a principle parameter in the synthesis of HA hydrogels, because it reflects the number of repeating disaccharide units. As stated, the HA polymer consists of repeating disaccharides units chemically bonded into a long chain. The term “ average HA molecular weight” is usually used to express this chain length which describes the relative molecular mass of the basic disaccharide and the number of disaccharide units connected in the chain. Therefore, the objective of this chapter was to study of the effect of HA molecular weight on the cross-linking efficiency of BDDE-HA hydrogels using three types of HA molecular weights Mw (100 kDa, 1000 kDa and 2000 kDa).

#### 6.2 HA molecular weight

##### 6.2.1 Materials

Hyaluronic acid with an average molecular weights (100 kDa, 1000 kDa and 2000 kDa). Hyaluronidase (3000 U/mg), BDDE, Ehrlich's reagent, phosphate buffer saline (PBS) and alkaline solutions.

##### 6.2.2 Synthesis

Three BDDE-HA hydrogels were prepared by mixing 1.0 g HA with 200  $\mu$ l BDDE in 10 ml basic solution (pH 13). The hydrogels were prepared from different types of HA molecular weight (100 kDa, 1000 kDa and 2000 kDa). The solutions were allowed to stand at 40 °C for 2 h. When reaction was complete, the hydrogels were neutralized by 0.1M HCl and purified using dialysis tubes.

Finally they were lyophilized and kept at 8 °C for studying purpose. The cross-linking efficiencies were estimated by measuring the *in-vitro* degradation rate, the swelling ratio and rheological behavior.

## **6.2.3 Measurements**

### **6.2.3.1 *In-vitro* degradation rate**

Equivalent portions from cross-linked hydrogels were cut and incubated with hyaluronidase solution for different intervals: 1, 2, 3 and 4 days. The enzymatic reactions were then stopped by heating each solution in boiling water for 5 min. The amount of *N*-acetyl glucosamine (NAG) found in each extract was quantified using the colorimetric method. The degradation rates of all samples were plotted as a function of time using the equation 4.1 described in section 4.2.3.1.

### **6.2.3.2 Swelling ratio**

Equivalent portions from cross-linked hydrogels were obtained and immersed in distilled water and phosphate buffer saline (PBS, pH = 7.4). The samples were left to reach their equilibrium states and then removed, excess water was gently dried by absorption paper. Measurements were carried out as described in section 4.2.3.2.

### **6.2.3.3 Rheological properties**

By varying HA molecular weight, the cross-linked hydrogels show varied strength and resistance towards compression applied from surrounding. So the measurements of rheological properties of prepared hydrogels will give further evidence about the relationship between HA molecular weight and cross-linking efficiency. The rheological measurements were performed on oscillatory shear mode to determine the elastic modulus  $G'$  (storage modulus) and the viscous modulus  $G''$  (loss modulus). The measurements were carried out using ARES rheometer (TA instruments, USA) equipped with a plate and plate geometry. Initially strain sweep tests were performed at a constant frequency over strain amplitude ranged between 0.01-100 % in order to determine the linear viscoelastic region (LVR).

Small Amplitude Oscillatory Strain (SAOS) tests were then applied to analyze the storage and loss modulus over a frequency range ( $0.01-100 \text{ s}^{-1}$ ) at a constant strain selected within the linear viscoelastic region. (*Appendix 1.6* describes the principle of rheometer and the oscillatory strain test)

## 6.2.4 Statistics

{As stated in section 4.2.4 }

## 6.2.5 Results and discussion

### 6.2.5.1 *In-vitro* degradation rate

The results of *in-vitro* degradation rate revealed that the percentage of NAG remaining in the hydrogel prepared with 2000 kDa HA molecular weight was larger than the NAG remaining in hydrogels prepared with 100 kDa and 1000 kDa HA molecular weight except on the third day where the hydrogel with 1000 kDa showed almost similar NAG content of that observed in the solid fraction of hydrogel with 2000 kDa. These data presented an evidence that the degradation rate was decreased with the increase of HA molecular weight. Fig 6.1 displays a graph comparing the degradation rates cross-linked hydrogels prepared at different HA molecular weight. The graph clearly shows the influence of HA molecular weight on cross-linked hydrogels.

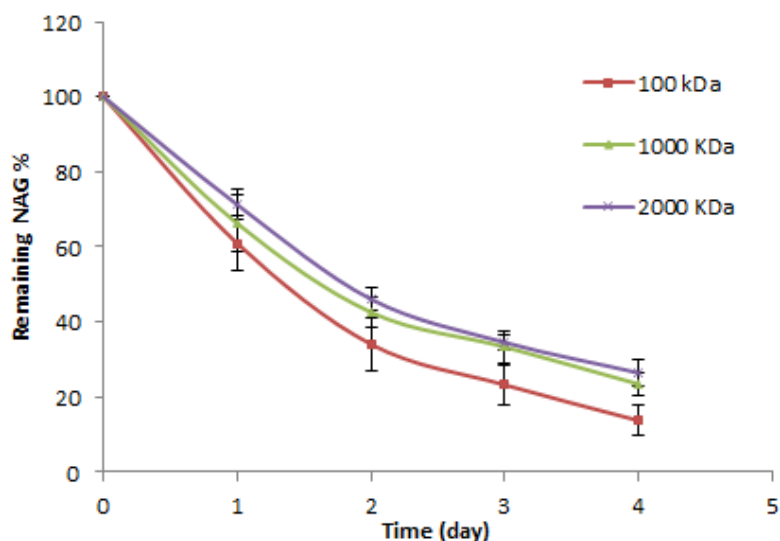


**Figure 6. 1** Degradation profiles of cross-linked hydrogels prepared at different HA molecular weight. They were plotted as a function of time with the 95% confidence interval

The influence of HA molecular weight on hydrogel stiffness could be rationalized to the number of repeating disaccharide units. Longer chain of HA monomer unit (higher molecular weight) involved in the chemical reaction promoted a larger number of hydroxyl groups to form ether bonds with BDDE. They also induced more polymer-polymer interactions and less pendants formation. Hydrogels with more chemical and physical interconnection produce less average mesh-width scaffold, subsequently they show a good ability to resist the attack of hyaluronidase. The (*appendix 6.5*) describes the relationship between the HA molecular weight and hydrogels' degradation rate.

### **6.2.5.2 Swelling ratio**

The swelling ratio (as shown in Fig. 6.2) was decreased when moving from the hydrogel prepared with 100 kDa HA molecular weight to the hydrogel prepared with 1000 kDa HA molecular weight and then showed a slight increase toward hydrogel prepared with 2000 kDa in distilled water and PBS. These data were relatively inconsistent with the *in-vitro* degradation data and showed less dependence on HA molecular weight. We stated previously that the hydrogel degradation and swelling ability were largely correlated with the cross-linking efficiency. The hydrogel synthesized at a high efficient cross-link showed a slower degradation rate and a lower swelling ability due to the hydrogel's stiffness. This inconsistency can probably be assigned to the physical structure formed in response to the different HA molecular weights or to the number of repeating disaccharide units rather than the chemical linkage occurred between the BDDE molecules and – OH groups. Despite the lower average pores-size exhibited by the hydrogel with a higher HA molecular weight, the longer HA chains had more hydrophilic sites attached to the hydrogel scaffold, and so more water was supposed to be absorbed. This probably explained why the hydrogel of 2000 kDa HA molecular weight did not show a lower swelling ratio in distilled water and PBS than hydrogel of 1000 kDa. In addition, the BDDE-HA hydrogel with a longer HA chain (2000 kDa) had probably some free HA fragments that were not released during the dialysis or purifying process. These trapped fragments did not form a limitation on the extent to which the hydrogel could swell, instead they contributed in the overall swelling and preserved a good water up-take ability. The results of swelling ratio are displayed in (*appendix 7.5*).

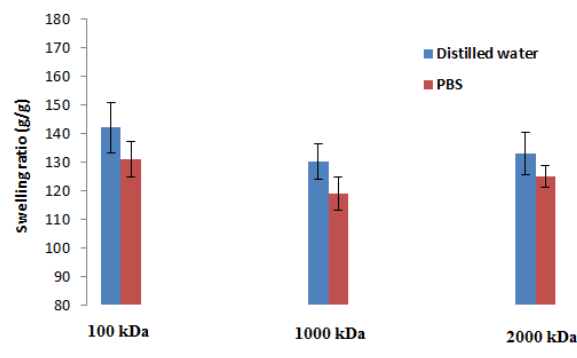


**Figure 6. 2** A bar graph represents swelling ratios (g/g) of hydrogels prepared at different HA molecular weight with the 95% confidence intervals

### 6.2.5.3 Rheological measurements

The results of rheological measurements proved that the moduli  $G'$  and  $G''$  were increased with the increase of HA molecular weight and became less dependent on the angular frequency. The storage modulus  $G'$  of hydrogel with the highest HA molecular weight is predominant over the loss modulus  $G''$  during the course of Small Amplitude Oscillatory Strain (SAOS) test. So, it shows a better viscoelastic property. It is important to note that the applied shear forces of all oscillation frequency tests felled within the linear viscoelastic range and that produced consistent data. Results of rheology were in good agreement with the results of *in-vitro* degradation rate. Figures (6.3- 6.6) demonstrate graphs presenting the rheological behavior (storage modulus, loss modulus) of native HA and cross-linked hydrogels prepared at various HA molecular weight.

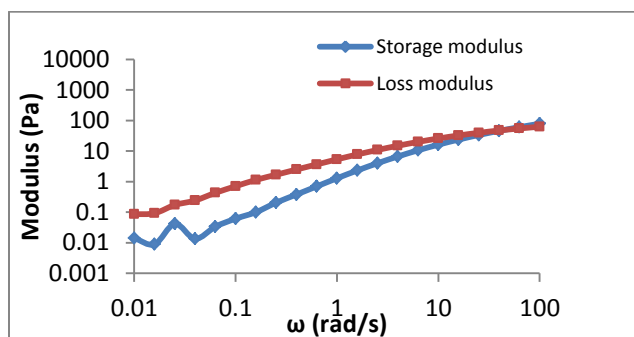


**Figure 6. 3** Storage modulus  $G'$  and Loss modulus  $G''$  (Pa) versus angular frequency in the range (0.01-100  $s^{-1}$ ) for native HA

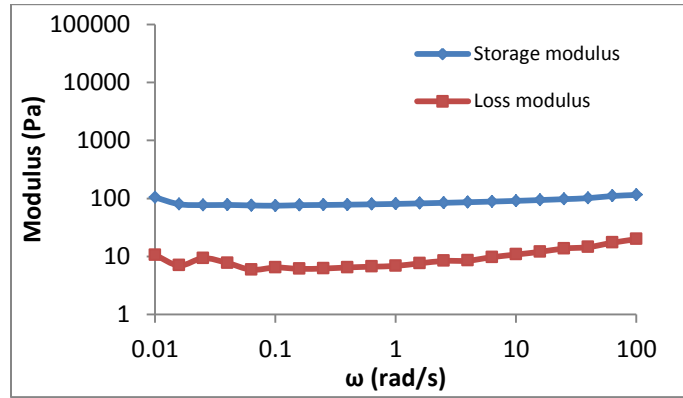


**Figure 6. 4** Storage modulus  $G'$  and Loss modulus  $G''$  (Pa) versus angular frequency in the range  $(0.01-100 \text{ s}^{-1})$  for cross-linked hydrogel prepared at 100,000 Da HA molecular weight

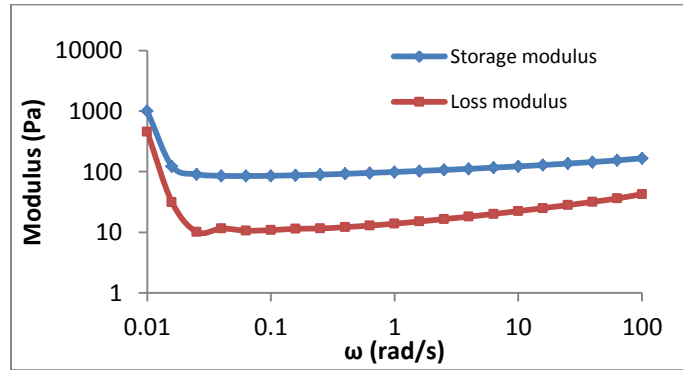


**Figure 6. 5** Storage modulus  $G'$  and Loss modulus  $G''$  (Pa) versus angular frequency in the range  $(0.01-100 \text{ s}^{-1})$  for cross-linked hydrogel prepared at 1,000,000 Da HA molecular weight

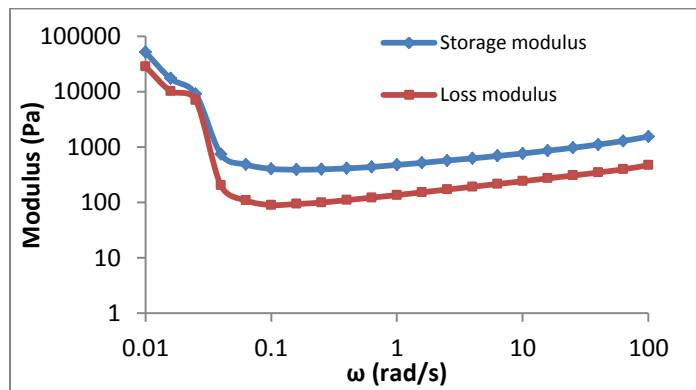


**Figure 6. 6** Storage modulus  $G'$  and Loss modulus  $G''$  (Pa) versus angular frequency in the range  $(0.01-100 \text{ s}^{-1})$  for cross-linked hydrogel prepared at 2,000,000 Da HA molecular weight

Over the course of oscillation test, the native HA did not demonstrate a viscoelastic property. At lower frequency value, it showed a viscous behavior and at a very high frequency, it turned into elastic. As shown in figure 6.3, the native HA was a highly frequency- dependent, because both moduli  $G'$  and  $G''$  varied significantly with the frequency between  $0.01 \omega$  (rad/s) and  $100 \omega$  (rad/s). In contrast, the cross-linked hydrogels were not frequency-dependent and showed viscoelastic properties where the storage modulus was predominant over the whole range of tested frequency. However, the cross-linked hydrogels experienced dehydrations when the measurements were carried out at a very low frequency rate particularly the hydrogel with 2000 kDa. Based on the analysis, the rheological behavior of the hydrogels prepared at 100 kDa (Fig. 6.4) and 1000 kDa (Fig. 6.5) is relatively similar. On the other hand, The hydrogel prepared at 2000 kDa HA molecular weight (Fig. 6.6) was the stiffest according to enzymatic degradation test and revealed a higher ability to restore deformation when pressure was applied. The 2000 kDa hydrogel exhibited the highest  $G'$  value (476 Pa) at 1.0 frequency in comparison to the hydrogel of 100 kDa (80.6 Pa) and the hydrogel of 1000 kDa (99.0 Pa).

By increasing the HA molecular weight, the number of substituted monomers to the total number of HA monomers is increased and so a larger cross-linked network is constructed. If the stoichiometric ratio between BDDE and HA is taken into account, increasing the length of HA chains will lead to the formation of more covalent bonds between HA and BDDE. The native and cross-linked hydrogels were also evaluated for their dynamic viscosity in a steady shear mode at 25 °C. All hydrogels showed a shear-thinning property; the shear viscosity decreased over the course of frequency sweep test (Fig. 6.7). This property confirmed the crucial role of HA molecular weight on cross-linking efficiency, because the formed hydrogels showed different shear-thinning response. The (*appendix 8*) displays all Excel data of native and cross-linked BDDE-HA hydrogels.



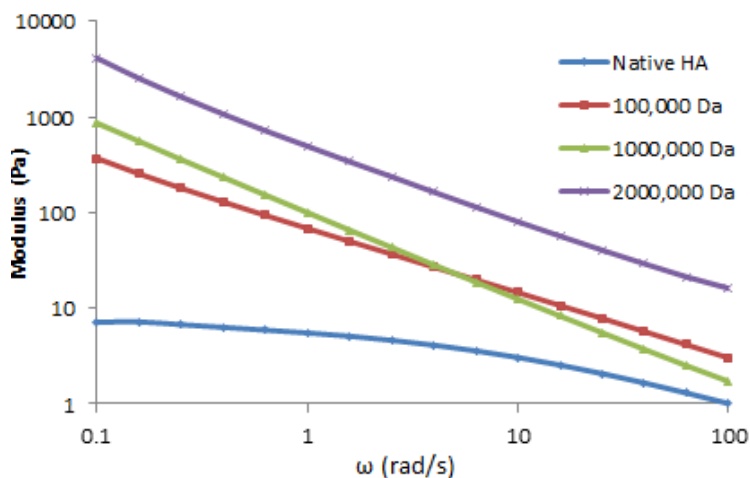


**Figure 6. 7** Measurements of dynamic viscosity for native HA and cross-linked hydrogels. The shear-thinning property was behaved in all cross-linked hydrogels.

### 6.3 Conclusion

The HA molecular weight showed a remarkable effect on cross-linking efficiency of BDDE-HA hydrogels. The increase of HA molecular weight led to the increase of hydrogel stability toward enzymatic digestion. The BDDE-HA hydrogel prepared from 2000,000 Da HA molecular weight showed the slowest degradation rate among tested hydrogels. The results of swelling ratio did not clearly reflect the effect of HA molecular weight. As observed, the hydrogel of 2000 kDa HA molecular weight swelled to a higher extent than the hydrogel of 1000 kDa with no significant difference. The storage modulus of the hydrogel prepared at (2000 kDa) HA molecular weight was higher than the storage modulus of hydrogels prepared at lower HA molecular weight. So the (2000 kDa) hydrogel was more resistant against deformation than the (100 kDa) and (1000 kDa) hydrogels subjected to the same oscillation frequency test. The native HA was a highly frequency- dependent compared to the cross-linked hydrogels which exhibited less frequency-dependence and more viscoelastic properties. Based on above analysis, we considered the HA molecular weight of 2000 kDa for our next investigation.

# CHAPTER 7

## 7. Mixing approach

### 7.1 Introduction

Mixing approach is a very important factor, particularly for heterogeneous reactions to limit mass loss or minimize impurity-uptake. Mixing of reaction components may be slow or fast to achieve complete blending or it may require a powered mixer or a hand mixing. Moreover, thorough mixing is critical to produce a homogenized hydrogel and increase the yields of physical cross-linking. Such conditions will have a significant impact on hydrogel properties including stability, swelling and modulus because they represent the way that HA powder is mixed with the BDDE solution. In this chapter we studied the effect of two mixing approaches: the large-batch mixing approach and the small-batches mixing approach. So, two cross-linked BDDE-HA hydrogels were synthesized: (*hydrogel 1*), by mixing the reaction quantities in one container; and (*hydrogel 2*), by dividing the reaction quantity into smaller batches at various HA/BDDE ratios. The results were compared with a native HA solution.

### 7.2 Mixing approach

#### 7.2.1 Materials

Hyaluronic acid with an average molecular weight 2000 kDa. Hyaluronidase (3000 U/mg), BDDE, Ehrlich's reagent, phosphate buffer saline (PBS) and alkaline solutions.

#### 7.2.2 Synthesis

Two cross-linking reagent solutions were prepared by adding 200  $\mu$ l of 1,4 – butandiol diglycidyl ether (BDDE) into 9.8 ml of 0.25M NaOH, (pH 13).

1.0 gram of HA powder was added to one reagent solution and mixed thoroughly at 40 °C for 2 h and then neutralized with 0.1M HCl to a pH of approximately 7.0. The resulted hydrogel was labeled with “hydrogel 1” and the mixing approach was suggested to be called “ the large-batch mixing approach”. Similar HA quantity was divided into smaller batches at different weights; 300 mg, 250 mg, 200 mg, 150 mg and 100 mg. Each batch was mixed with 2.0 ml of the second reagent solution in separate containers for 30 min at room temperature. All batches were then combined in one reaction container and left under continuous mixing at 40 °C for 90 min. The combined mixture was then neutralized with 0.1M HCl to a pH of approximately 7.0. The resulted hydrogel was labeled with “ hydrogel 2 ” and the mixing approach was suggested to be called “ the small-batches mixing approach”. Both solutions were then dialyzed for 2 days against distilled water to remove BDDE residue and non-reacted HA fragments. Finally the cross-linked hydrogels were lyophilized and kept at 8 °C until the characterization studies were carried out. The cross-linking efficiencies were estimated by measuring the *in-vitro* degradation rate using the colorimetric method, the swelling ratio using gravimetric balance, surface morphology using scanning electron microscope (SEM) and modulus using rheometer. All hydrogels were analyzed by Fourier-transformed infrared (FTIR) and nuclear magnetic resonance spectroscopy (NMR) to confirm the occurrence of modification between HA chains and BDDE molecules. For a comparison purpose, the cross-linked hydrogels were compared with a native HA polymer.

## **7.2.3 Measurements**

### **7.2.3.1 *In-vitro* degradation rate**

Equivalent portions from cross-linked hydrogels were cut and incubated with hyaluronidase in PBS solution for different intervals: 1, 2, 3 and 4 days. The enzymatic reactions were then stopped by heating each solution in boiling water for 5 min. The amount of *N*-acetyl glucosamine (NAG) found in each extract was quantified using the colorimetric method. The degradation rates of all samples were plotted as a function of time using the equation 4.1 described in section 4.2.3.1

### 7.2.3.2 Swelling ratio

Equivalent portions from cross-linked hydrogels were immersed in distilled water and phosphate buffer saline (PBS) until equilibrium state. Measurements were carried out as described in section 4.2.3.2.

### 7.2.3.3 Scanning Electron Microscope SEM

The morphologies of prepared hydrogels were visualized by scanning electron microscope (SEM) from JEOL (Tokyo, Japan). The lyophilized samples were first coated with platinum using an ion sputter and then imaged with SEI mode at 10 Kv.

### 7.2.3.4 Rheological measurements

Rheological measurements were carried out using ARES rheometer (TA instruments, USA) equipped with a plate and plate geometry. Initially a strain sweep test was performed to determine the linear viscoelastic region (LVR) and then an oscillatory test was applied to determine the storage and loss modulus over a frequency range (0.01-100 s<sup>-1</sup>) at a constant strain.

### 7.2.3.5 Fourier-transformed infrared (FT-IR) analysis

Portions from native HA and cross-linked hydrogels were obtained and characterized using Bruker Tensor 37 Fourier Transform Infrared Spectroscopy FT-IR (Ettlingen, Germany). All spectra were recorded between 4000 and 400 cm<sup>-1</sup> with a resolution of 4 cm<sup>-1</sup> and the data was manipulated using OPUS software.

### 7.2.3.6 NMR spectroscopy

Known samples of native and cross-linked hydrogels were mixed with bovine testicular hyaluronidase (BTH) enzyme solution until complete digestion. The extracts were centrifuged at 2000 rpm for 2 min and then lyophilized. The samples were then dissolved in D<sub>2</sub>O and transferred into NMR tubes. The <sup>1</sup>H NMR spectroscopy was carried out on a Bruker 600 MHz (Zurich, Switzerland) instrument operating at a frequency of 600 MHz. The spectra were acquired by Bruker Topspin 3.2 software.

## 7.2.4 Statistics

{As stated in section 4.2.4 }

## 7.2.5 Results and discussion

### 7.2.5.1 *In-vitro* degradation test

Although HA hydrogels can be degraded by bovine testicular hyaluronidase (BTH) enzyme, the cross-linked polymer matrix can slow down enzymatic invasion and increase duration of hydrogel residence. Fig. 7.1 represents degradation profiles of native and cross-linked hydrogels for four consecutive days of treatment. As stated, the degradation rates were evaluated by determining the % NAG remaining in the non-digested fractions as a function of incubation time with the hyaluronidase.

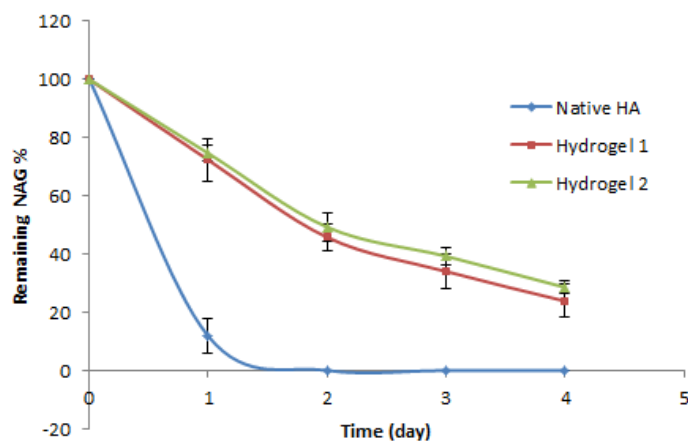


**Figure 7. 1** Degradation profiles of native and cross-linked BDDE-HA hydrogels 1 & 2 prepared at different mixing approaches. Results are expressed as mean  $\pm$  95% confidence represented by the error bars (n=3).

Based on results, the native HA solution and hydrogels 1 and 2 showed different sensitivities towards enzyme activity, and it was observed that almost 90% of native HA was lost in the first day of incubation with hyaluronidase compared to hydrogels 1 and 2, which showed a much higher stability towards enzymatic digestion and lost approximately 26 % and 24 % respectively of their original content of NAG after a similar duration.

Although hydrogels 1 and 2 did not exhibit a significant difference ( $p > 0.05$ , t-test,  $n=3$ ) towards hyaluronidase on the first and second days of incubation, they showed different degradation on subsequent days. Hydrogel 1 degraded faster than hydrogel 2 on the third and fourth days, indicating that the polymer matrix of hydrogel 1 was relatively affected by the mixing approach. Hydrogel 2, overall, presented a higher resistance to enzyme, and approximately one-fourth of its original content of NAG remained after the course of treatment. In contrast, the remaining NAG of hydrogel 1 was less by almost 5.0%. These data reveal that the mixing approach is critical and leads to a different degradation profile in cross-linked hydrogels. The small-batches mixing approach showed a better blending of hydrogel components and seemed to produce a more homogenized cross-linked matrix.

Although, the two solutions were mixed for the same period, the small-batches mixing approach allowed HA powder to disperse into the reagent solution in lower volumes, and different HA / BDDE molar ratios that led to a better movement of solution components. Each separate mixing step added a distinct feature to the total mixture, so the small HA batches in hydrogel 2 had a greater chance to bind with BDDE molecules than did the single lump in hydrogel 1. In addition, the small-batches mixing may play a crucial role in keeping HA chains close together and form more HA entanglement and conformation. The HA chains in the hydrogel 2 composite became shorter than those in hydrogel 1, thus strengthening the overall network. This highly cross-linked network served as an inhibitor for the enzyme attack. All degradation rate values with uncertainty intervals are demonstrated in (*appendix 6.6*).

## 7.2.5.2 Swelling measurements

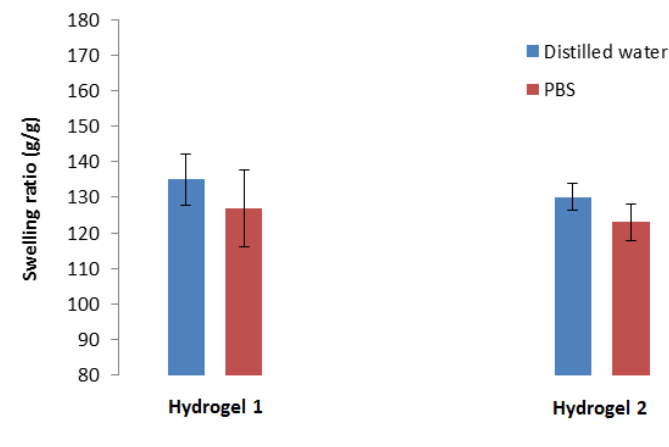


**Figure 7. 2** Swelling ratios of cross-linked BDDE-HA hydrogels 1 & 2

The swelling ratios of the cross-linked hydrogels 1 and 2 in distilled water and phosphate buffer saline are demonstrated in Fig. 7.2. Native HA was excluded because it showed solubility and did not form a well-defined three-dimensional scaffold. The results of swelling ratio measurements were in good agreement with the results of the *in-vitro* degradation rate. Hydrogels 1 and 2 reached their equilibrium states at different water-absorption capacity explaining the relative effect of mixing methodology on hydrogel swelling properties. Swelling ratios of hydrogels 1 and 2 in distilled water showed a significant difference and reached to maximum average values at  $135 \pm 7.2$  g/g and  $130 \pm 3.8$  g/g respectively. However, their swelling ratios in phosphate buffer saline (PBS) showed no significant difference with average values at  $127 \pm 10.8$  g/g for hydrogel 1 and  $123 \pm 5.2$  g/g for hydrogel 2. On the other hand, it was observed that the extent to which the cross-linked hydrogels swelled in PBS was less than their swelling in distilled water pointing out to the influence of ionic strength of buffer. The (*appendix 7.6*) displays the swelling ratio of cross-linked hydrogels prepared at different mixing approach. Based on these findings, a slight change in BDDE-HA synthesis process including mixing process can alter the chemical and physical properties of HA hydrogels.

This can be plausibly attributed to the fact that hydrogel 2 formed more physical entanglements and covalent bonds with BDDE than hydrogel 1 that kept the polymer chains in close proximity and limited its possibility for swelling. It is also noteworthy mentioning that incorporation of various HA contents with a fixed level of cross-linking reagent solution (as happened with hydrogel 2) resulted in various exposures of HA chains to BDDE molecules. This mixing enhanced formation of efficient cross-links and led to a more densely cross-linked network, so the hydrogel became stiffer and subsequently showed a lower swelling ratio. The hydrogel 2 cross-linking efficiency was also verified by the narrower 95% confidence interval (n=3) observed around the average swelling ratios and degradation rates of hydrogel 2 compared to hydrogel 1. The wide 95% confidence interval usually reflects inhomogeneity and irregular distribution of BDDE molecules in the reaction mixture forming rich and poor cross-linking density regions throughout the hydrogel scaffold and that may explain the slight increase in the uncertainty level of hydrogel 1.

Based on hydrogel degradation and swelling capacity, it is necessary to highlight that these two significant factors depend basically on the degree of cross-linking which is of great relevance to *in-vivo* hydrogel profile. Despite differences between *in-vivo* and *in-vitro* conditions, measurements of the *in-vitro* hydrogel degradation rate and swelling ratio are observed to be substantial. It is of large benefit to predict *in-vivo* performance of cross-linked hydrogel from *in-vitro* data. The slower degradation rate of a studied hydrogel expresses tighter structure, slower erosion rate and better mechanical integrity, thus it exhibits more robust behavior necessary for tissue growth and long-lasting effect. On the other hand, the modified hydrogels are highly water-swollen that can swell in water under biological conditions but do not dissolve in it (Zhu and Marchant, 2011). This high swelling expresses several features such as low surface tension with surrounding biological fluids or low mechanical irritation to surrounding tissues and excellent nutrients diffusion into the gel and cellular waste removal out of the gel (Jeon et al., 2007). The ability of molecules to diffuse into and out of swollen hydrogels, enable the use of hydrogels in a variety of biomedical applications including skin augmentation, regenerative medicine and recently as delivery vehicles of bioactive substances (Satish et al., 2006).



Drugs can be easily incorporated into swollen hydrogel matrix and then injected to the defect site. So fundamental measurements of hydrogel degradation and swelling ability have become crucial, particularly for drugs diffusion tended to be released in the living body through matrix swelling or matrix erosion. The mechanism of drug release in matrix swelling occurs when diffusion of drug is faster than hydrogel swelling while in surface matrix erosion, the release occurs when the rate of enzymatic degradation is much faster than the transport of enzyme into the hydrogel (Zarzycki et al., 2010). The success of a tissue engineering approach is also dependent on the properties of scaffolding hydrogel (Park et al., 2009), so carrying out such measurements could provide valuable means of assessing hydrogel erosion and structural integrity outside the organism and thus it helps developing a tailored scaffold that mimics tissue of native extracellular matrix. A study showed that the *in-vivo* erosion of selected hydrogels that degraded by hydrolytic or enzymatic degradation linearly correlated with the *in-vitro* erosion (Artzi et al., 2012).

This correlation enables successful predication of material erosion that can be extended to monitor material stabilization, cell viability and scaffold fate in tissue-engineering formulations. Based on such work, a significant advance in the design of artificial matrices has been made from a simple scaffold to a more complex dynamic 3-dimensional network that supports cell growth, facilitates nutrient transfer and provides appropriate mechanical and chemical characteristics (Geckil et al., 2010). Furthermore, the *in-vitro* degradation measurements allow producing materials with a controllable degradation which is necessary for the *in-vivo* application. For instance, materials with a degradation time of 25-day is suitable for burn and skin excision, and with an 8-week degradation time is suitable for diabetic ulcer or pressure ulcer (Xu et al., 2009). However, a specific set of physiological conditions need to be established *in-vitro* to attain *in-vivo* correlation because the *in-vivo* erosion profile is more complex and it is site-dependent (Artzi et al., 2012).

### 7.2.5.3 SEM

Although SEM cannot confirm the presence of ether bond in the cross-linked hydrogel, it offers unique information about porosity and scaffold interconnection. Fig. 7.3 shows SEM surface images of native HA and cross-linked hydrogels, all images were obtained at identical magnification conditions (x100, x500, SEI and 10kv). In our results, the SEM images demonstrated differences in the hydrogel's microstructure. It was obvious that the cross-linking process produced a scaffold with larger density and lower pore sizes. The images of native HA showed a very thin layer and open pores with some collapse that probably occurred during the freeze-drying process. In contrast, hydrogels 1 and 2 showed rigidity and cross-linked composites. The SEM images of cross-linked hydrogels exhibited almost identical matrices with relative different porous structures where hydrogel 2 appeared denser and showed smaller pores size in comparison with hydrogel 1.

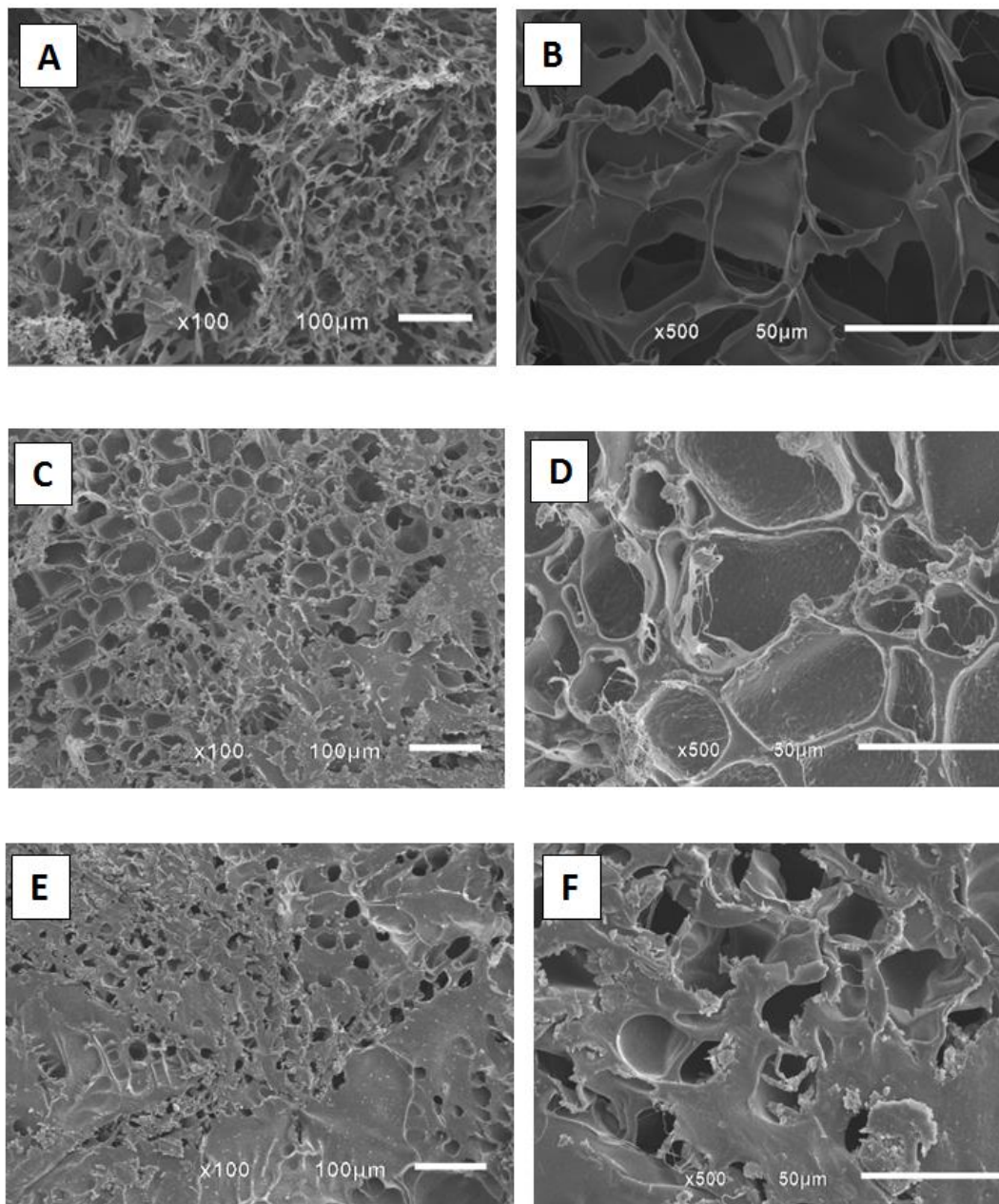


**Figure 7. 3** Morphological structure imaged by SEM using SEI mode (10 Kv) at x100 and x 500 for lyophilized native HA (A & B), hydrogel 1 (C & D), and hydrogel 2 (E & F)

### 7.2.5.4 Rheological measurements

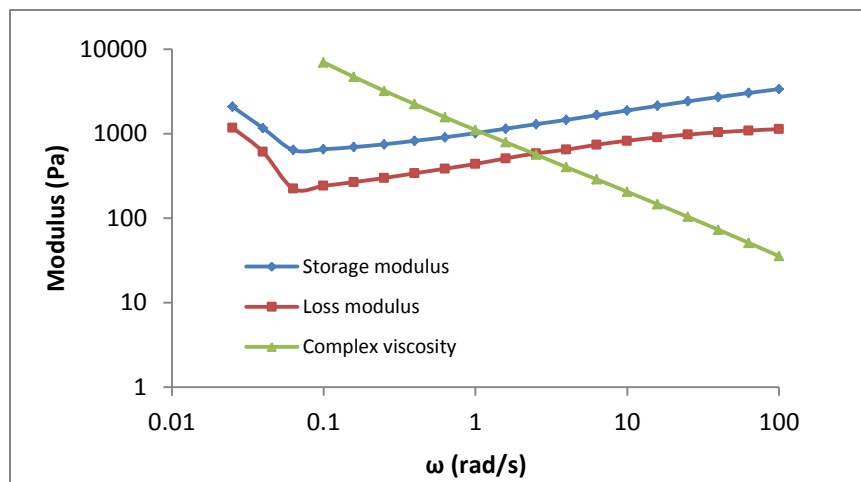


**Figure 7. 4** Storage modulus  $G'$  and Loss modulus  $G''$  (Pa) versus angular frequency in the range (0.01-100  $s^{-1}$ ) for hydrogel 1 prepared by large-batch mixing approach

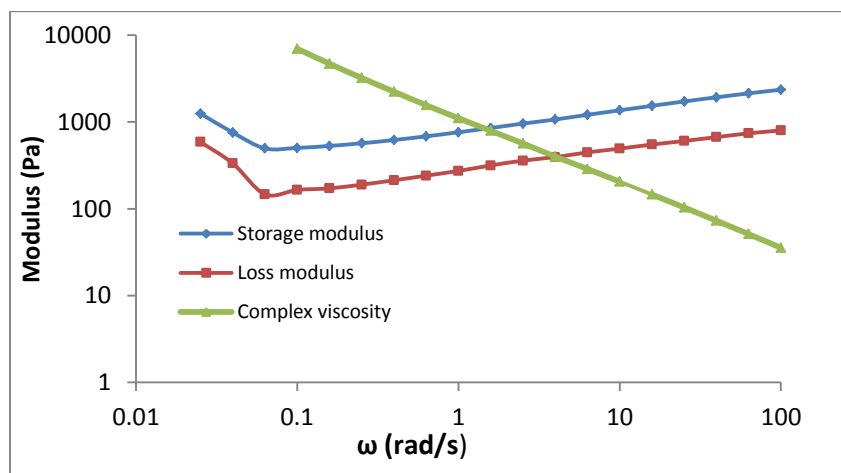


**Figure 7. 5** Storage modulus  $G'$  and Loss modulus  $G''$  (Pa) versus angular frequency in the range (0.01-100  $s^{-1}$ ) for hydrogel 2 prepared by small-batches mixing approach

Figures 7.4 and 7.5 show the modulus graphs of cross-linked BDDE-HA hydrogels prepared at different mixing approaches. Both hydrogels experienced a solvent dehydration at lower frequency. The analysis of rheological data (*appendix 8*) revealed that the modulus did not exhibit a noticeable difference between the two hydrogels.

It was shown that the storage and loss modulus increased slowly with the increase of angular frequency, this indicated that both hydrogels were not frequency-dependent. The elastic modulus was always higher than the viscous modulus over the whole range of analysis and the two hydrogels showed a shear-thinning and a viscoelastic property. However, the high storage value observed with the hydrogel 2 reflected its restitution ability after deformation and relaxation stress. These data confirmed that the small-batches mixing approach promoted the cross-linking reaction and formed a better cross-lined network than the large-batch mixing approach.

### **7.2.5.5 FTIR and NMR**

The chemical modification of HA with BDDE was confirmed by FTIR and  $^1\text{H}$  NMR analysis (Fig. 7.6). The difference in the FTIR and NMR spectra between native HA and BDDE-HA hydrogels confirmed that a chemical modification occurred to the native HA structure. As stated in chapter 2, spectra of FTIR shows three characteristic peaks: peak 1 at  $3343\text{ cm}^{-1}$  observed in native and cross-linked hydrogel; peak 2 at  $2900\text{ cm}^{-1}$  observed in cross-linked hydrogels and relatively in native HA; peak 3 at  $1300\text{ cm}^{-1}$  observed in the cross-linked hydrogels. Peak 1 was assigned to the hydroxyl group, whereas peaks 2 and 3 represented the C-H stretching and ether linkage. The peak 1 corresponding to the hydroxyl group appeared with a higher intensity in native HA than its counterpart peaks in cross-linked hydrogels.

This noticeable decrease explained that under alkaline conditions, the cross-linking reaction targeted one of the reactive hydroxyl groups in native HA and by increasing the modification process, the total amount of ( $-\text{OH}$ ) decreased. In terms of the mixing approach, the BDDE molecule blocked a larger amount of ( $-\text{OH}$ ) groups in hydrogel 2 and more ether bonds were formed in comparison to hydrogel 1. This finding was consistent with previous analysis and confirmed the efficiency of the small-batches mixing approach. NMR results revealed a distinctive signal at 1.5 ppm in the cross-linked BDDE-HA hydrogels which is absent in native HA. This peak represents the ( $-\text{CH}_2-$ ) group of the BDDE molecule.

The peak at about 1.9 ppm which appeared in native HA and cross-linked hydrogels could be assigned to the acetyl glucosamine. As we explained in chapter 2, Integration of the signal at 1.5 ppm with regard to the acetyl glucosamine at 1.9 ppm gives the number of BDDE molecules linked to HA chains which explains the total degree of modification occurred in the formed hydrogel. Based on NMR data, the degree of modification of hydrogels 1 and 2 equaled to about 14% and 24 % respectively. Commercially available injectable dermal fillers usually exhibit a wide range of degree of modification depending on purpose of implantation. For instance, lower-modification hydrogels may be better suited for less-dynamic wrinkles such as lips or periorbital region, high-modified HA hydrogels are probably better suited to areas where correction is very important such as nasolabial folds and marionette lines ([Kablik et al, 2009](#)). Examples of HA-based fillers with low HA modification (less than 10 %) include Juvederm and Restylane ([Edsman et al, 2012](#) ) and products with high HA modification include Hylaform, and Prevelle that show a degree of modification reaching to 23 % ([Kablik et al, 2009](#)).

The NMR data also supported the previous measurements presenting further evidence for the occurrence of modification and proved that hydrogel 2 underwent a higher degree of modification when compared to hydrogel 1. However, it is important to note that the obtained values of the degree of modification were far less than the theoretical degree of modification according to molar ratio of HA and BDDE involved in the chemical reaction, this means that a large portion of BDDE molecules was not bound with HA chains particularly in hydrogel 1.

CHAPTER 7: MIXING APPROACH

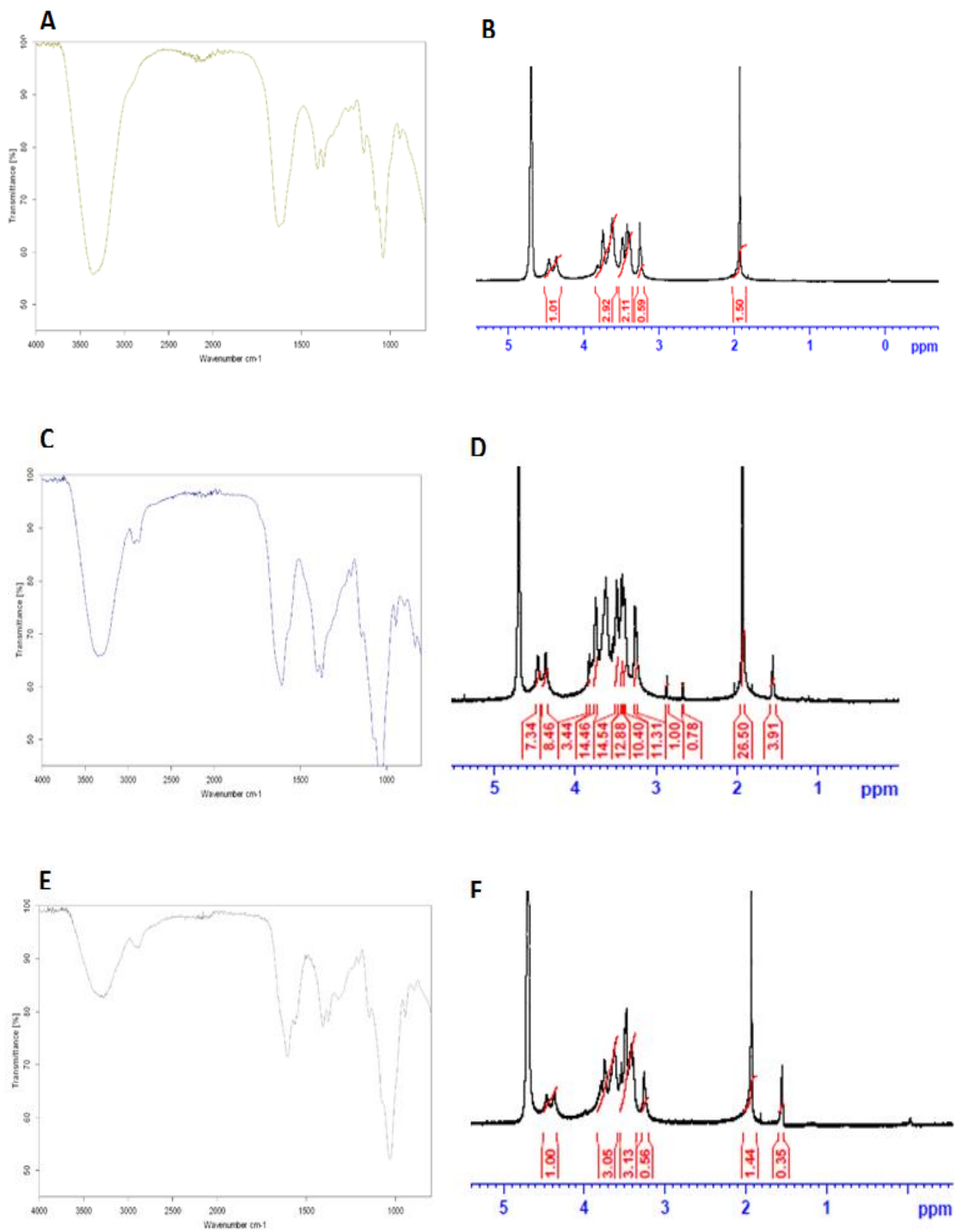


**Figure 7. 6** FTIR and <sup>1</sup>H NMR spectra for native HA ( A & B), hydrogel 1 (C & D) and hydrogel 2 ( E & F)

The difference between the degrees of modification of hydrogels 1 and 2 was significantly large ( $p = 0.004$ ), which was not clearly observed in the *in-vitro* degradation rates and swelling measurements. This was probably due to the formation of pendant groups along with the efficient cross-links in hydrogel 2. As we explained in chapter 1, pendant modification does not contribute to hydrogel stability and does not produce a covalently cross-linked network. During the cross-linking reaction, the BDDE reacts with HA chains at both ends forming the double-linked molecules. However, some portion of BDDE reacts with HA at one end leaving the other end pendent (mono-linked) or reacted with water/hydroxide (Kenne et al. 2013). The mechanism of this interaction is mainly dependent on reaction conditions or relative tendency of epoxides binding with the hydroxyl groups of HA. The data of NMR describe the total change happened in hydrogel modification which includes both mono-linked BDDE molecules and those involved in the actual cross-linkages. Overall, the small-batches mixing approach produced higher yields of physical and chemical cross-links than the large-batch mixing approach. Despite the similarities in some results and the formation of pendant, we could demonstrate that the cross-linked BDDE-HA hydrogel prepared through the small-batches mixing approach showed a higher strength and stability against the action of hyaluronidase than the hydrogel prepared by the large-batch mixing approach.

### **7.3 Conclusion**

In this work, we studied the influence of mixing approach on two cross-linked BDDE-HA hydrogels prepared by two different mixing approaches; the large-batch mixing approach in which the hydrogel quantities were all mixed as a single lump in one container (*hydrogel 1*), and the small-batches mixing approach in which the hydrogel quantities were divided into smaller batches, mixed separately at various HA/BDDE ratios then combined in one reaction mixture (*hydrogel 2*). The result showed that the cross-linking reaction was mixing process-dependent. Degradation tests proved that, in relation to hydrogel 1, hydrogel 2 was more stable, and exhibited a higher resistance toward hyaluronidase activity.



The swelling ratio of hydrogel 1 was significantly higher than that of hydrogel 2 in distilled water; however, in phosphate buffer saline, both hydrogels showed no significant difference. SEM images demonstrated that hydrogel 2 composite showed a denser network structure and smaller pore-size than hydrogel 1. In comparison to native HA, the occurrence of chemical modification in the cross-linked hydrogels was confirmed by FTIR and NMR distinctive peaks. These peaks also provided evidence that hydrogel 2 exhibited a higher degree of modification than hydrogel 1. In conclusion, the small-batches mixing approach proved to be more effective than large-batch mixing in promoting HA-HA entanglement and increasing the probability of BDDE molecules for binding with HA chains.

## SUMMARY AND OUTLOOK

The main objective of our study was to enhance the cross-linking efficiency of HA hydrogels cross-linked with 1, 4-butanediol diglycidyl ether BDDE via studying method conditions including reaction time, pH, temperature, HA concentration, HA molecular weight and mixing approach. Based on hydrogel's properties (e.g. *in-vitro* degradation rate, swelling ability, morphological and rheological behavior) resulting from each cross-linking process, the cross-linking efficiency was evaluated. The results revealed that there was a noticeable correlation between method conditions and cross-linking efficiency. The BDDE-HA hydrogels synthesized at a reaction time equaled or longer than 2 h showed slower degradation rates and lower swelling ratios than those synthesized at shorter time. The two-hour interval was subsequently determined as a minimum reaction time required for cross-linking 1.2 g HA powder with 200  $\mu$ l BDDE. The resistance towards enzymatic degradation and swelling ability demonstrated by the BDDE-HA hydrogel prepared at pH 13 confirmed the potential impact of strong alkaline medium on cross-linking efficiency of HA.

The temperature was also an effective parameter, the 40 °C was determined as an ideal heated medium to carry out the HA chemical modification because it produced the stiffest hydrogel against enzymatic destruction. The BDDE-HA hydrogel prepared at 10.0 % HA initial concentration proved to be the idlest concentration level corresponding to the 2.0 % v/v BDDE. On the other side, the two millions Da (HA) molecular weight formed a more stable cross-linked network towards hyaluronidase compared to the hydrogels prepared at one million Da or 100 kDa. However, the swelling ratio of two millions Da (HA) hydrogel was slightly larger than the swelling ratio of one million Da hydrogel in both water and PBS. Furthermore, mixing approach showed a remarkable influence on BDDE-HA cross-linked network. The small-batches mixing approach produced a more homogenized cross-linked texture than the large-batch mixing.

Based on the above summary, we hypothesize that, the method with the new optimum conditions can relatively enhance the cross-linking efficiency of BDDE-HA hydrogel to a certain degree while the BDDE content is possible to be kept constant. The desirability and suitability of cross-linked hydrogels as a dermal filler or scaffolding materials are largely correlated with longevity. Preparation of a rigid HA hydrogel in the absence of BDDE is challenging. The chemical cross-linker usually forms a major constituent in HA modification and a greater contributor in the increase of cross-linking efficiency. In spite of the fact that the physical crosslinking has recently gained a considerable attention, the physical cross-linking alone cannot exhibit a significant resistant against depolymerization. Therefore, more studies are required in this area particularly for the formation of physically cross-linked hydrogels by either HA-HA interaction or hybrid networks in which HA is combined with other biopolymers. An alternative approach could be the use of physical cross-linking strategy with a minimum quantity of the chemical cross-linker in order to produce a rigid hydrogel with a low potential of hazards and adverse reactions. However, more studies are required to evaluate the amounts of BDDE to be activated in order to cross-link larger amounts of HA chains and to not form pendants or dangling chains. We may recommend here a development of a chromatographic method using high performance liquid chromatography to monitor the BDDE residue in the solution after the synthetic reaction.

Pendant or dangling chains are probably formed when BDDE molecule is physically restricted from one side to reach HA chain or the epoxide rings are not active enough to open and react with HA chain. To avoid pendants, we also recommend to investigate how HA chains can be made close enough to reach each other and to reach the cross-linker molecules. Study of the effect of di- or tri-valent counter ions on cross-linking efficiency is also recommended. For instance, cross-linking of hyaluronic acid with BDDE in the presence of a multivalent ion of opposite charge (e.g.  $\text{CaCl}_2$  or  $\text{MgCl}_2$ ) is worthwhile. These ions will lead to an interaction between anionic groups on HA ( $\text{COO}^-$ ) with the positive charge of the metal ( $\text{Ca}^+$ ,  $\text{Mg}^+$ ), subsequently the distances between HA strands become shorter.

## ACKNOWLEDGMENT

I would like to express my deepest thanks and appreciation to my supervisor Prof. Dr. Dr. Reinhard Neubert who provided me the opportunity to carry out this project with him. I am really grateful to his continuous help and support that enabled me to complete my work on time. His vision, knowledge and experience have all kept me motivated always and looked forward to increase my interest in this area of study. My deepest appreciation is also expressed to my co- supervisor Prof. Ahmed Al-Harrasi who gave me knowledge and support, particularly when I held a part of my project at Nizwa University. I also gratefully acknowledge Dr. yahya mrestani for his advice and guidance, especially when I settled in Germany. A special thanks goes to Dr. Klaus Schröter at the Institute of Physics for his technical support and rheological measurements. I would like also to thank Ms. Manuela Woigk who assisted in the preparation of HPLC work. I would like also to acknowledge Mr. Khamis Omair Al Riyami for SEM work and Mr. Muhammed Adil and Ahmed Al-Abri for NMR analysis. Furthermore, all colleagues and friends who assisted me in my research are gratefully acknowledged. I also would like to appreciate Vivatis Pharma (Hamburg, Germany) who kindly donated the sodium salt of hyaluronic acid. Finally, I have to appreciate my parents, wife and whole family for their large encouragement and support.

## REFERENCES

**Akdamar, H.,** Sariözlü, N., Özcan, A., Ersöz, A., Denizli, A., Say, R. (2009). Separation and purification of hyaluronic acid imprinted microbeads. *Materials Science and Engineering*, C29,1404-1408.

**Alijotas-Reig, J.,** García-Giménez, V. (2008). Delayed immune-mediated adverse effects related to hyaluronic acid and acryl hydrogel dermal fillers: clinical findings, long-term follow-up and review of the literature. *Journal of the European Academy of Dermatology and Venereology*, 22,150-61.

**Alkrad, J.,** Merstani, Y., Neubert, R. (2002). New approaches for quantifying hyaluronic acid in Pharmaceutical semisolid formulation using HPLC and CZE. *Journal of pharmaceutical and Biomedical Analysis*, 30, 913-919.

**Allemann, I.B.,** Baumann, L.(2008). Hyaluronic acid gel (Juvederm) preparations in the treatment of facial wrinkles and folds. *Clinical Interventions in Aging*, 3(4), 629-634.

**Amargier, C.,** Marchacl, P., Payan, E., Netter, P., Dellacheri, E. (2006). New physically and chemically cross-linked hyaluronate (HA)-based hydrogels for cartilage repair. *Journal of Biomedical Material Research*, 76 A, 416-424.

**Andre, P.** (2004). Hyaluronic acid and its use as a “rejuvenation” agent in cosmetic dermatology. *Seminars in Cutaneous Medicine and Surgery*, 23, 218–222.

**Argin-Soysal, S.,** Kofinas, P., Martin Lo, Y. (2009). Effect of complexation conditions on xanthan-chitosan polyelectrolyte complex gels. *Food Hydrocolloids*, 23, 202-209.

**Arrich, J.,** Pirbauer, F., Mad, P., Schmid, D., Klaushofer, k., Mullner, M. (2005). Intra-articular hyaluronic acid for treatment of osteoarthritis of the knee systematic review and meta-analysis. *Canadian Medical Association Journal*, 172-1039.

**Artzi, N.,** Oliva, N., Puron, C., Shitreet, S., Artzi, S., Ramos, A., Groothuis, A., Sahagian, G., Edelman, E. (2012). In vivo and in vitro tracking of erosion in biodegradable materials using non-invasive fluorescence imaging. *Natural Materials*, 10 (9), 704-709.

**Athre, R.** (2007). Facial filler agents. *Operative Techniques in Otolaryngology*, 18 : 243-247.

**Barbucci, R.,** Leone, G., Chiumiento, A., Di Cocco, M., D’Orazio, G., Gianferri, R., Delfini, M. (2006). Low-and high-resolution nuclear magnetic resonance (NMR) characterization of hyaluronan-based native and sulfated hydrogels. *Carbohydrate Research*, 341, 1848-1858.

**Baumann, L.** (2004). Replacing dermal constituents lost through aging with dermal fillers. *Seminars in Cutaneous Medicine and Surgery*, 23,160-166.

## REFERENCES

- Beasley, K. L.,** Weiss, M. A., Weiss, R. A. (2009). Hyaluronic acid fillers: A comprehensive review. *Facial Plastic Surgery*, 25, 86–94.
- Bencherif, S.,** Srinivasan, A., Horkay, F., Hollinger, J., Matyjaszewski, K., Washburn, N. (2008). Influence of the degree of methacrylation on hyaluronic acid hydrogels properties. *Biomaterials*, 29 (12), 1739–1749.
- Berkó, S.,** Maroda, M., Bondár, M., Erós, G., Hartmann, P., Szentner, K., Szabó-Révész, P., Kemény, L., Borbély, J., Csányi, E. (2013). Advantages of cross-linked versus linear hyaluronic acid for semisolid skin delivery systems. *European Polymer Journal*, 49, 2511-2517.
- Bingol, A.O.,** Dogan, A. (2012). Physical properties of hyaluronic acid fillers and their relevance for clinical performance. *MÄC Magazin für ästhetische Chirurgie*, 2112 (6), 6-12.
- Boogaard, P.J.,** Denneman, M.A., Van Sittert, N.J. (2000). Dermal penetration and metabolism of five glycidyl ethers in human, rat and mouse skin. *Xenobiotica*, 5, 469-83.
- Borrell, M.,** Leslie, D., Tezel, A. (2011). Lift capabilities of hyaluronic acid fillers. *Journal of Cosmetic and Laser Therapy*, 13, 21-27.
- Brandt, F.,** Cazzaniga, A. (2008). Hyaluronic acid gel fillers in the management of facial aging. *Clinical Interventions in Aging*, 3 (1), 153-159.
- Brown, T. J.,** Laurent, U. B. G. & Fraser, J. R. E. (1991). Turnover of hyaluronan in synovial joints: Elimination of labelled hyaluronan from the knee joint of the rabbit. *Experimental Physiology*, 76(1), 125–134.
- Caillard, R.,** Remondetto, GE., Mateescu, MA., Subirade, M. (2008). Characterization of amino cross-linked soy protein hydrogels. *Journal of Food Science*, 73(5), C283-291.
- Cardoso, D.A.,** Ulset, A.S., Bender, J., Jansen, J.A., Christensen, B.E., Leeuwen-burgh, S.C. (2014). Effects of physical and chemical treatments on the molecular weight and degradation of alginate–hydroxyapatite composites. *Macromolecular Bioscience*, 14(6) , 872–880.
- Carruthers, J.D.,** Glogau, R.G., Blitzer, A., et al. (2008). Advances in facial rejuvenation: Botulinum toxin type a, hyaluronic acid dermal fillers, and combination therapies—consensus recommendations. *Plastic and Reconstructive Surgery*, 121(Suppl), 5S-30S.
- Chung, C. W.,** Kang, J. Y., Yoon, I. S., Hwang, H. D., Balakrishnan, P., Cho, H. J., et al. (2011). Interpenetrating polymer network (IPN) scaffolds of sodium hyaluronate and sodium alginate for chondrocyte culture. *Colloids and Surfaces B: Biointerfaces*, 88, 711–716.
- Cirillo, P.,** Benci, M., Bartoletti, E., et al. (2008). Proposed guidelines for use of dermal and subdermal fillers. *Giornale Italiano Di Dermatologia E Venereologia*, 143, 187-193.
- Clark, C.P.** (2007). Animal-based hyaluronic acid fillers: scientific and technical considerations. *Plastic and Reconstructive Surgery*, 120 (Suppl), 27S-32S.

## REFERENCES

- Collins, M. N.** Birkinshaw, C. (2007). Comparison of the effectiveness of four different crosslinking agents with hyaluronic acid hydrogel films for tissue-culture applications. *Journal of Applied Polymer Science*, 104(5), 3183–3191.
- Davidenko, N.,** Campbell, J.J., Thian, E.S., Watson, C.J., Cameron, R.E. (2010). Collagen-hyaluronic acid scaffolds for adipose tissue engineering. *Acta Biomaterialia*, 6, 3957-3968.
- De Boule, K.,** Glogau, R., Kono, T., Nathan, M., Tezel, A., Roca-Martinez, J.X., Paliwal, S., Stroumpoulis, D. (2013). A Review of the Metabolism of 1,4-Butanediol Diglycidyl Ether–Cross-linked Hyaluronic Acid Dermal Fillers. *Dermatologic Surgery*, 12, 1758-66.
- Della Valle, F.,** Romeo, A. (1986). US4851521.
- Edsman, K.,** Nord, L., Ohrlund, A., Larkner, H., Kennf., A. (2012). Gel properties of hyaluronic acid dermal fillers. *Dermatologic Surgery*, 38, 1170-1179.
- Eenschooten, C.,** Vaccaro, A., Delie, F., Guillaumie, F., TA, mmeraas, K., Kontogeorgis, G. M., et al. (2012). Novel self-associative and multiphasic nanostructured soft carriers based on amphiphilic hyaluronic acid derivatives. *Carbohydrate Polymers*, 87(1), 444–451.
- Esposito, E.,** Menegatti, E., Cortesi, R. (2005). Hyaluronan-based microspheres as tools for drug delivery: A comparative study. *International Journal of Pharmaceutics*, 288(1), 35–49.
- Esteban, C.** Severian, D. (2000) Polyionic hydrogels based on xanthan and chitosan for stabilising and controlled release of vitamins, Vol. WO0004086 (A1) (ed. U. United States Patent), Kemestrie Inc [CA], USA.
- Fakhari, A.,** Berkland, C. (2013). Applications and emerging trends of hyaluronic acid in tissue engineering as a dermal filler and in osteoarthritis treatment. *Acta Biomaterialia*, 9, 7081-7092.
- Falcone, S. J.,** Berg, R. A. (2008). Crosslinked hyaluronic acid dermal fillers: A comparison of rheological properties. *Journal of Biomedical Materials Research*, 87A, 264–271.
- Fan, H.B.,** Hu, Y.Y., Qin, L., Li, X.S., Wu, H., Lv, R. (2006). Porous gelatin–chondroitin–hyaluronate tri-copolymer scaffold containing microspheres loaded with TGF- $\beta$ 1 induces differentiation of mesenchymal stem cells *in vivo* for enhancing cartilage repair. *Journal of Biomedical Materials Research*, (77A), 785–94.
- Ferretti, M.,** Marra, K.G., Kobayashi, K., Defail, A.J., Chu, C.R.(2006). Controlled *in vivo* degradation of genipin crosslinked polyethylene glycol hydrogels within osteochondral defects. *Tissue Engineering*, 12 (9), 2657–63.
- Frazier, S.,** Roodhouse, K., Hourcade, D., Zhang, L. (2008). The Quantification of Glycosaminoglycans: A Comparison of HPLC, Carbazole, and Alcian Blue Methods. *Open Glycoscience*, (1), 31-39.

## REFERENCES

**Gatta, A.,** Schiraldi, C., Papa, A., D'Agostino, A., Cammarota, M., Rosa, A., Rosa, M. (2013). Hyaluronan scaffolds via diglycidyl ether cross-linking: Toward improvements in composition and performance. *Carbohydrate Polymers*, 96, 536–544.

**Gatta, A.,** Schiraldi, C., Papa, A., Rosa, M. (2011). Comparative analysis of commercial dermal fillers based on cross-linked hyaluronan: Physical characterization and in vitro enzymatic degradation. *Polymer Degradation and Stability*, 96, 630-636.

**Geckil, H.,** Xu, F., Zhang, X., Moon, S. Demirci, U. (2010). Engineering hydrogels as extracellular matrix mimics. *Nanomedicine*, 5 (3), 469-484.

**Grimshaw, J.,** Kane, A., Trocha-Grimshaw, J., Douglas, A., Chakravarthy, U., Archer, D. (1994). Quantitative analysis of hyaluronan in vitreous humor using capillary electrophoresis. *Electrophoresis*, (15), 936–940.

**Guarise, C.,** Pavan, M., Pirrone, L., Renier, D. (2012). SEC determination of cross-link efficiency in hyaluronan fillers. *Carbohydrate Polymers*, 88, 428-434.

**Gulrez, S.,** Al-Assaf, S., Phillips, G. (2011). *Hydrogels: Methods of Preparation, Characterisation and Applications, Progress in Molecular and Environmental Bioengineering - From Analysis and Modeling to Technology Applications*, Prof. Angelo Carpi (Ed.), ISBN: 978-953-307-268-5.

**Hennink, W.E.,** van Nostrum, C.F. (2012). Novel crosslinking methods to design hydrogels. *Advanced Drug Delivery Reviews*, 64, 223-236.

**Hoffman, A.S.** (2002). Hydrogels for biomedical applications. *Advanced Drug Delivery Reviews*, 43,3-12.

**Holzer, M.P.,** Tetz, M.R., Auffarth, G.U., Welt, R., & Voelcker, H. (2001). Effect of healon 5 and 4 other viscoelastic substances on intraocular pressure and endothelium after cataract surgery. *Journal of Cataract and Refractive Surgery*, 27, 213–8.

**Huang-Lee, L.L.H.,** Nimmi, M. (1994). Crosslinked CNB-activated hyaluronan-collagen matrices: effects on fibroblast contraction. *Matrix Biology*, 14,147–57.

**Huin-Amargier, C.,** Marchal, P., Payan, E., Netter, P., Dellacherie, E. (2006). New physically and chemically crosslinked hyaluronate (HA)-based hydrogels for cartilage repair. *Journal of Biomedical Materials Research Part A*, 76(2), 416–424.

**Hwang, H. D.,** Cho, H. J., Balakrishnan, P., Chung, C. W., Kang, J. Y., Yoon, I. S., et al. (2012). Cross-linked hyaluronic acid-based flexible cell delivery system: Application for chondrogenic differentiation. *Colloids and Surfaces B: Biointerfaces*, 91, 106–113.

**Iannitti, T.,** Bingol, A., Rottigni, V., Palmieri, B. (2013). Biocompatibility and rheological properties of a new highly viscoelastic hyaluronic acid in a rat model for biomaterial implants and first – in – man clinical investigation in esthetic and restorative medicine. *International Journal of Pharmaceutics*, in press.



## REFERENCES

- Iannitti, T.,** Bingölc, Ö. A., Rottignib, V., Palmierib, B. (2013). A new highly viscoelastic hyaluronic acid gel: rheological properties, biocompatibility and clinical investigation in esthetic and restorative surgery. *International Journal of Pharmaceutics*, 456, 583-592.
- Ibrahim, S.,** Kang, Q. K., Ramamurthi, A. (2010). The impact of hyaluronic acid oligomer content on physical, mechanical, and biological properties of divinyl sulfone-crosslinked hyaluronic acid hydrogels. *Journal of Biomedical Materials Research*, 94A, 355-370.
- Jafari, B.,** Rafie, F., Davaran, S. (2011). Preparation and Characterization of a Novel Smart Polymeric Hydrogel for drug delivery of insulin. *BioImpacts*, 1(2), 135-143.
- Jansson, P.,** Kenne, L., Lindberg, B. (1975). Structure of extracellular polysaccharide from *Xanthomonas campestris*. *Carbohydrate Research*, 45, 275-282.
- Jeon, O.,** Song, S., Lee, K., Park, M., Lee, S., Hahn, S., Kim, S., Kim, B. (2007). Mechanical properties and degradation behaviors of hyaluronic acid hydrogels cross-linked at various cross-linking densities. *Carbohydrate Polymers*, 70, 251-257.
- Johl, S.S.,** Burgett, R.A. (2006). Dermal filler agents: a practical review. *Current Opinion in Ophthalmology*, 17, 471-9.
- John, H.E.,** Price, R.D., 2009. Perspectives in the selection of hyaluronic acid fillers for facial wrinkles and aging skin. *Patient Preference and Adherence*, 3, 225-230.
- Kablik, J.,** Monheit, G., Yu, L., P.H.D., Chang, G., Gershkovich, J. (2009). Comparative physical properties of hyaluronic acid dermal fillers. *Dermatology Surgery*, 35, 302-312.
- Kandasamy, R.,** Shaikh, S., Khalil, P., Muneera, M.S. & Thusleem, O.A. (2013). Determination of sodium hyaluronate in pharmaceutical formulations by HPLC-UV. *Journal of Pharmaceutical Analysis*, 3(5), 324-329.
- Kang, J. Y.,** Chung, C. W., Sung, J. H., Park, B. S., Choi, J. Y., Lee, S. J., et al. (2009). Novel porous matrix of hyaluronic acid for the three-dimensional culture of chondrocytes. *International Journal of Pharmaceutics*, 369, 114-120.
- Kaufmann, J.,** Mohle, K., Hofmann, H., Arnold, K. (1998). Molecular dynamics study of hyaluronic acid in water. *Journal of molecular structure (Theochem)*, 422, 109-121.
- Kenne, L.,** Gohil, S., Nilsson, E., Karlsson, A., Ericsson, D., Kenne, A., Nord, L. (2013). Modification and cross-linking parameters in hyaluronic acid hydrogels- Definitions and analytical methods. *Carbohydrate Polymers*, 91, 410- 418.
- Kim, J. K.,** Lee, J. S., Jung, H. J., Cho, J. H., Heo, J. I., Chang, Y. H. (2007). Preparation and properties of collagen/modified hyaluronic acid hydrogel for biomedical application. *Journal of Nanoscience and Nanotechnology*, 7, 3852-3856.

## REFERENCES

- Kim, I.L.,** Mauck, R.L., Burdick, J.A. (2011). Hydrogel design for cartilage tissue engineering: a case study with hyaluronic acid. *Biomaterials*, 32, 8771–82.
- Kupiec, T.** (2004). Quality-Control Analytical Methods: High Performance Liquid Chromatography. *International Journal of Pharmaceutical Compounding*, 8-3, 223-227.
- Lai, J.** (2014). Relationship between structure and cytocompatibility of divinyl Sulfone cross-linked hyaluronic acid. *Carbohydrate Polymers*, 101, 203-212.
- Lai, J.** (2012). Solvent Composition is Critical for Carbodiimide Cross-Linking of Hyaluronic Acid as an Ophthalmic Biomaterial. *Materials*, 5, 1986-2002.
- Leach, J.,** Bivens, K., Patrick, C., Jr., Schmidt, C. (2003). Photocrosslinked hyaluronic acid hydrogels: Natural, biodegradable tissue engineering scaffolds. *Biotechnology and Bioengineering*, 82(5), 578–589.
- Lee, F.,** Chung, J.E., Kurisawa, M. (2009). An injectable hyaluronic acid-tyramine hydrogel system for protein delivery. *Journal of Control Release*, 134 (3), 186-193.
- Lepperdinger, G.,** Fehrer, C., Reitingner, S. (2004). Biodegradation of hyaluronan. In H. G. Garg, & C. A. Hales (Eds.), *Chemistry and biology of hyaluronan* (pp. 71–82). Oxford: Elsevier Ltd.
- Limberg, M.B.,** McCaa, C., Kissling, G.E., Kaufman, H.E. (1987). Topical application of hyaluronic acid and chondroitin sulfate in the treatment of dry eyes. *American Journal of Ophthalmology*, 103, 194–7.
- Linhardt, R.J.,** Liu, J., Han, X.J. (1993). Mapping and sequencing of oligosaccharides by electrophoresis. *Trends in Glycoscience and Glycotechnology*, (5), 181–192.
- Linhardt, R.J.,** Pervin, A. (1996). Separation of acidic carbohydrates by capillary electrophoresis. *Journal of Chromatography*, (720), 323–335.
- Liu, L.,** Liu, D., Wang, M., Du, G., Chen, J. (2007). Preparation and characterization of sponge-like composites by cross-linking hyaluronic acid and carboxymethyl cellulose sodium with adipic dihydrazide. *European Polymer Journal*, 43, 2672–2681.
- Loewe, N.J.,** Maxwell, A., Loewe, P., Duick, M.G., Shan, K. (2001). Hyaluronic acid skin fillers: adverse reactions and skin testing. *Journal of the American Academy of Dermatology*, 45, 930-3.
- Luo Y,** Kirker KR, Prestwich GD (2000) Cross-linked hyaluronic acid hydrogel films: new biomaterials for drug delivery. *Journal of Control Release* 69 : 169–84.
- Malson, T.,** Lindqvist, B. (1986). Gels of crosslinked hyaluronic acid for use as a vitreous humor substitute. WO1986000079.
- Manna, F.,** Dentini, M., Desideri, P., De Pita, O., Mortilla, E., Maras, B. (1999). Comparative chemical evaluation of two commercially available derivatives of hyaluronic acid (Hylaform from rooster combs and Restylane from streptococcus) used for soft tissue augmentation. *Journal of the European Academy of Dermatology and Venereology*, 13, 183-192.

## REFERENCES

**Mao, W.,** Thanawiroon, C., Linhardt, R. (2002). Capillary electrophoresis for the analysis of glycosaminoglycans and glycosaminoglycan- derived oligosaccharides. *Biomedical Chromatography*, (16) 77-94.

**Masters KS,** Shah DN, Leinwand LA, Anseth KS (2005) Crosslinked hyaluronan scaffolds as a biologically active carrier for valvular interstitial cells. *Biomaterials* 26: 2517–25.

**Medscape Dermatology.** (2008). Dermal Fillers: Focus on Hyaluronic Acid. [www.medscape.org/viewarticle](http://www.medscape.org/viewarticle)

**Medvedovici, A.,** Farca, A., David, V. (2009). Derivatization reactions in liquid chromatography for drug assaying in biological fluids. *Advances in chromatography*,47, 283–314.

**Mellergaard, M.,** Larsen, M., Malle, B. (2011). Rheological properties of cross-linked hyaluronic acid for dermal fillers. *Annual Transaction of The Nordic Rheology Society*, 19.

**Micheels, P.** (2001). Human anti-hyaluronic acid antibodies. Is it possible?. *Dermatologic Surgery*, 27,185-91.

**Nakagawa, Y.,** Nakasako, S., Ohta, S., Ito, T. (2015). A biocompatible calcium salt of hyaluronic acid grafted with polyacrylic acid. *Carbohydrate Polymers*, 117, 43-53.

**Narins, R.S.,** Bowman, P.H. (2005). Injectable skin fillers. *Clin Plast Surg*, 32, 151-162.

**Necas, J.,** Bartosikova, L, Brauner, P., Kolar, J. (2008). Hyaluronic acid (hyaluronan): a review. *Journal of Veterinary Medicine*, 53, 397–411

**Nimni, M.E.,** Cheung, D., Strates, B., Kodama, M., & Sheikh, K. (1987). Chemically modified collagen: a natural biomaterial for tissue replacement. *Journal of Biomedical Materials Research*, 21,741–71.

**Palumbo, F. S.,** Pitarresi, G., Mandracchia, D., Tripodo, G., Giammona, G. (2006). *Carbohydrate Polymers*, 66, 379–385. Pouyani, T., Harbison, G. S., & Prestwich, G. D. (1994). *Journal of the American Chemical Society*, 116(17), 7515–7522.

**Park, H.,** Guo, X., Temenoff, J., Tabata, Y., Caplan, A., Kasper, F., Mikos, A. (2009). Effect of swelling ratio of injectable hydrogel composites on chondrogenic differentiation of encapsulated rabbit marrow mesenchymal stem cells *in vitro*. *Biomacromolecules*, 10(3), 541-546.

**Pastorini, E.,** Rotini, R., Guardigli, M., Vecchiotti, S., Persiani, S., Trisolino, G., Antonioli, D., Rovati, L.C., Roda, A. (2009). Development and validation of a HPLC–ES-MS/MS method for the determination of glucosamine in human synovial fluid. *Journal of Pharmaceutical and Biomedical Analysis*, 50, 1009–1014.

**Pelletier, S.,** Hubert, P., Lapique, F., Payan, E., Dellacherie, E. (2000). Amphiphili derivatives of sodium alginate and hyaluronate: Synthesis and physico-chemical properties of aqueous dilute solutions. *Carbohydrate Polymers*, 43(4), 343–349.

## REFERENCES

**Piron, E.,** Tholin, R., 2002. WO2002006350.

**Pitarresi, G.,** Palumbo, F.S., Tripodo, G. Cavallaro, G., & Giammona, G. (2007). Preparation and characterization of new hydrogels based on hyaluronic acid and  $\alpha$ ,  $\beta$ -polyaspartylhydrazide. *European Polymer Journal*, 43, 3953-3962.

**Prata, J.,** Barth, T., Bencherif, S., Washburn, N. (2010). Complex fluids based on methacrylated hyaluronic acid. *Biomacromolecules*, 11(3), 769–775.

**Prestwich, G.,** Marecak, D., Marecek, J., Vercruyse, K., Ziebell, M., (1998). Controlled chemical modification of hyaluronic acid: synthesis, applications, and biodegradation of hydrazide derivatives. *Journal of Controlled Release*, 53, 93–103.

**Raghu, S.,** Athre, MD. (2007). Facial filler agents. *Operative Techniques in Otolaryngology*, 18, 243-247.

**Reddy, K.,** Karunakaran, K. (2013). Purification and characterization of hyaluronic acid produced by *Streptococcus zooepidemicus* strain 35237. *Journal of BioScience and Biotechnology*, 2(3), 173-179.

**Reissig, J.L.,** Strominger, J.L., Leloir, L.F. (1995). A modified colorimetric method for the estimation of N-acetylamino sugars. *Journal of Biological Chemistry*, 270, 959-996.

**Rhodes, J.M.,** Simons, M. (2007). The extracellular matrix and blood vessel formation; not just a scaffold. *Journal of Cellular and Molecular Medicine*, 11,176-205.

**Robinson, D.,** Aasi, S.(2011).Cosmetic concerns and management strategies to combat aging. *Maturitas*, 70, 256-260.

**Rosiak, J. M. &** Yoshii, F. (1999) Hydrogels and their medical applications. *Nuclear Instruments and Methods in Physics Research B* 151, 56-64.

**Romagnoli, M.,** Belmontesi, M. (2008). Hyaluronic acid-based fillers: theory and practice. *Clinics in Dermatology*, 26, 123-159.

**Ruckmani, K.,** Shaikh, S., Khalil, P., Muneera, M., Thusleem, O.A. (2013). Determination of sodium hyaluronate in pharmaceutical formulation by HPLC-UV. *Journal of Pharmaceutical Analysis*, 3 (5), 324-329.

**Sadick, N.,** Karcher, C., Palmisano, L. (2009). Cosmetic dermatology of the aging face. *Clinics in Dermatology*, 27, S3-S12.

**Sánchez-Carpintero.** Candelas, D., Ruiz-Rodríguez, R. (2010). Dermal Fillers: Types, Indications, and Complications. *Actas Dermo-Sifiliográficas*, 101(5), 381–393.

## REFERENCES

- Satish, C.S.,** Satish, K.P., Shivakumar, H.G. (2006). Hydrogels as controlled drug delivery system: synthesis, crosslinking, water and drug transport mechanism. *Indian Journal of Pharmaceutical Sciences*, 68 (2), 133-140.
- Schanté, C.,** Zuber, G., Herlin, C., Vandamme, T. (2012). Improvement of hyaluronic acid enzymatic stability by the grafting of amino-acids. *Carbohydrate Polymer*, 87, 2211-2216.
- Schante, C.,** Zuber, G., Herlin, C., Vandamme, T. (2011). Chemical modification of hyaluronic acid for the synthesis of derivatives for a broad range of biomedical application. *Carbohydrate polymers*, 85, 469-489.
- Schanté, C.,** Zuber, G., Herlin, C., Vandamme, T. (2011). Synthesis of N-alanyl-hyaluronamide with high degree of substitution for enhanced resistance to hyaluronidase-mediated digestion. *Carbohydrate Polymers*, 86, 747-752.
- Scott, J.E.** (1995). Extracellular matrix, supramolecular organization and shape. *Journal of Anatomy*, 187, 259-69.
- Scott, J.E.** (1989). Secondary structures in hyaluronan solutions: chemical and biological implications. *Ciba Foundation J*, 143, 6–20.
- Segura, T.,** Anderson, B. C., Chung, P. H., Webber, R. E., Shull, K. R., Shea, L. D. (2005). Crosslinked hyaluronic acid hydrogels: A strategy to functionalize and pattern. *Biomaterials*, 26, 359–371.
- Serban, M.,** Yang, G., Prestwich, G. (2008). Synthesis, characterization and chondroprotective properties of a hyaluronan thioethyl ether derivative. *Biomaterials*, 29, 1388-1399.
- Sherman, L.** (May2004). Rheometers : Which type is right for you?. *Plastic Technology*.  
[www.ptonline.com/articles/rheometers-which-type-is-right-for-you](http://www.ptonline.com/articles/rheometers-which-type-is-right-for-you)
- Šimković, I.,** Hricovíni, M., Šoltés, L., Mendichi, R., Cosentino, C. (2000). Preparation of water-soluble/insoluble derivatives of hyaluronic acid by cross-linking with epichlorohydrin in aqueous NaOH/NH<sub>4</sub>OH solution. *Carbohydrate Polymers*, 41, 9–14.
- Sung, H.W.,** Huang, R.N., Huang, L.L.H., Tsai, C.C., Chiu, C.T. (1998). Feasibility study of a natural crosslinking reagent for biological tissue fixation. *Journal of Biomedical Materials Research*, (42), 560–7.
- Tan, H.,** Chu, C., Payane., K., Marra., K. (2009). Injectable in situ forming biodegradable chitosan-hyaluronic acid based hydrogels for cartilage tissue engineering. *Biomaterials*, 2499-2506.
- Vejlens, L.** (1971). Glycosaminoglycans of human bone tissue. *Calcified Tissue International*, 7, 175–90.
- Verpaele, A.,** & Strand, A. (2006). Restylane Sub Q, a non-animal stabilized hyaluronic acid gel for soft tissue augmentation of the mid- and lower face. *Aesthetic Surgery*, 26,10-17.
- Water, J.,** Schack, M., Velazquez-Campoy, A., Maltesen, M., Van de Weert, M., Jorgensen, L. (2014). Complex coacervates of hyaluronic acid and lysozyme: Effect on protein structure and physical stability. *European Journal of Pharmaceutics and Biopharmaceutics*, 88, 325-331.

## REFERENCES

- Weng, L.,** Gouldstone, A., Wu, Y., Chen, W. (2008). Mechanically strong double network photocrosslinked hydrogels from N,N-dimethylacrylamide and glycidyl methacrylated hyaluronan. *Biomaterials*, 29(14), 2153–2163.
- Wollina, U.,** Goldman., A. (2013). Dermal fillers: Facts and controversies. *Clinics in Dermatology*, 31, 731-736.
- Wong, R.,** Ashton, M., Dodou, K. (2015). Effect of crosslinking agent concentration on the properties of unmedicated hydrogels. *Pharmaceutics*, 7, 305-319.
- Xu, S.,** Li, J., He, A., Liu, W., Jiang, X., Zheng, J., Han, C., Hsiao, B., Chu, B., Fang, D. (2009). Chemical cross-linking and biophysical properties of electrospun hyaluronic acid based ultra-thin fibrous membranes. *Polymer*, 50, 3762-3769.
- Yamanlar, S.,** Sant, S., Boudou, T., Picart, C., Khademhosseini, A. (2011). Surface functionalization of hyaluronic acid hydrogels by polyelectrolyte multilayer films. *Biomaterials*, 32, 5590–9.
- Yokoi, N.,** Komuro, A., Nishida, K., Kinoshita, S. (1997). Effectiveness of hyaluronan on corneal epithelial barrier function in dry eye. *British Journal of Ophthalmology*, 81, 533–6.
- Yoon, I. S.,** Chung, C. W., Sung, J. H., Cho, H. J., Kim, J. S., Shim, W. S., et al. (2011). Proliferation and chondrogenic differentiation of human adipose-derived mesenchymal stem cells in porous hyaluronic acid scaffold. *Journal of Bioscience and Bioengineering*, 112(4), 402–408.
- Zarzycki, R.,** Modrzejewska, Z., Nawrotek, K. (2010). Drug release from hydrogel matrices. *Ecological chemistry and engineering*, 17 (2), 117-136.
- Zawko, S.,** Suri, S., Truong, Q., Schmidt, C. (2009). Photopatterned anisotropic swelling of dual-crosslinked hyaluronic acid hydrogels. *Acta. Biomaterialia*, 5, 14–22.
- Zhao, X.** (2000). Process for the production of multiple cross-linked hyaluronic acid derivatives. WO/2000/046253.
- Zhong, S.P.,** Campoccia, D., Doherty, P.J., Williams, R.L., Benedetti, L., Williams, D.F. (1994). Biodegradation of hyaluronic acid derivatives by hyaluronidase. *Biomaterials*, 15, 359- 365.
- Zhu, J.,** Marchant, R. (2011). Design properties of hydrogel tissue-engineering scaffolds. *Expert Review of Medical Devices*, 8(5), 607-626.
- Zhu, J.** (2010). Bioactive modification of poly(ethylene glycol) hydrogels for tissue engineering. *Biomaterials*, 31, 4639-4.

# APPENDICES

## **Appendix 1:** Introduction to the analytical instruments employed for the characterization of HA hydrogels

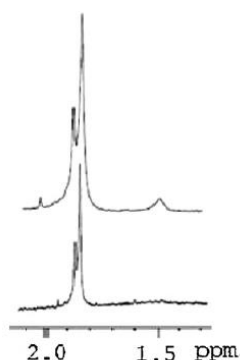
### **1.1 Fourier transform infrared (FTIR)**

FTIR spectroscopy is a powerful method for identification of functional groups of molecules by evaluating the transition between vibrational states of bonds within the molecule (Reddy & Karunakaran, 2013). When sample is introduced into the FTIR spectrometer, some radiation is absorbed by the sample and some of it is passed through, the resulting spectrum represents a molecular fingerprint of the sample. Therefore, it is mainly used to confirm the occurrence of cross-linking bonds rather than quantitative analysis. With FTIR measurements, HA sample does not require a tedious preparation method and the spectra may be recorded between  $4000\text{-}400\text{ cm}^{-1}$  ( $2.5\text{-}25\text{ }\mu\text{m}$ ). A typical FTIR spectrum of HA solution shows three main peaks corresponding to the presence of C-H stretching, O-H stretching and C-O-C stretching. All these peaks present a characteristic spectrum and could differentiate the native HA and cross-linked HA hydrogel (Pitarresi et al., 2007).

### **1.2 Nuclear magnetic resonance spectroscopy (NMR)**

NMR spectrometry is a common method used to confirm the presence of crosslinking and to determine the total change of chemical modification occurred within HA polymer. The pretreatment of samples is essential, because dissolution of cross-linked HA hydrogels in NMR solvents becomes challenge. The NMR spectrum of native HA dissolved in  $\text{D}_2\text{O}$  shows broad signals due to the high viscosity of HA solution (Schante, Zuber, Herlin, & Vandamme, 2011).

Dissolution of cross-linked hydrogels has also been reported in DMSO-d<sub>6</sub>/D<sub>2</sub>O mixture ( Palumbo et al., 2006 ; Guarise, Pavan, Pirrone & Renier, 2012). (Appendix 1.2 A) shows a typical <sup>1</sup>H NMR spectra comparing native HA and cross-linked BDDE-HA hydrogel carried out by (Guarise, Pavan, Pirrone & Renier, 2012). In the cross-linked HA, a signal appearing at 1.8 ppm attributed to N-CH<sub>3</sub> of HA and also a peak at approximately 1.5 ppm which represents the –(CH<sub>2</sub>)<sub>2</sub> of BDDE. However, in the native HA, there is no peak appearing at 1.5 ppm, these data confirmed that the HA hydrogel had been modified with BDDE molecules.



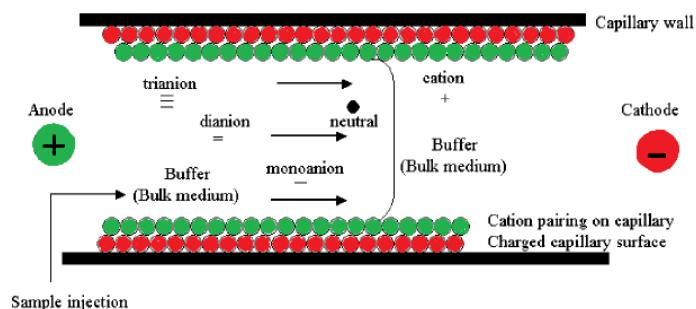
**Appendix 1.2 A** NMR spectra of native HA (lower) and BDD-HA (higher) (Guarise, Pavan, Pirrone & Renier, 2012)

### 1.3 Capillary electrophoreses (CE)

Capillary electrophoreses (CE) is a high resolution analytical technique that has been widely used for the analysis of disaccharide compositional molecules particularly glycosaminoglycans (GAGs) in the biological samples (Linhardt , Liu & Han, 1993). CE has a different mechanism of analysis and it is used to separate ions according to their electrophoretic mobility under the influence of an applied voltage across a field that the ions exist. The ions of opposite charge to electrodes on either end of the voltage migrate toward that electrode in a narrow capillary tube which is made of fused silica and provides a flat flow due to electroosmotic flow. At a high voltage, ions that are positively charged migrate toward the negatively charged electrode (the cathode) and the negative ions migrate to the positively charged electrode (the anode).



The rate of migration of each single ion is based on its quantity of charge compared to its relative hydrodynamic size. Electrophoretic mobility is the term used to describe ions affinity for its opposite electrode. The rate of migration is directly proportional to the applied voltage. If the sample contains neutral and ionic analytes, the electroosmotic flow drives all species from the injector to the detector through the capillary eluting first the positive species followed by the neutral and later the negative (Linhardt & Pervin, 1996). On the other hand, if two ions have same size, the one with greater charge moves faster and for ions with the same charge, the smaller size migrates first due to its less friction. A typical capillary electrophoresis system consists of a voltage power supply, a capillary tube, a sample introduction system and a detector. Two different analysis mode are applied for the analysis of GAGs which are normal polarity mode and reversed polarity mode. The normal polarity mode as shown in (appendix. 1.3 A) is the most common analysis mode by which the sample is injected at the anode and detected at the cathode.



**Appendix 1.3 A** Diagram showing capillary electrophoresis separation mechanism of neutral and charged species by normal polarity mode (Wenjun, Thanawiroon & Linhardt, 2002)

Hyaluronic acid can be identified and detected by CE following various reported methods. The one which is well-established, is that when hyaluronic acid is analyzed in normal polarity mode and detected by direct UV detection at wavelength 185-214 nm. The HA oligomers migrate at a buffer of phosphate borate, pH 9.0 containing sodium dodecyl sulfate. Identification and separation of hyaluronic acid from synovial fluid and vitreous humor can be analyzed by this method.

The migration of HA, however, is affected by the interaction with proteins, but adding sodium dodecyl sulfate may decrease such interaction (Grimshaw et al., 1994). Despite the ability of CE for oligosaccharides separation, a well-designed and efficient method for quantification of cross-linked BDDE-HA fragments by the CE has not yet been established. So, we used it as a confirmation tool for the occurrence of cross-linking reaction in the cross-linked BDDE-HA hydrogels when compared with native HA.

#### **1.4 High performance liquid chromatography (HPLC)**

HPLC is a separation technique used to separate mixtures into their components based on their molecular structures. HPLC is better than normal column chromatography for oligosaccharides separation, because the solvent is allowed to drip through the column under a high pressure force than under gravity. So, it is widely employed for the evaluation of *in-vitro* degradation rate of HA hydrogels and also to confirm the occurrence of cross-linking process. HPLC involves a stationary phase (commonly column filled with non-polar silica) and a mobile phase (polar solvent) carrying the components of the mixture. A stronger interaction is displayed between the solvent and the polar components, thus they will travel through the column more quickly than less polarity-components (Kupiec, 2004). Different chromatographic methods have been developed for quantification of HA content in pharmaceutical formulations or to separate HA oligosaccharides following a digestion procedure. Determination of HA oligosaccharides by HPLC is a challenge and is largely influenced by method conditions (e.g. mobile phase, pH and the concentration of buffer) which affect sensitivity, linearity, accuracy and retention time. Therefore, for the development of a robust HPLC method, different compositions of the mobile phase have to be tested to reduce the overlapping and to obtain best signal response for HA fragments. Some HPLC methods were established with post-chromatographic derivatization reactions. However, the HA products obtained with this process are not stable and have a short half-life due to the possible spontaneous intermolecular rearrangement (Medvedovici, Farca, & David, 2009). A novel chromatographic method with no pre-analytical derivatization step for HA analysis was developed by (Pastorini et al., 2009).

The method was set for the determination of glucosamine in human synovial by HPLC coupled with electro-spray tandem mass spectrometry. The analyte was separated using 10 mM acetic acid in water with ammonia and acetonitrile under isocratic elution at 0.3 ml/min flow rate. On the other hand, the analysis of HA components by HPLC coupled with UV detector has also become a challenge. This problem, fortunately, was overcome by developing a size- exclusion liquid chromatography (SEC) with UV detection using variable wavelength set at 205 nm (Ruckmani et al., 2013). The method was performed on an isocratic mode with a mobile phase consisting of buffer 0.05 M potassium dihydrogen phosphate and the pH was adjusted at 7.0. In our study, we applied HPLC for the quantification of *N*-acetyl glucosamine (NAG) remaining in the cross-linked BDDE-HA hydrogel after a specific treatment with the enzyme “ hyaluronidase “. High (NAG) content in the tested extract indicated faster degradation rate and lower cross-linking efficiency.

### **1.5 The scanning electron microscope (SEM)**

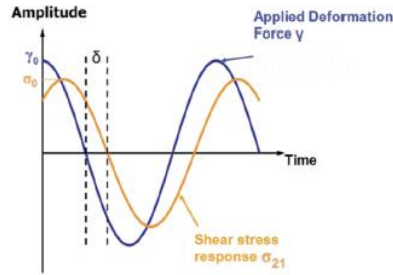
The scanning electron microscope (SEM) is a microscope that uses electrons to create a magnified image for advanced characterization of polymers. The electrons are generated at the top of microscope and then directed down the column toward the sample. Secondary electrons are then emitted that contain information about sample surface composition. In this study, we used the SEM to characterize the morphology (form and structure) of native HA and cross-linked BDDE-HA hydrogels (Esposito et al., 2005). The cross-linked hydrogels display different porous structure and cohesively as a result of the degree of cross-linking. The SEM images of native HA show some collapse within their substrate structures and wider pores-size comparing to the cross-linked hydrogels synthesized at high degrees of cross-linking (Gatta et al., 2013).

### **1.6 Rheometer**

Rheometer is a mechanical spectrometer used to measure deformation and flow of materials under applied force. The Measurement includes various physical properties such as: viscosity, shear stress, storage modulus ( $G'$ ) and loss modulus ( $G''$ ).

The storage modulus measures the stored energy representing the elastic portion in viscoelastic materials, whereas the loss modulus measures the energy dissipated as heat representing the viscous portion in viscoelastic materials. Rheometer provides also an effective indication about critical gel point, the point when the material changes from a viscoelastic liquid to a viscoelastic solid during cross-linking reaction. The rheometers are of two types: rotational that work with controlled stress or strain and extensional that work with extensional stress or strain. Most measurements of HA cross-linked hydrogels are performed on a rotational rheometer using a parallel geometry at controlled temperature of 25 °C. The rotational rheometer operates in continuous rotation and oscillations mode. It consists of a motor, optical encoder and torque-sensing mechanism. There are three types of stress attachments: cone and plate, plate and plate, or concentric cylinder (Sherman, 2004). The viscosity of HA solution varies with the shear rate, so it is classified as a shear rate – dependent material (Bingol & Dogan, 2012). Rheology has become a differentiating factor for cross-linked hydrogels, because it reflects the viscoelastic property. The native HA solution shows a different behavior than cross-linked HA when subjected to a frequency sweep test; the native HA behaves viscous at the lower frequency range, while at the higher range, it behaves elastic. However, the moduli of cross-linked hydrogels do not vary significantly with the frequency and show almost similar viscoelastic properties over the testing range (Mellergaard, Larsen & Malle, 2011).

This phenomenon is referred to the Maxwell-type behavior and single relaxation time, the storage  $G'$  and loss  $G''$  modulus in cross-linked hydrogels are independent of oscillation frequency (Omari et al., 2006 ; Gulrez, Al-Assaf & Phillips, 2011). Determinations of storage and loss moduli are usually carried out by Small Amplitude Oscillatory Strain (SAOS) measurements over a frequency range of (0.01-100 s<sup>-1</sup>) at a constant strain (appendix 1.6 A). However, a strain sweep test should initially be performed at a constant frequency over a strain amplitude ranged from 0.01-100% in order to determine the linear viscoelastic region (LVR) (Borrell, Leslie & Tezel, 2011).



**Appendix 1.6 A** Diagram of SAOS with deformation signal  $\gamma$ , response signal  $\sigma$  and phase shift  $\delta$ . (Bingol & Dogan, 2012)

When hydrogel sample is exposed to sinusoidal deformation at radial frequency  $\omega$ , there is a delay between excitation and the response known as phase shift  $\delta$ . From the experiment, the elastic modulus and the viscous modulus can be calculated according to the following equations:

$$G' = \frac{\sigma_0}{\gamma_0} \cdot \cos\delta$$

$$G'' = \frac{\sigma_0}{\gamma_0} \cdot \sin\delta$$

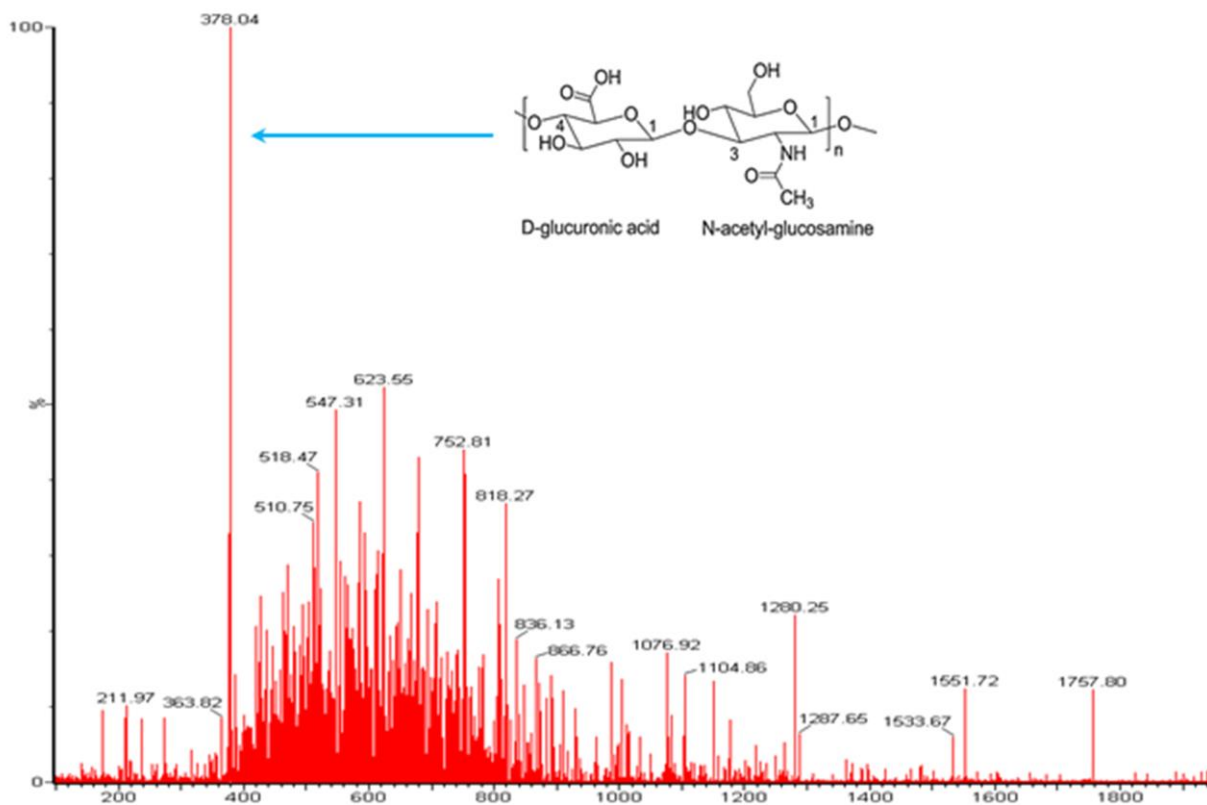
Where  $G'$  represents elastic or storage modulus,  $G''$  represents viscous or loss modulus,  $\gamma$  for strain or deformation,  $\sigma$  for stress or response,  $\delta$  for phase shift. In order to distinguish between different viscoelastic fluids, it is necessary to determine the loss tangent factor “ $\tan \delta$ ” that describes the ratio between the elastic and viscous share of polymer fluid according to the equation below. If “loss tangent  $\delta$ ” is greater than 1, the hydrogel is predominantly viscous and if it is smaller than 1, the hydrogel is predominantly elastic (Bingol & Dogan, 2012).

$$\tan \delta = \frac{G''}{G'}$$

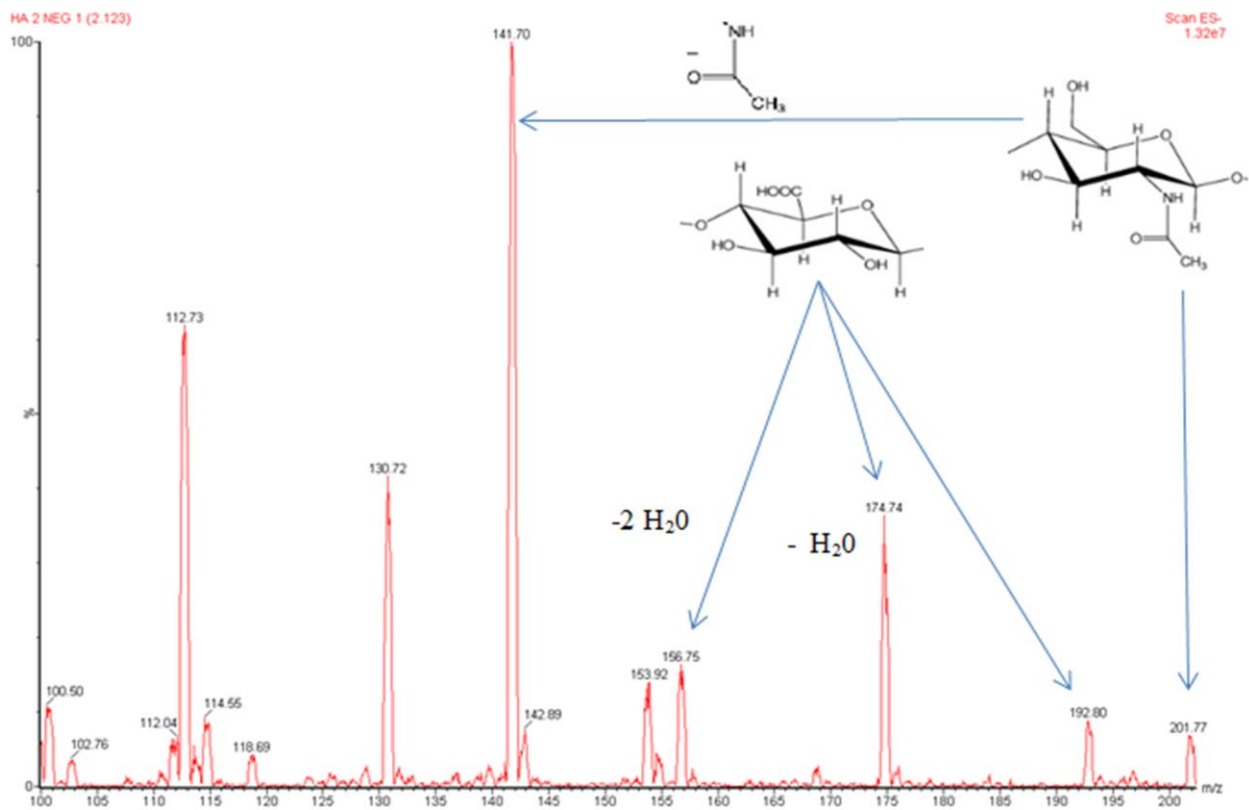
The viscoelastic property is highly correlated to the degree of cross-linking. It was stated by (Segura et al., 2005) that the complex modulus increases when the theoretical cross-links increases suggesting that the network with more cross-links becomes more resistance towards mechanical changes.

## Appendix 2: ESI-Mass spectrometry analysis

### 2.1 The MS spectrum of disaccharide unit of HA

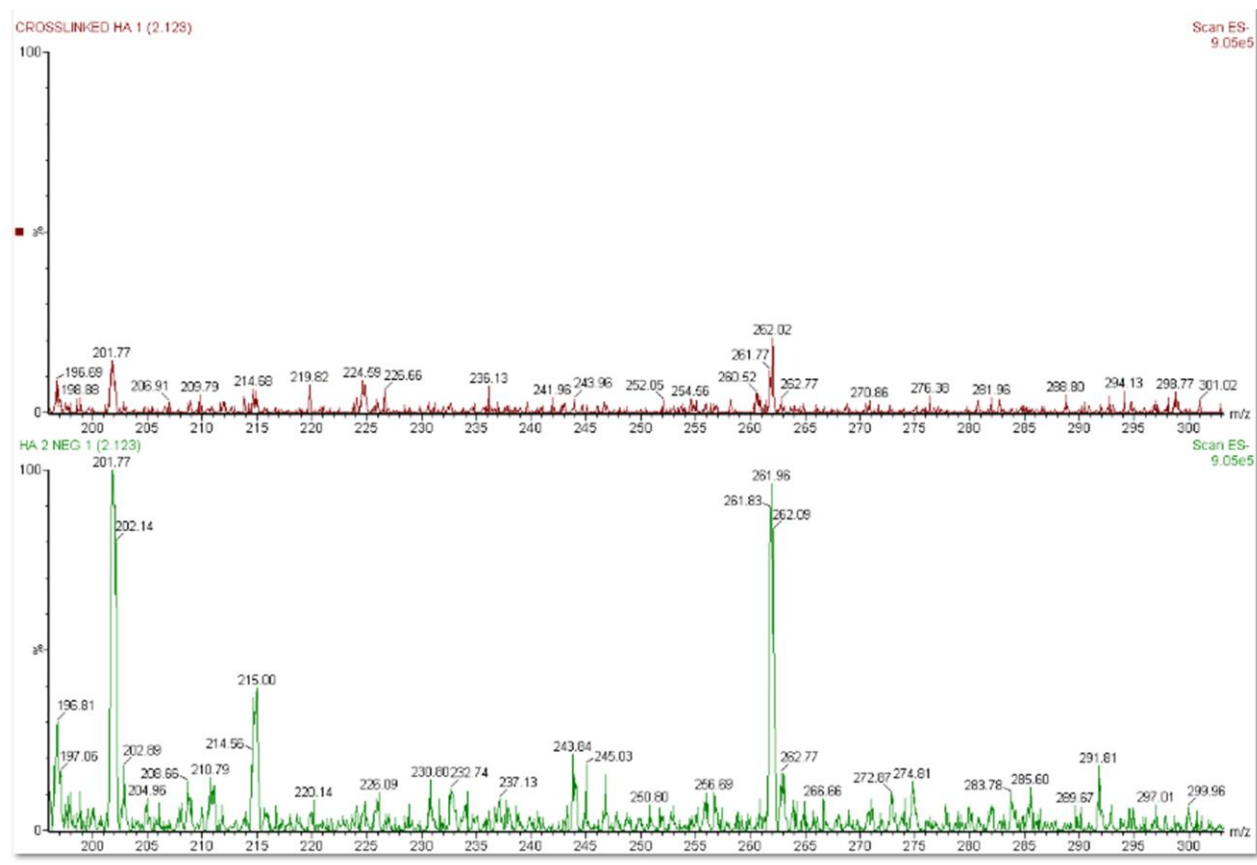


**Appendix 2. 1** A ESI-MS spectra of native HA showing the base peak of the disaccharide unit at m/z 378 with a singly charged negative ion  $[M-H]^-$



**Appendix 2. 1 B** ESI-MS spectra of native HA showing the peaks of the glucuronic acid (GlcA) at  $m/z$  192.8 and *N*-acetyl-D-glucosamine (GlcNAc - H<sub>2</sub>O) at  $m/z$  201.89

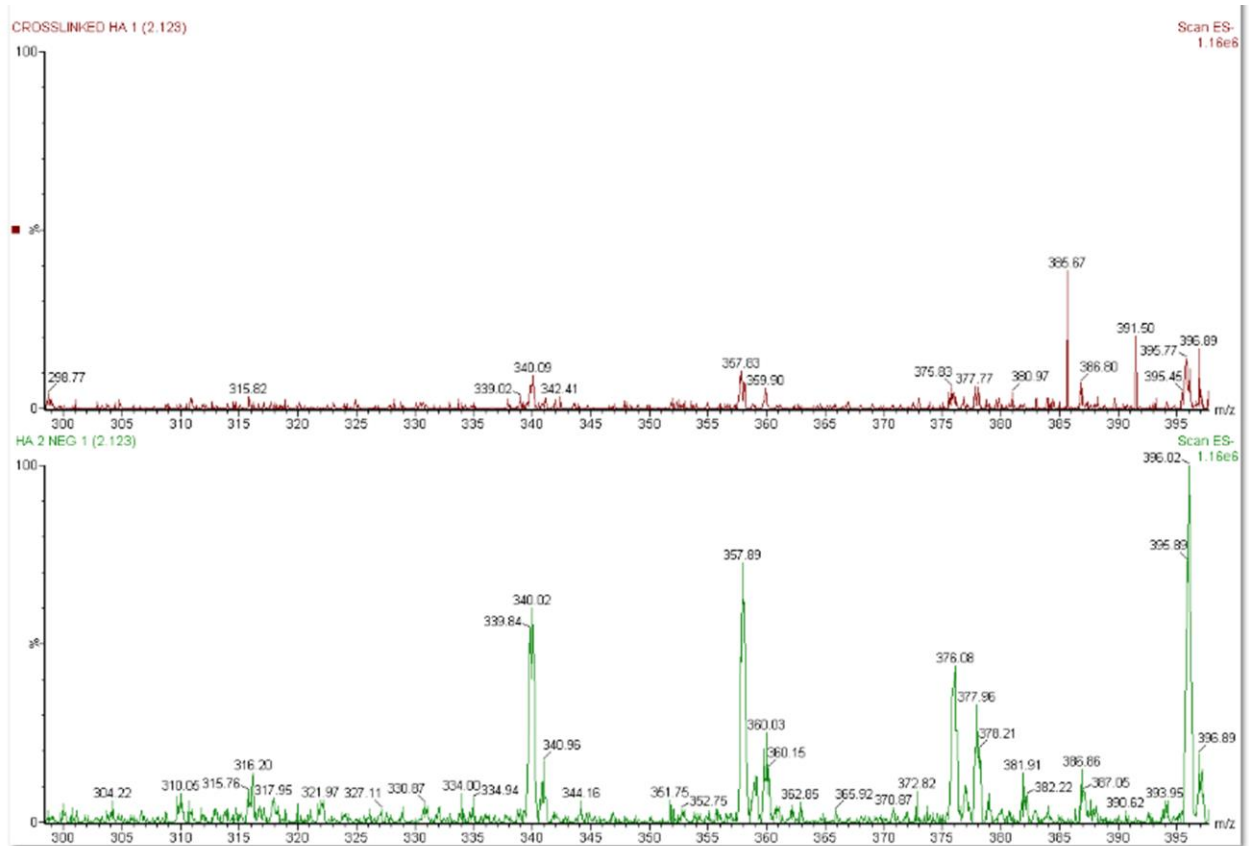
## 2.2 The MS spectrum of extended range of native and cross-linked hydrogel



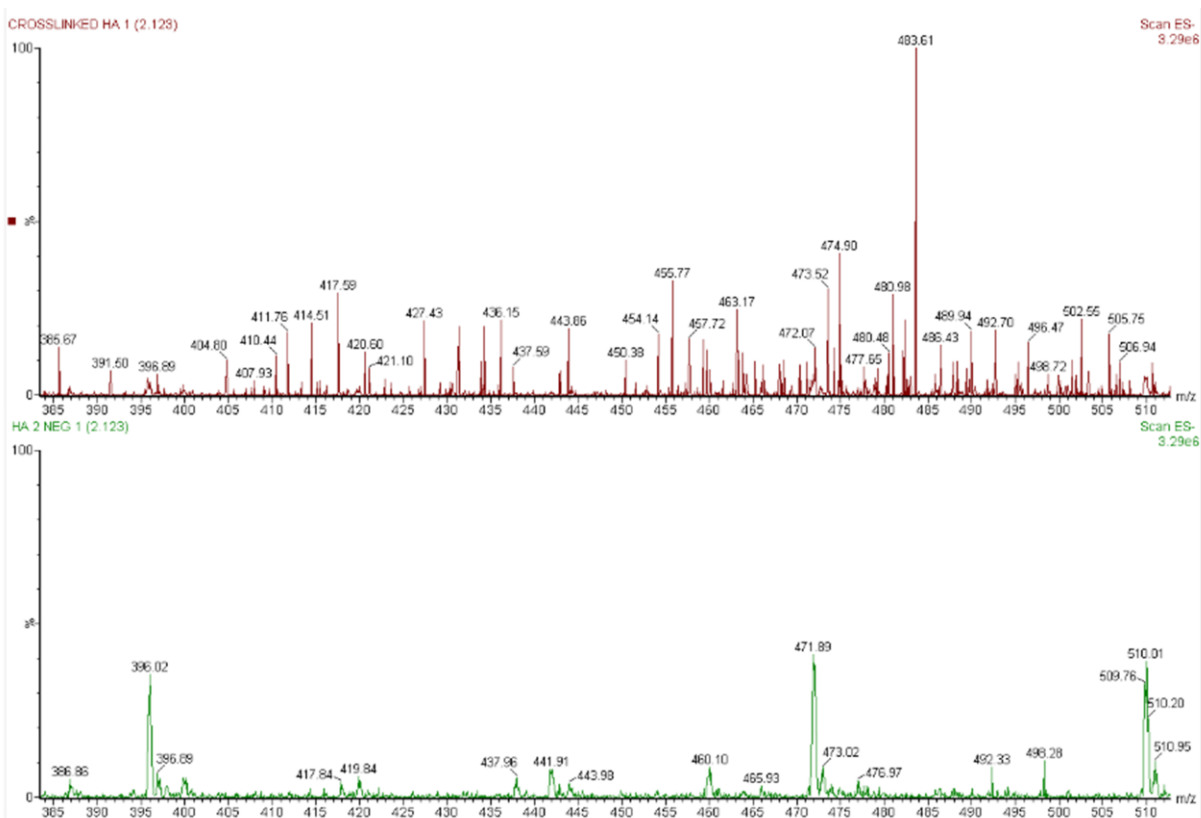
**Appendix 2. 2 A** ESI-MS spectra of extended range from  $m/z$  200 to  $m/z$  300 for native HA (green color) and cross-linked HA (red color)



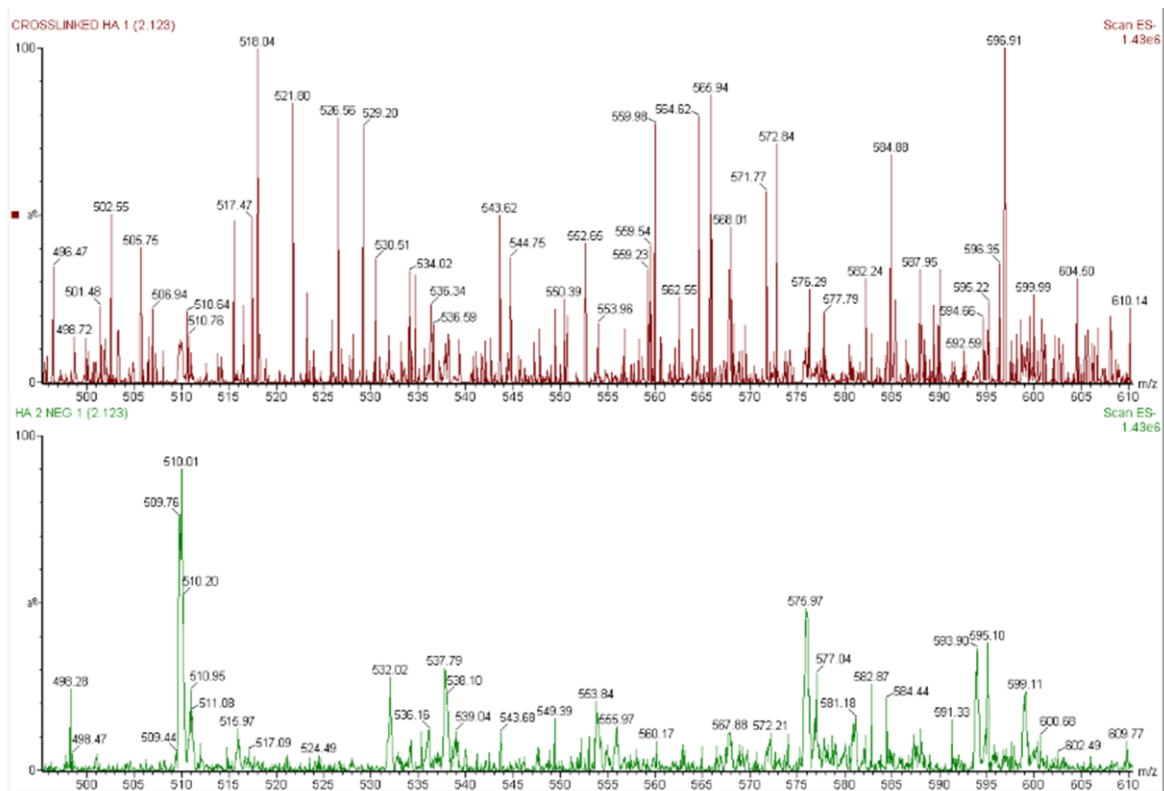
APPENDICES



**Appendix 2. 2 B** ESI-MS spectra of extended range from  $m/z$ . 300 to  $m/z$ . 400 for native HA (green color) and cross-linked HA (red color)



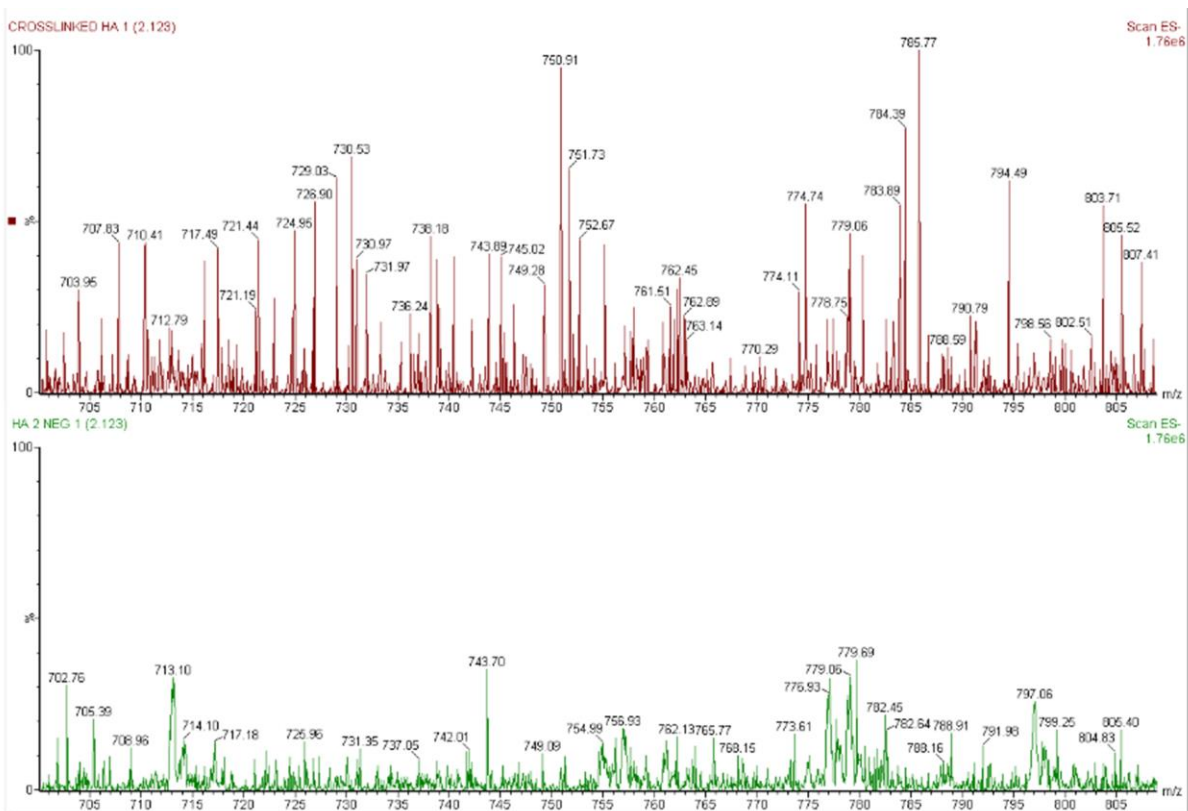
**Appendix 2. 2 C** ESI-MS spectra of extended range from  $m/z$  400 to  $m/z$  500 for native HA (green color) and cross-linked HA (red color)



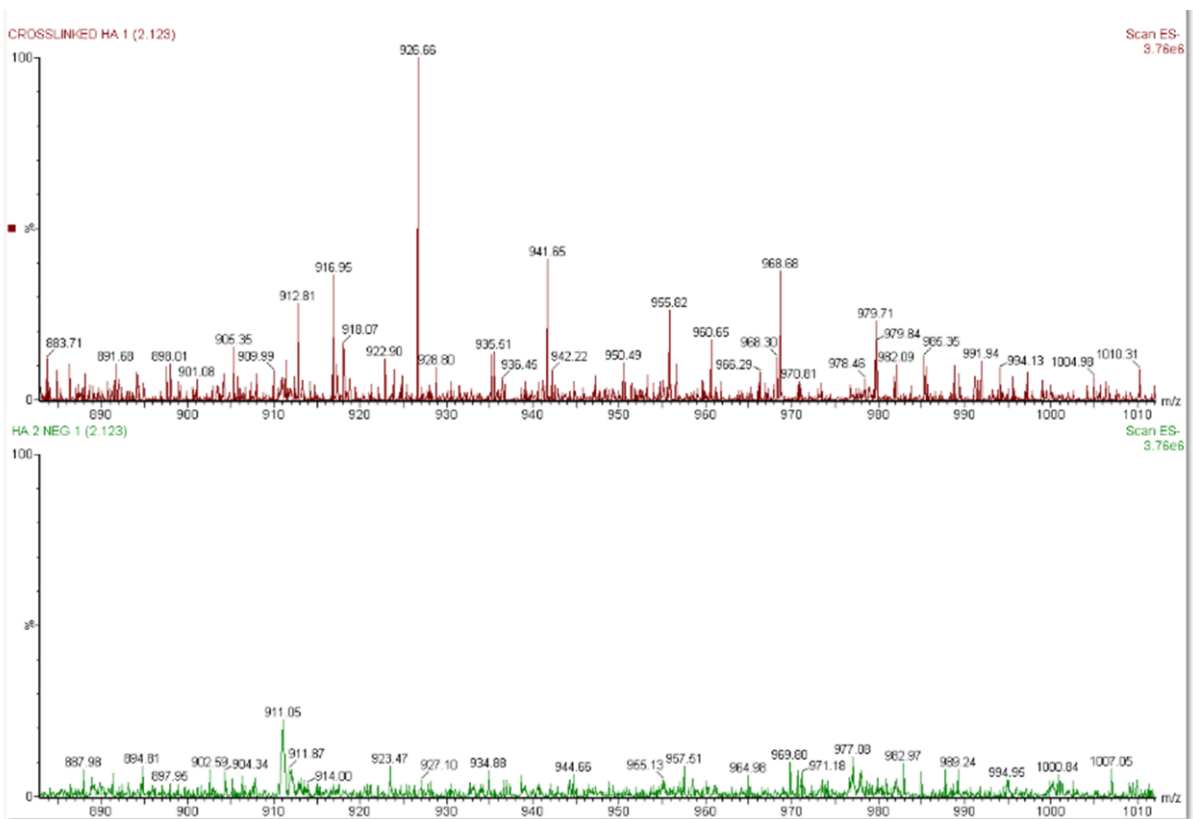
**Appendix 2. 2 D ESI-MS spectra of extended range from  $m/z$  500 to  $m/z$  600 for native HA (green color) and cross-linked HA (red color)**



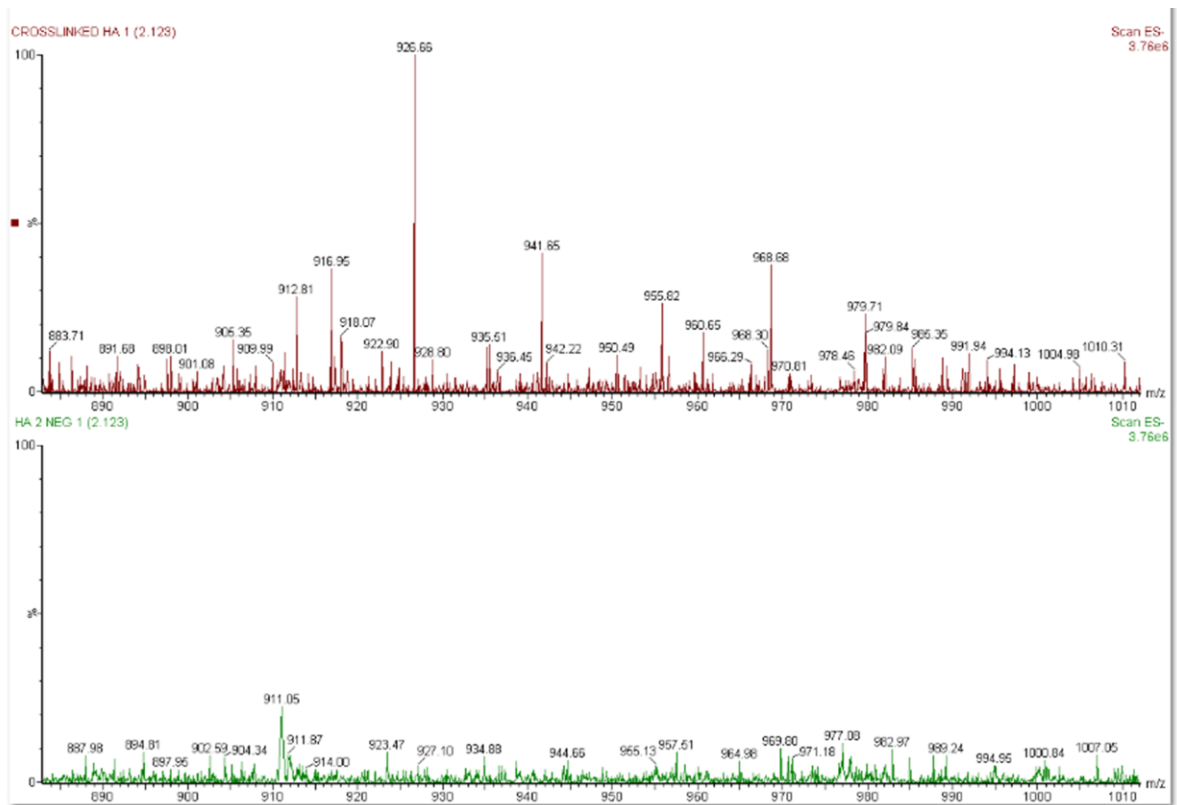
APPENDICES



**Appendix 2. 2 F** ESI-MS spectra of extended range from  $m/z$  700 to  $m/z$  800 for native HA (green color) and cross-linked HA (red color)

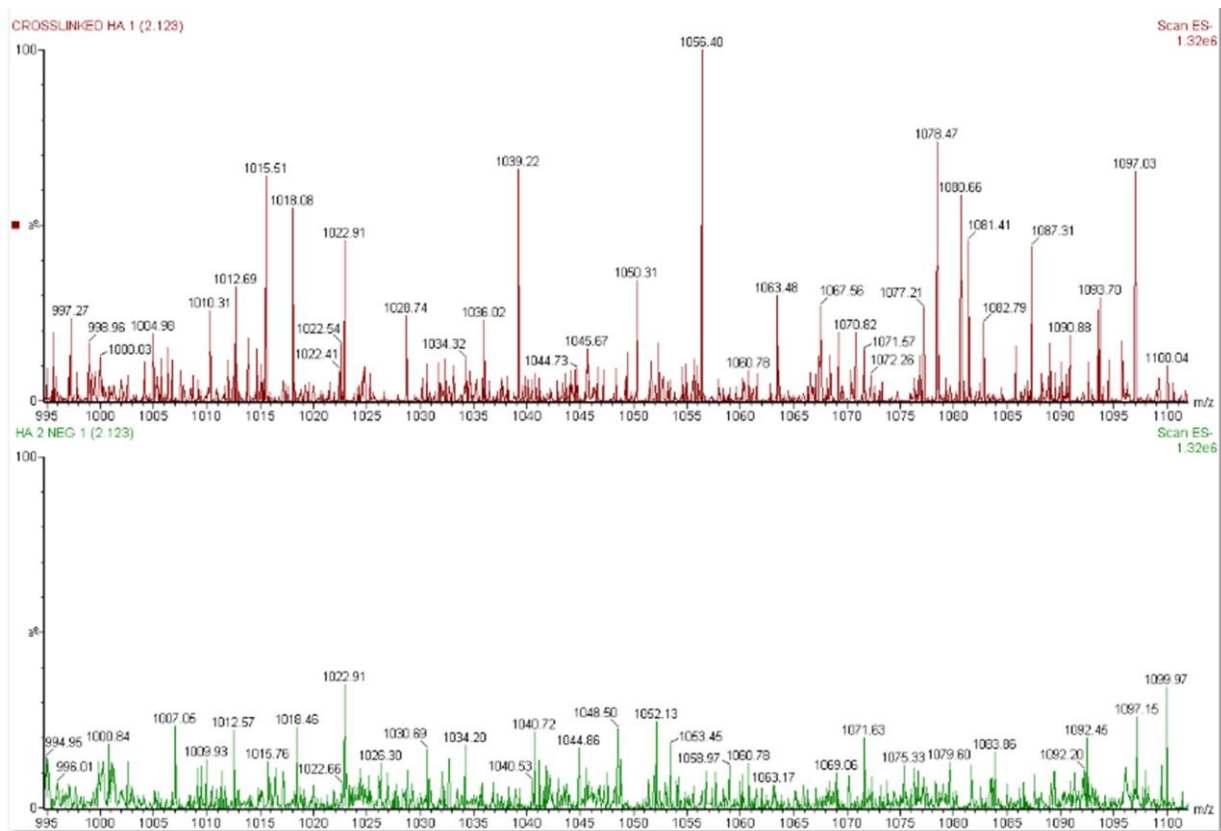


**Appendix 2. 2 G** ESI-MS spectra of extended range from  $m/z$  800 to  $m/z$  900 for native HA (green color) and cross-linked HA (red color)



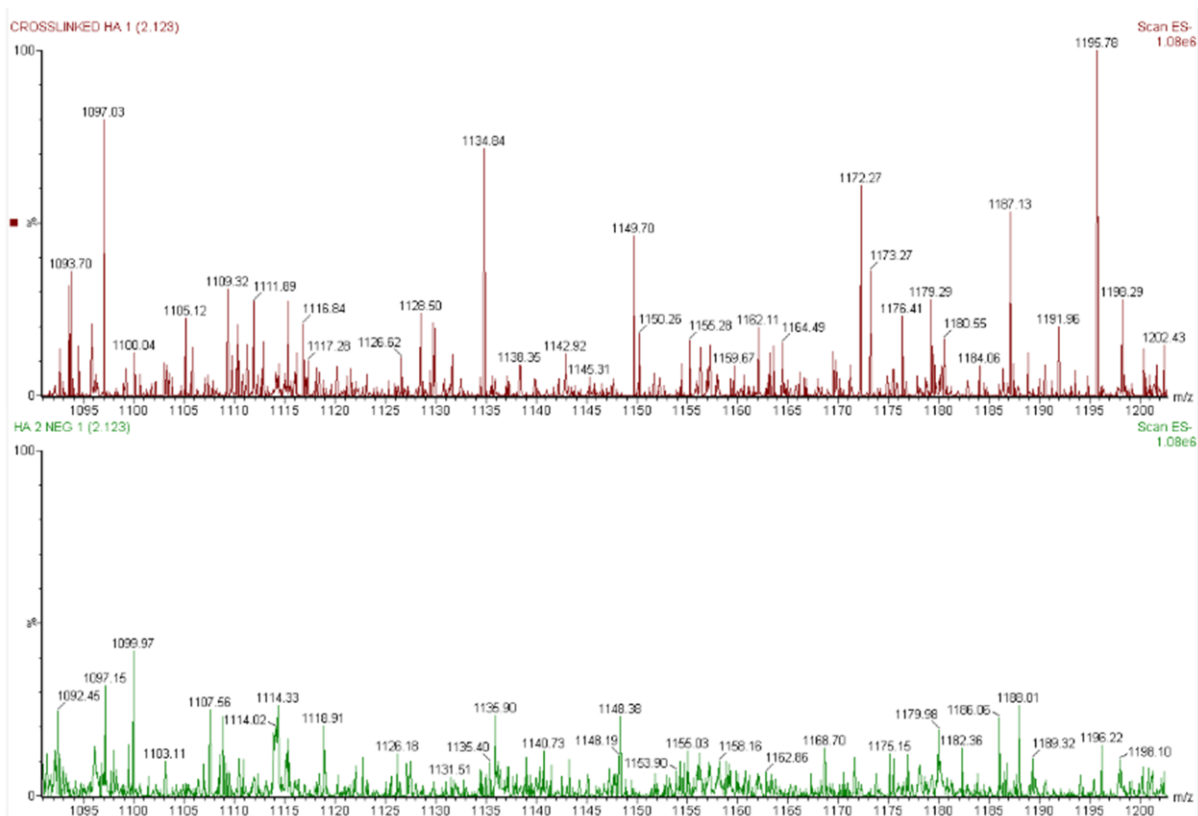
**Appendix 2. 2 H** ESI-MS spectra of extended range from  $m/z$  900 to  $m/z$  1000 for native HA (green color) and cross-linked HA (red color)

APPENDICES

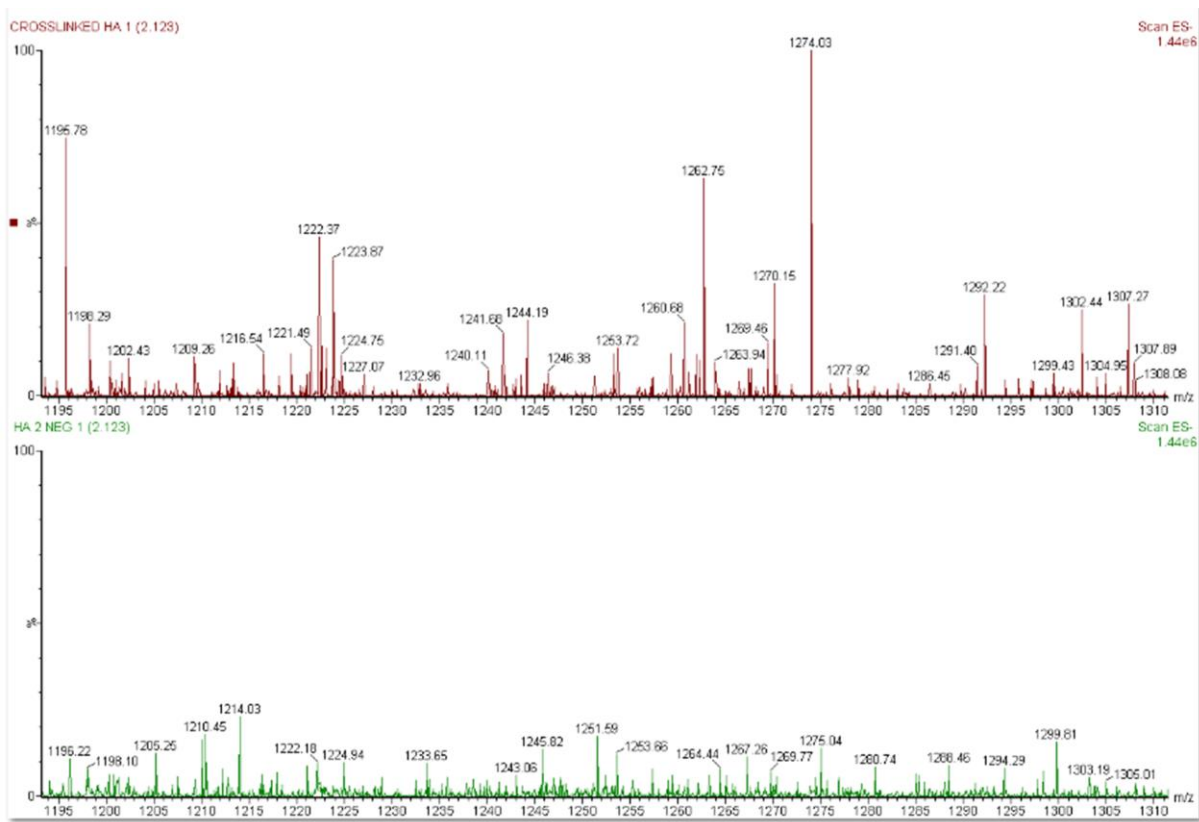


**Appendix 2. 2 I** ESI-MS spectra of extended range from  $m/z$  1000 to  $m/z$  1100 for native HA (green color) and cross-linked HA (red color)

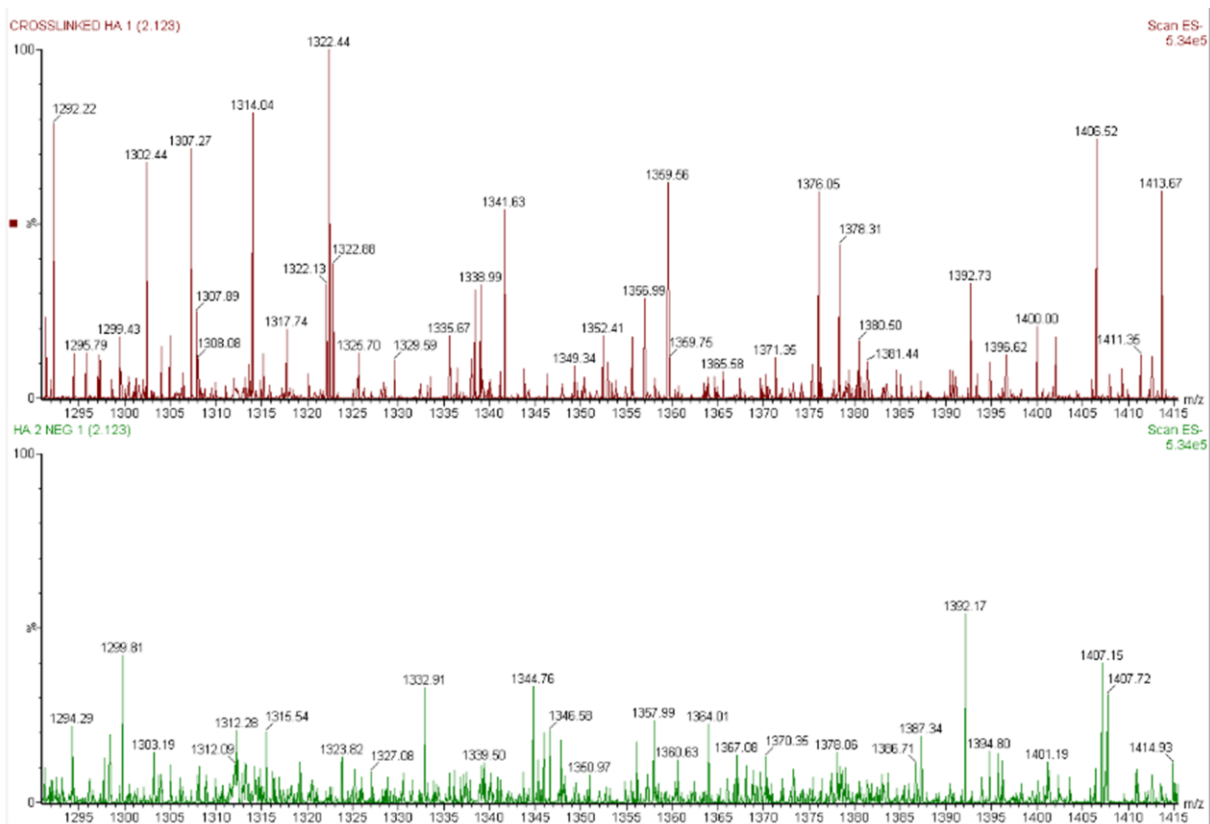




**Appendix 2. 2 J** ESI-MS spectra of extended range from  $m/z$  1100 to  $m/z$  1200 for native HA (green color) and cross-linked HA (red color)

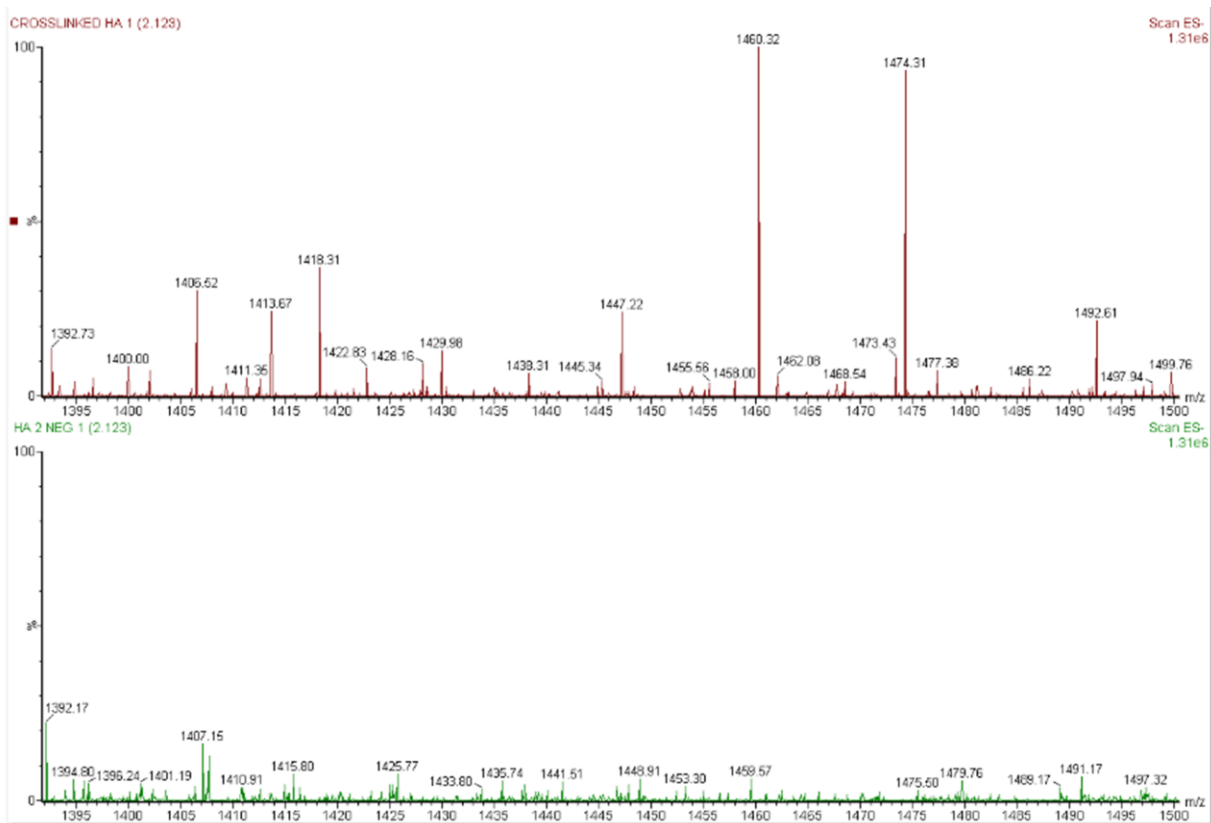


**Appendix 2. 2 K** ESI-MS spectra of extended range from  $m/z$  1200 to  $m/z$  1300 for native HA (green color) and cross-linked HA (red color)

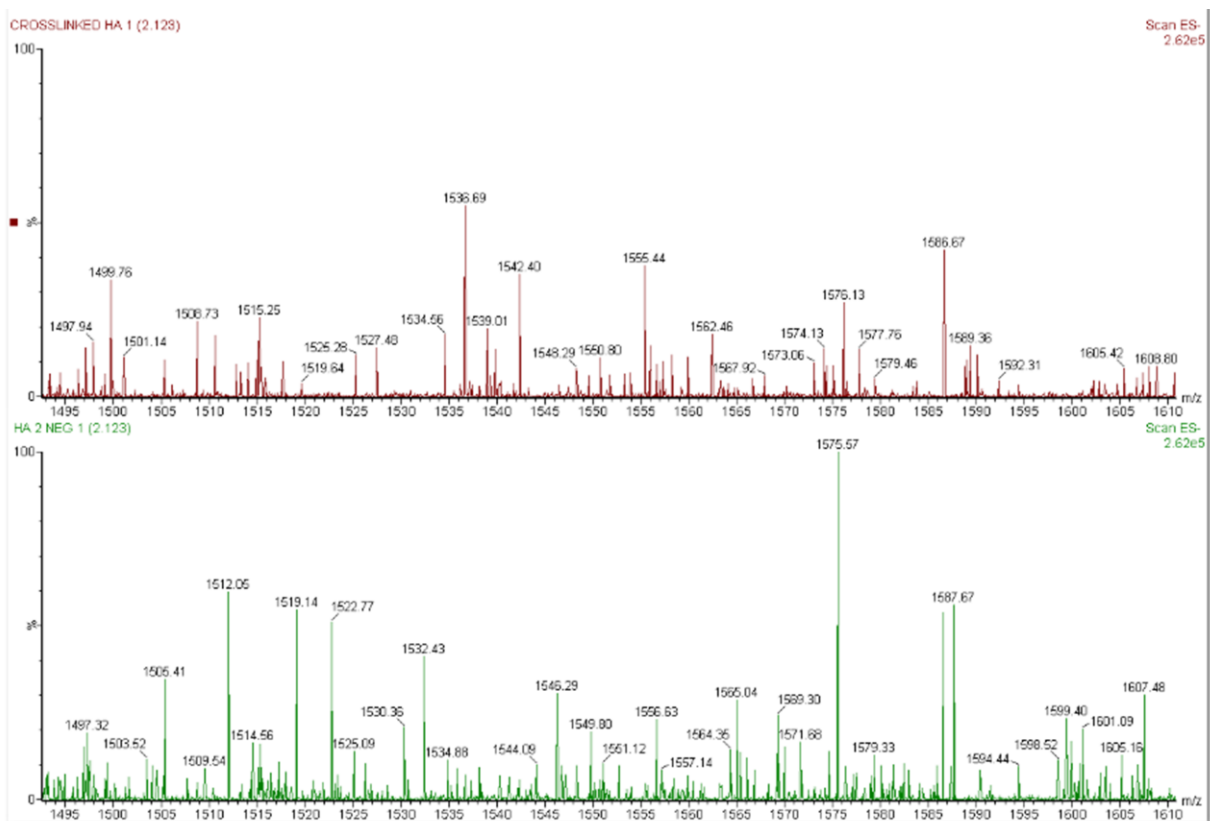


**Appendix 2. 2 L** ESI-MS spectra of extended range from  $m/z$  1300 to  $m/z$  1400 for native HA (green color) and cross-linked HA (red color)

APPENDICES

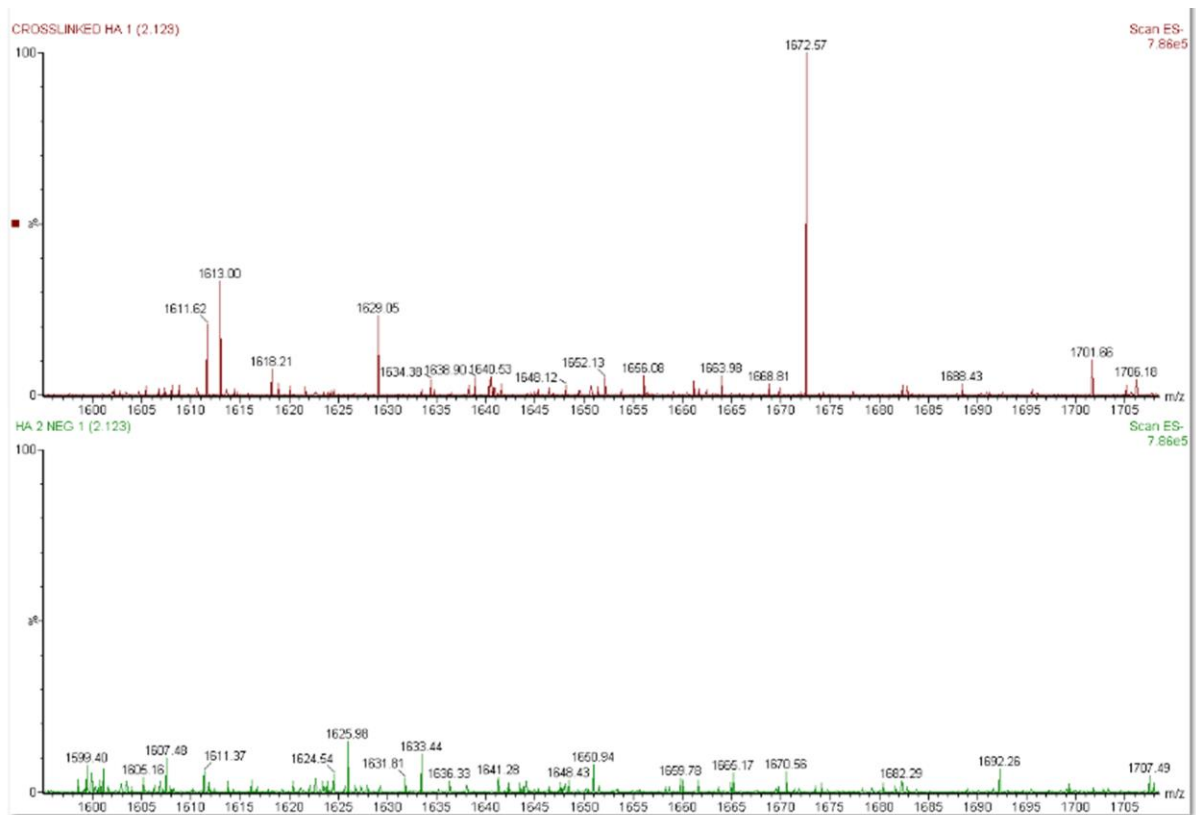


**Appendix 2.** 2 M ESI-MS spectra of extended range from  $m/z$  1400 to  $m/z$  1500 for native HA (green color) and cross-linked HA (red color)



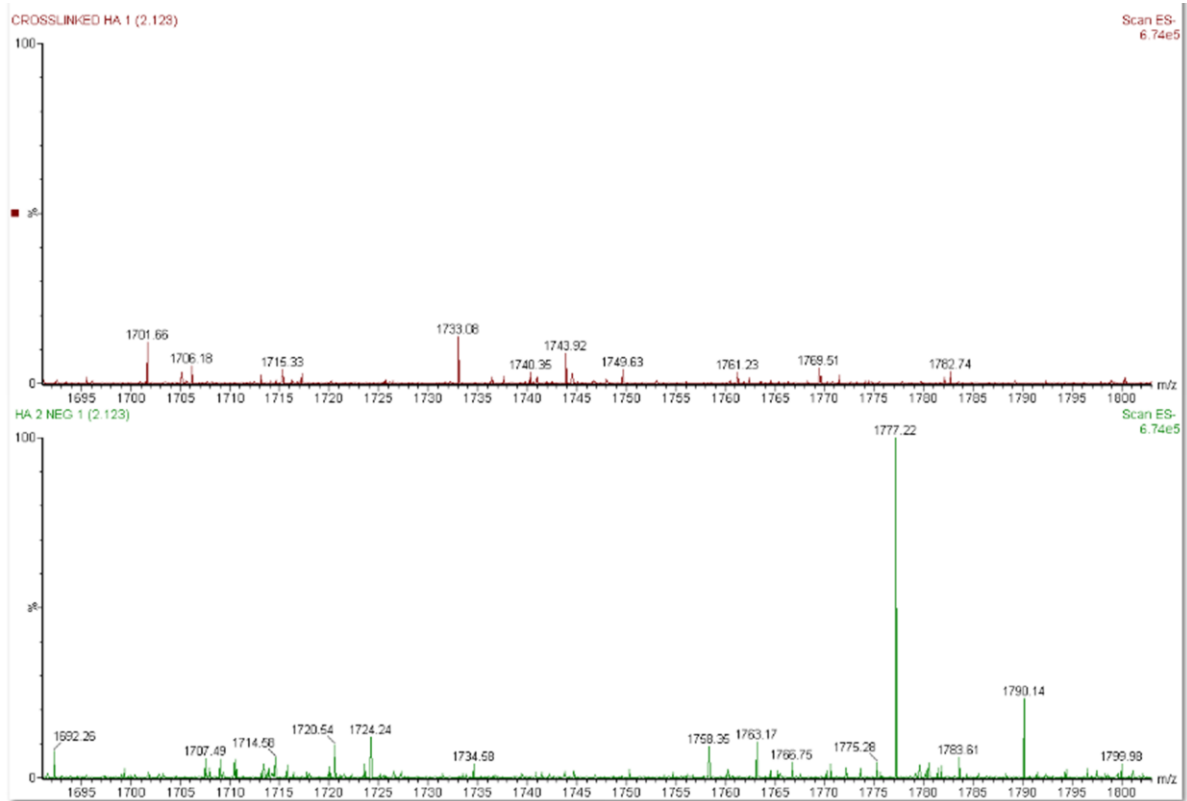
**Appendix 2. 2 N** ESI-MS spectra of extended range from  $m/z$  1500 to  $m/z$  1600 for native HA (green color) and cross-linked HA (red color)

APPENDICES



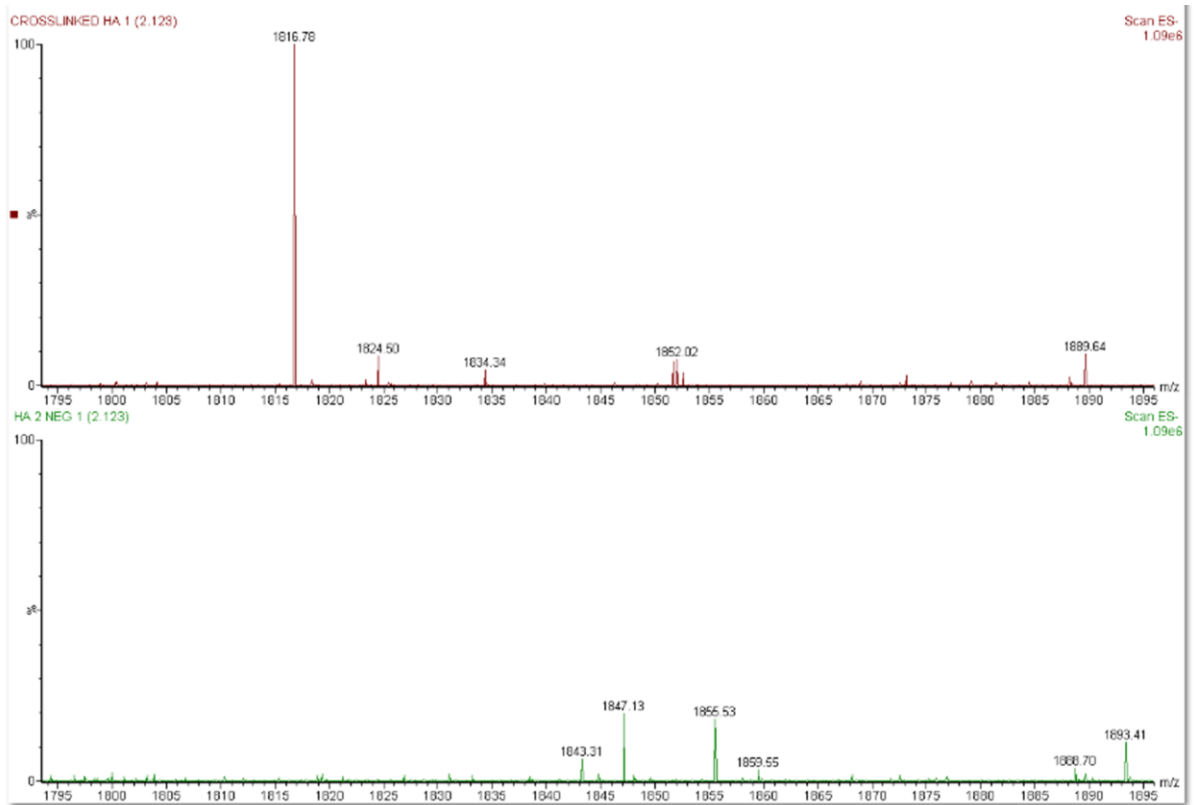
**Appendix 2. 2 O** ESI-MS spectra of extended range from  $m/z$  1600 to  $m/z$  1700 for native HA (green color) and cross-linked HA (red color)

APPENDICES



**Appendix 2. 2 P** ESI-MS spectra of extended range from  $m/z$  1700 to  $m/z$  1800 for native HA (green color) and cross-linked HA (red color)

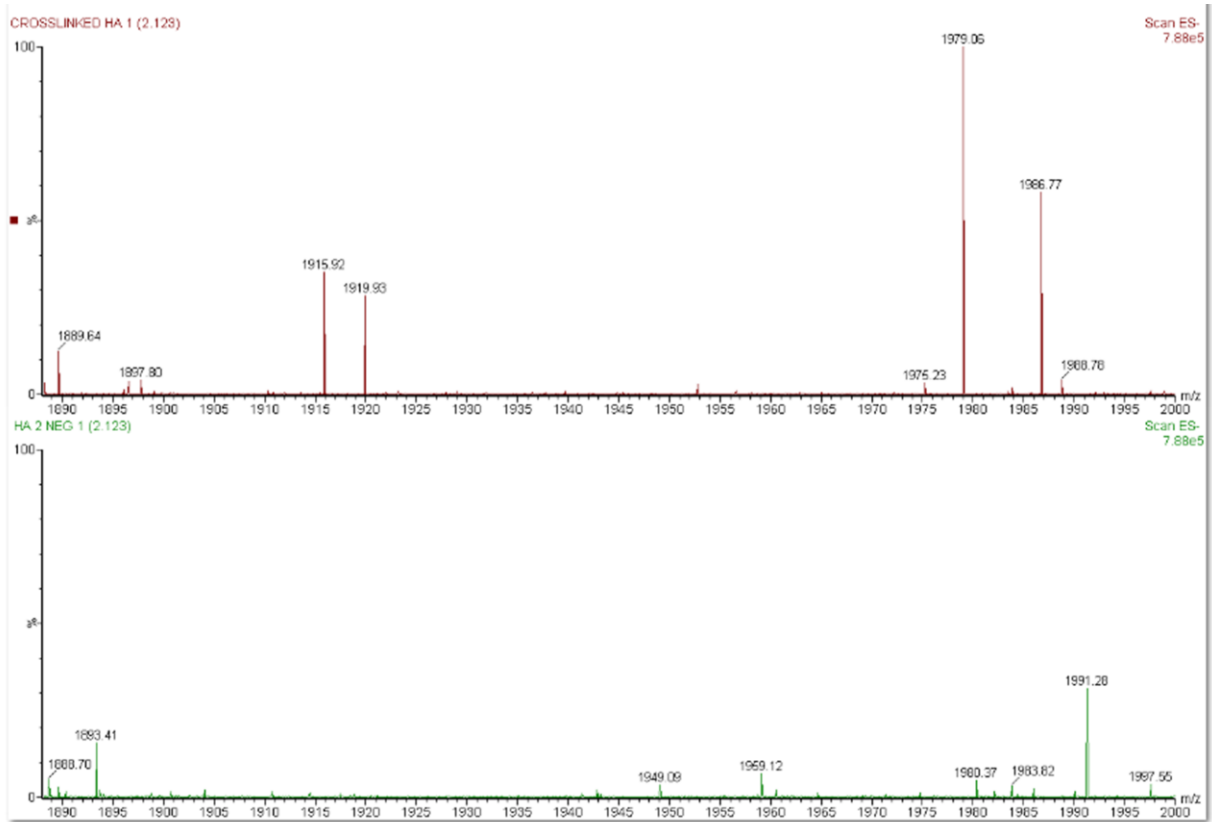
APPENDICES



**Appendix 2. 2 Q** ESI-MS spectra of extended range from  $m/z$  1800 to  $m/z$  1900 for native HA (green color) and cross-linked HA (red color)

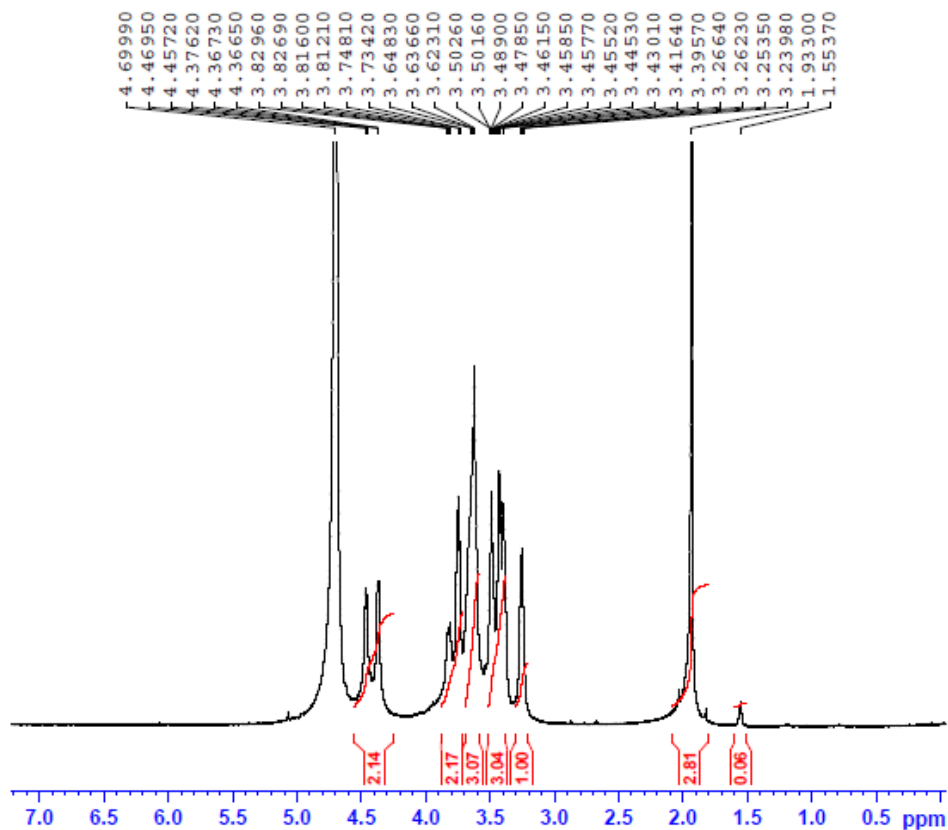


APPENDICES

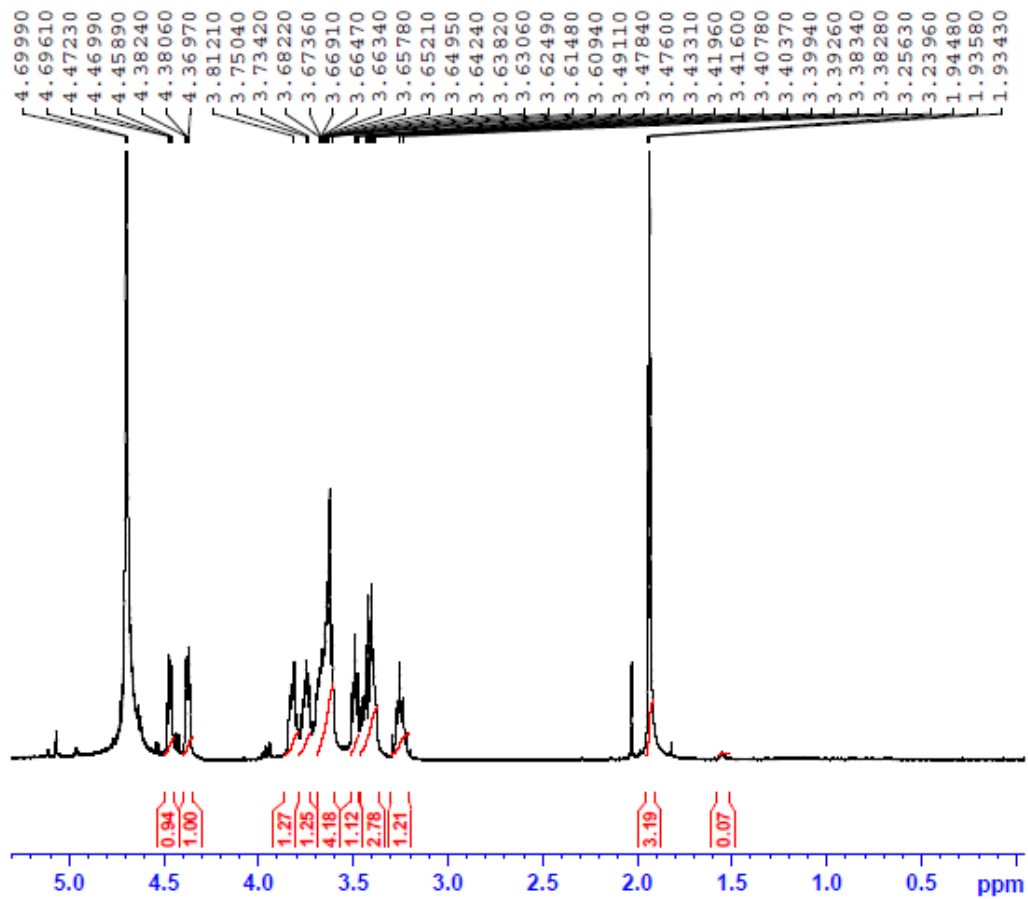


**Appendix 2. 2 R** ESI-MS spectra of extended range from  $m/z$  1900 to  $m/z$  2000 for native HA (green color) and cross-linked HA (red color)

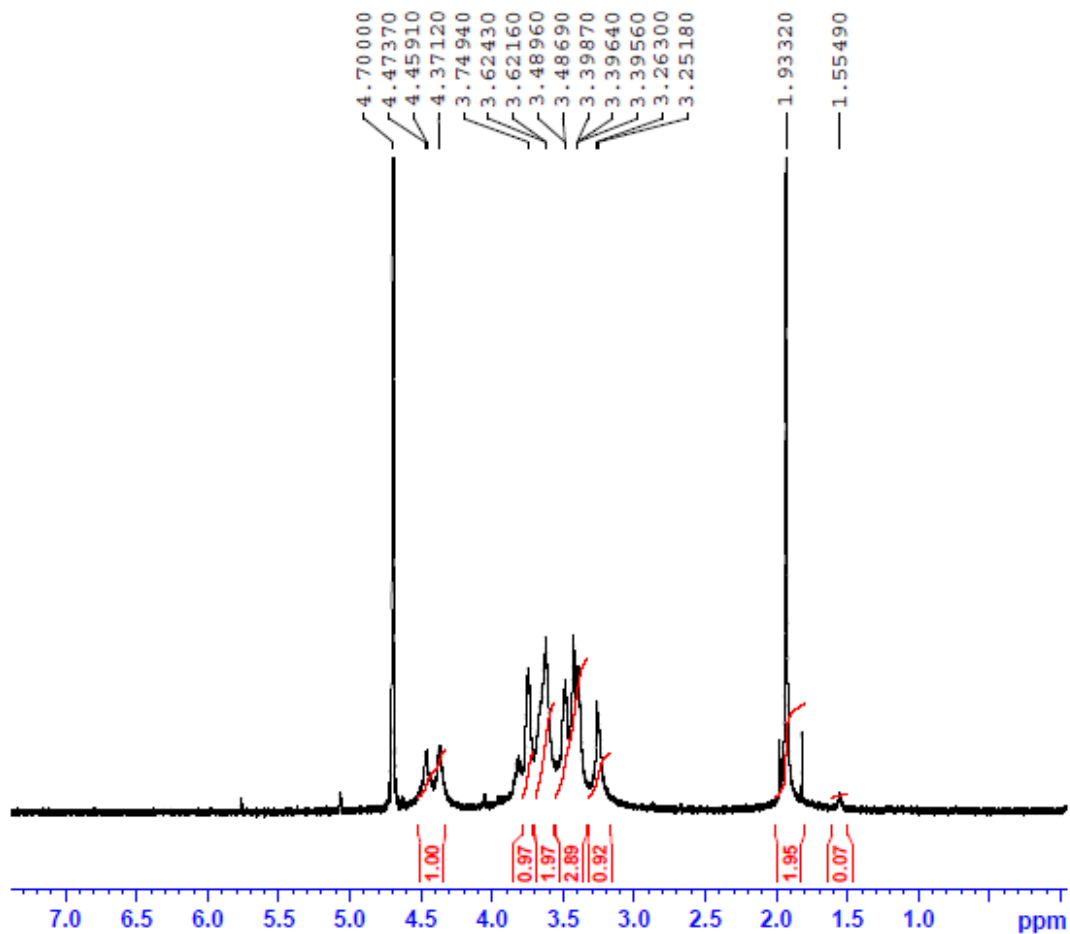
### Appendix 3: The relation between degree of modification and BDDE concentration.



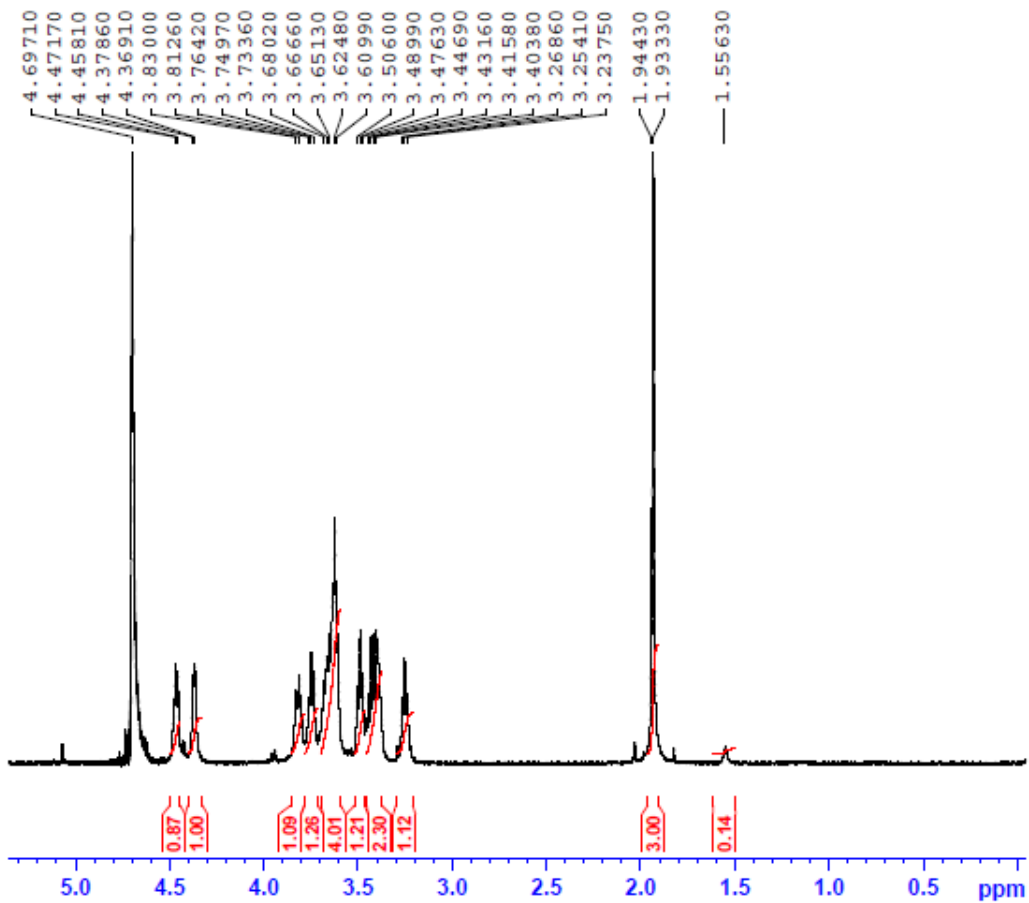
**Appendix 3. 1** A NMR spectra of lyophilized BDDE- HA digested fragments obtained at 25 °C , pH 13, reaction time 60 min, initial HA concentration 5.0 % and BDDE 0.25% . The degree of modification was 2.1% based on the integration of BDDE peak at 1.55 ppm with respect to the peak of *N*-acetyl glucosamine at approximately 1.9 ppm.



**Appendix 3.1 B** NMR spectra of lyophilized BDDE- HA digested fragments obtained at 25 °C , pH 13, reaction time 60 min, initial HA concentration 5.0 % and BDDE 0.5% . The degree of modification was 2.2% based on the integration of BDDE peak at 1.55 ppm with respect to the peak of *N*-acetyl glucosamine at approximately 1.9 ppm.



**Appendix 3.**  $^{13}\text{C}$  NMR spectra of lyophilized BDDE- HA digested fragments obtained at  $25\text{ }^{\circ}\text{C}$ , pH 13, reaction time 60 min, initial HA concentration 5.0 % and BDDE 0.75% . The degree of modification was 3.6% based on the integration of BDDE peak at 1.55 ppm with respect to the peak of *N*-acetyl glucosamine at approximately 1.9 ppm.



**Appendix 3. 1 D** NMR spectra of lyophilized BDDE- HA digested fragments obtained at 25 °C , pH 13, reaction time 60 min, initial HA concentration 5.0 % and BDDE 1.0 % . The degree of modification was 4.7% based on the integration of BDDE peak at 1.55 ppm with respect to the peak of *N*-acetyl glucosamine at approximately 1.9 ppm.

## **Appendix 4: Chromatographic analysis**

### **4.1 How HPLC is able to discriminate native HA from cross-linked BDDE-HA hydrogel.**

#### **Materials**

Samples of native HA and cross-linked BDDE-HA hydrogel, enzyme hyaluronidase (solid powder) with 3000 U/mg. Ehrlich's reagent, phosphate buffer saline (PBS) and alkaline solution.

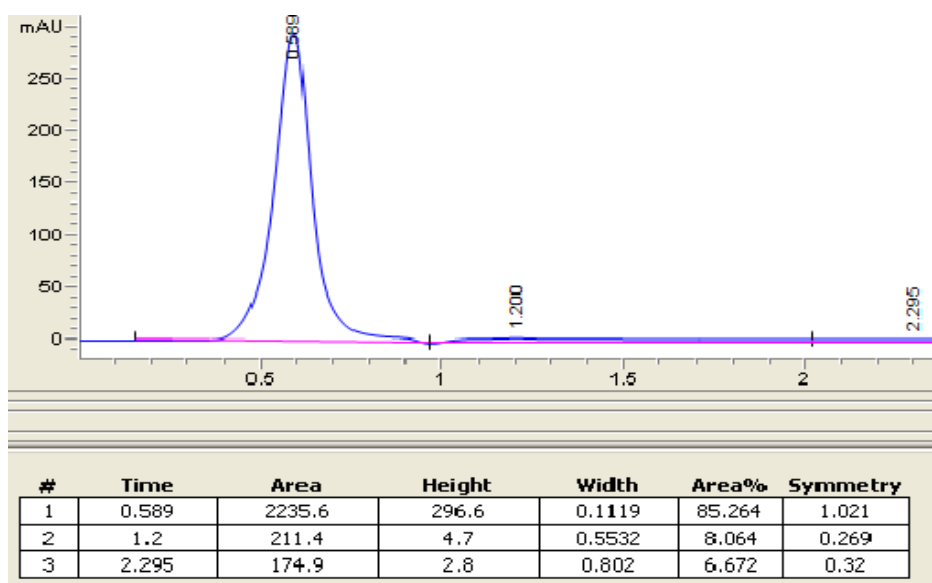
#### **Measurements**

Equivalent portions from lyophilized native HA and cross-linked BDDE-HA were obtained and digested with hyaluronidase solution until complete degradation. The extracts were filtered using 45  $\mu\text{m}$  Watmaan filtration paper. Each extract was analyzed by a reverse-phase HPLC (Agilent 1220 infinity, Waldbronn, Germany) and detected by a built-in diode-array detector. The stationary phase was C18 end-capped column (100 cm x 2mm) with 5  $\mu\text{m}$  particle size from (Knauer, Berlin, Germany) and the mobile phase was composed of two solutions: A: 96% (water 96% + acetonitrile 4%), B: methanol 4%. The method was performed on an isocratic mode and optimized with an injection volume of 2  $\mu\text{l}$ , flow rate of 0.4 ml/min and run time of 10 min. The detection was achieved at 195 nm.

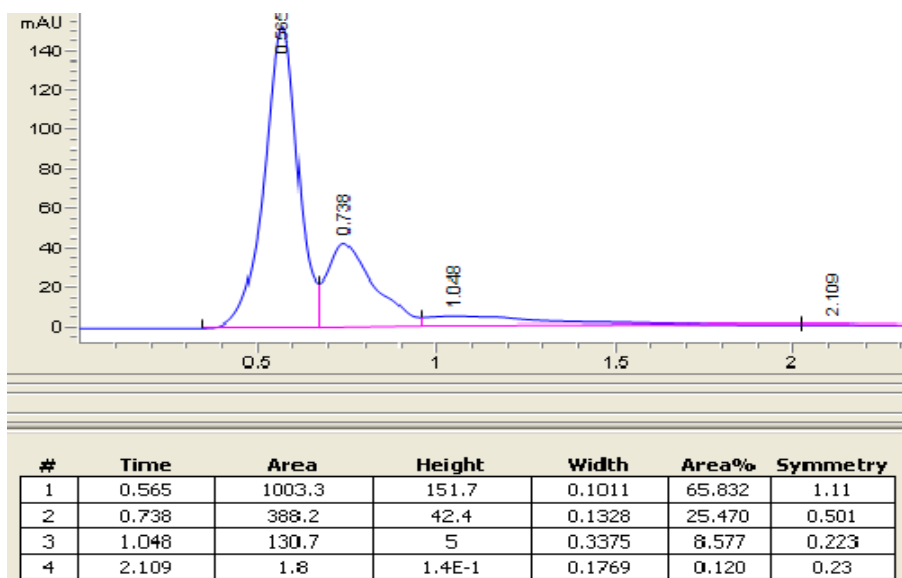
## Results and discussion

The native HA and cross-linked hydrogel were eluted relatively at different retention times. Chromatogram of native HA hydrogel showed a single broad peak eluting at 0.589 min (appendix 4.1 A) which was attributed to the variation in hydrodynamic radius of HA fragments.

However, the cross-linked hydrogel showed less overlapping components (appendix 4.1 B). It showed a large peak at 0.565 min representing the total volume of BDDE-HA fragments accompanied with a small one at 0.738 min representing the enzyme.



**Appendix 4.1 A** HPLC chromatogram of native HA hydrogel obtained at 198 nm in isocratic mode with a flow rate of 0.4 ml/min. The chromatogram displays a broad peak retained at 0.589 min which represents the total hyaluronic acid fragments



**Appendix 4. 1 B** HPLC chromatogram of BDDE-HA hydrogel obtained at 198 nm in isocratic mode with a flow rate of 0.4 ml/min. Chromatogram displays two peaks retained at 0.565 min which represents total BDDE-HA fragments and 0.738 mint which represents hyaluronidase.

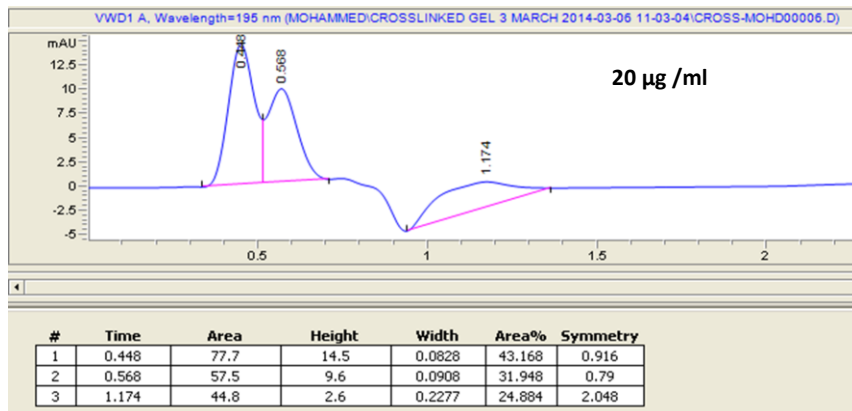
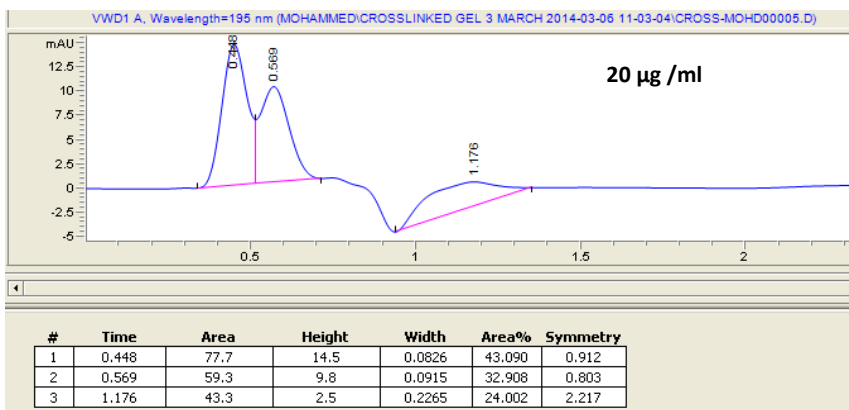
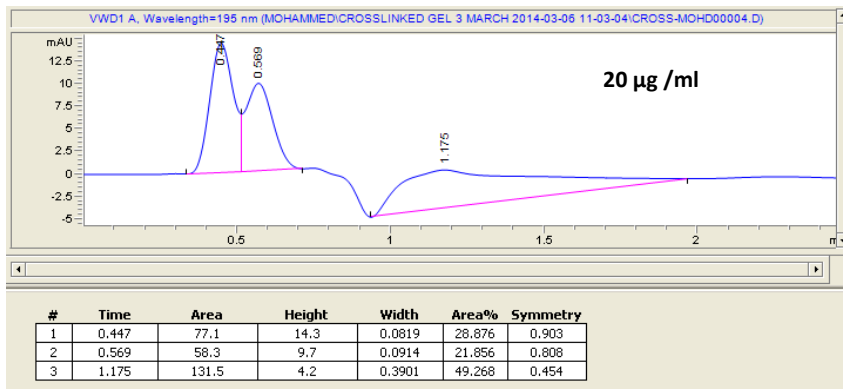
Although, the bovine testicular hyaluronidase exhibits efficient de-polymerization cleavage and produces different oligo-saccharides including disaccharides, tetra-saccharides, and hexa- saccharides, it was very difficult under our HPLC conditions to separate HA fragments or even to get a clear distinction between the native HA and BDDE-HA hydrogel . The application of RP-HPLC is challenging to separate such overlapped fragments even if the cross-linked hydrogel is digested with the hyaluronidase. As described earlier, due to the silanol groups found in silica or the chemical interaction between the polar mobile phase and non-polar stationary phase, the native HA and cross-linked HA are mostly eluted with peak tailing. The strongly acidic silanol groups work as cation-exchange sites for ionized bases of HA fragments.



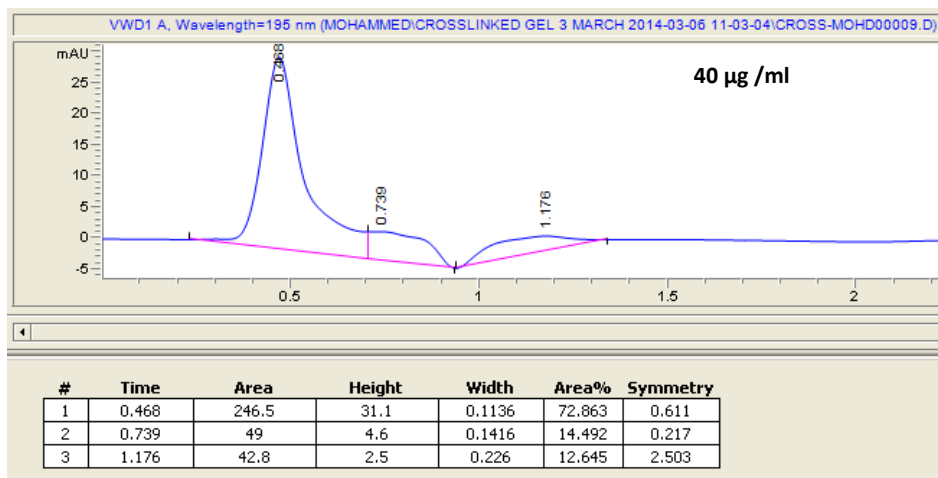
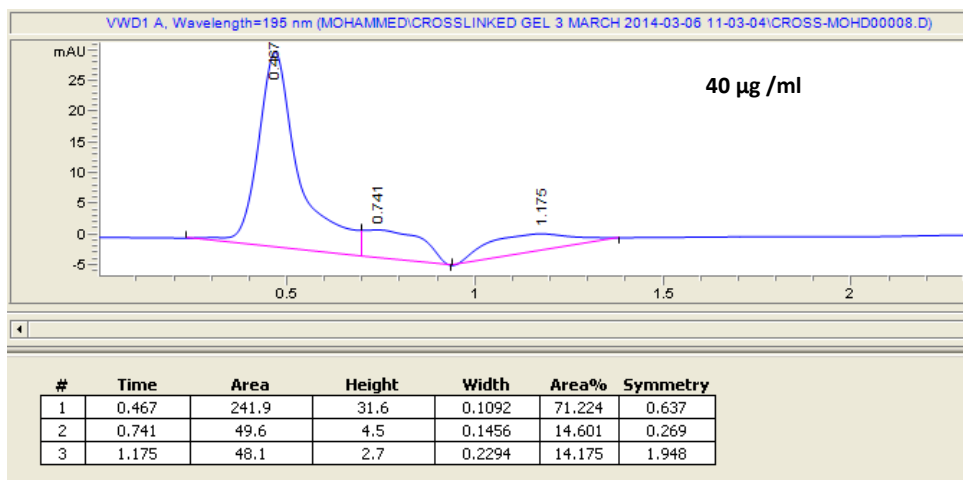
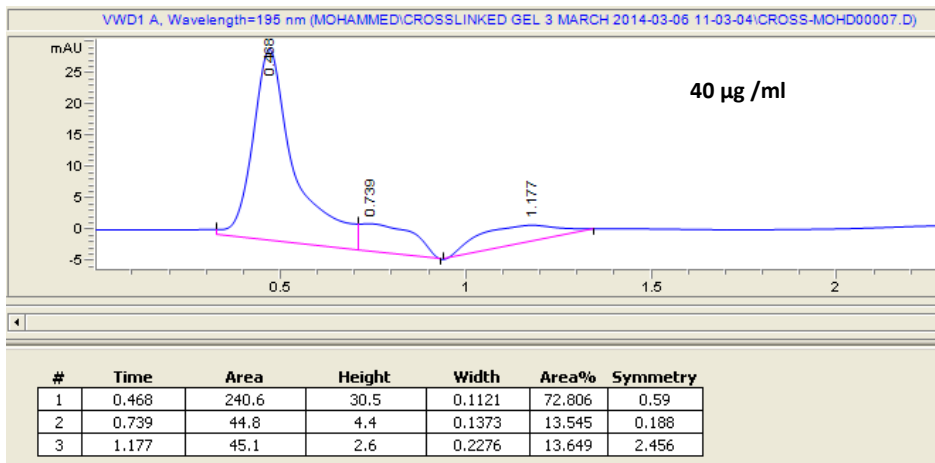
On the other hand, hyaluronic acid (HA) and hyaluronidase (HAase) have closely related structures, subsequently two overlapped peaks may be observed. If HA concentration is higher than (HAase), the (HAase) peak disappear. In contrast, if HA concentration is lower than (HAase), the (HAase) peak can suppress HA peak. This phenomenon is clearly observed in the next section (appendix 4.2). The physicochemical properties of HA and the digestion process could also affect resolution , separation and retention time. If the stationary phase becomes saturated or blocked over the course of analysis, that will lead to a variation in the retention time. The retention time also experiences a drift with increased HA content. This phenomenon is apparently correlated to the hydrodynamic radius and quantities of HA fragments found in the extract. As the amount of HA fragments increases like in native HA, it stays longer in the column and thus, has a slower retention time. .

## 4.2 Evaluation of *in vitro* degradation rate of cross-linked BDDE by HPLC.

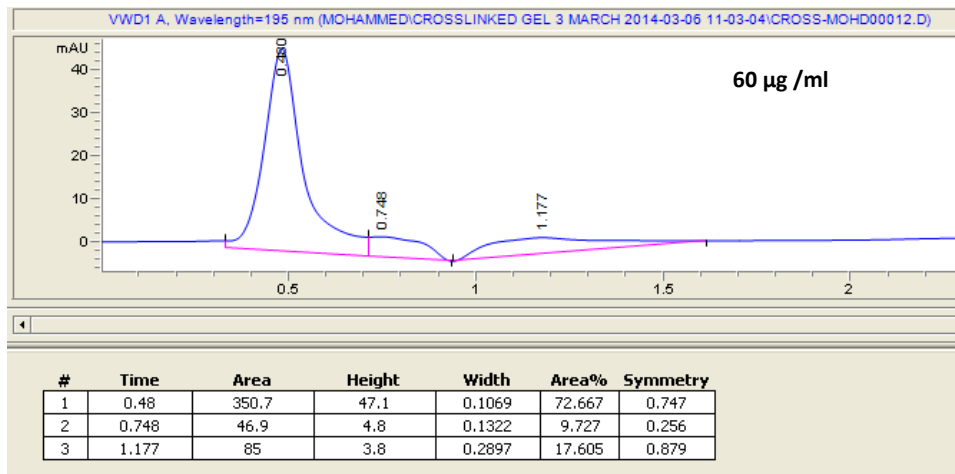
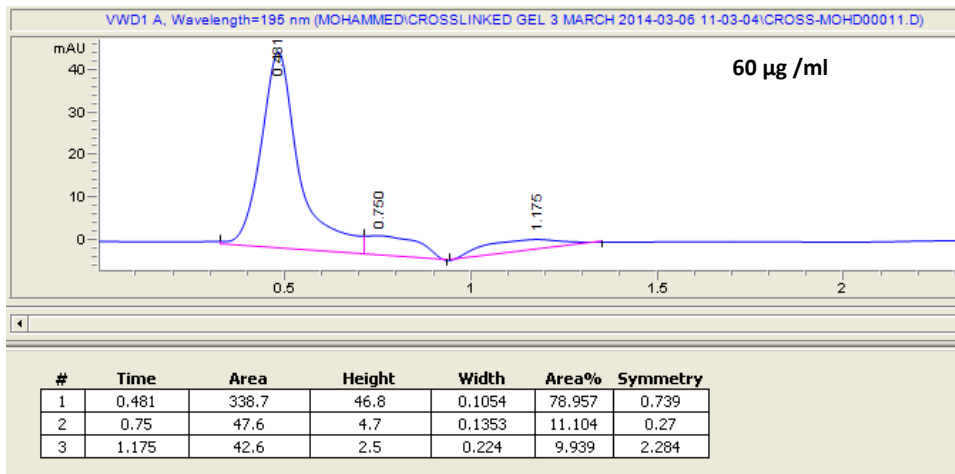
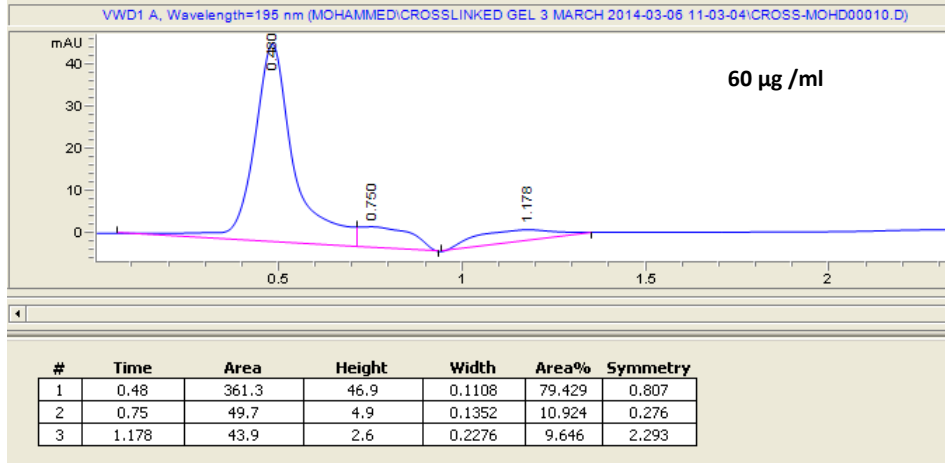
### 4.2.1. Preparation of standard solutions



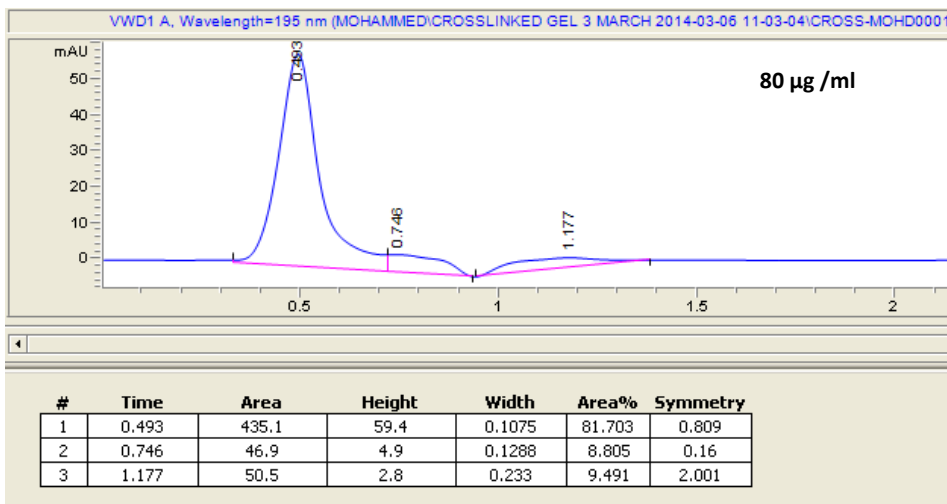
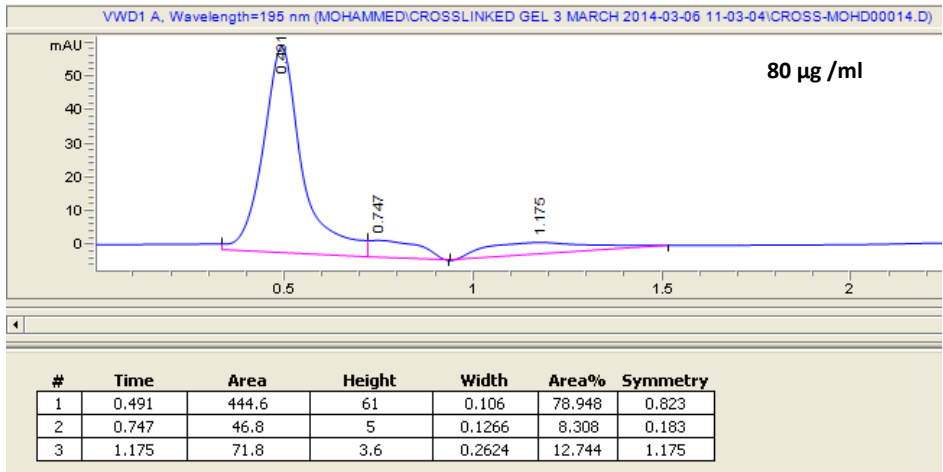
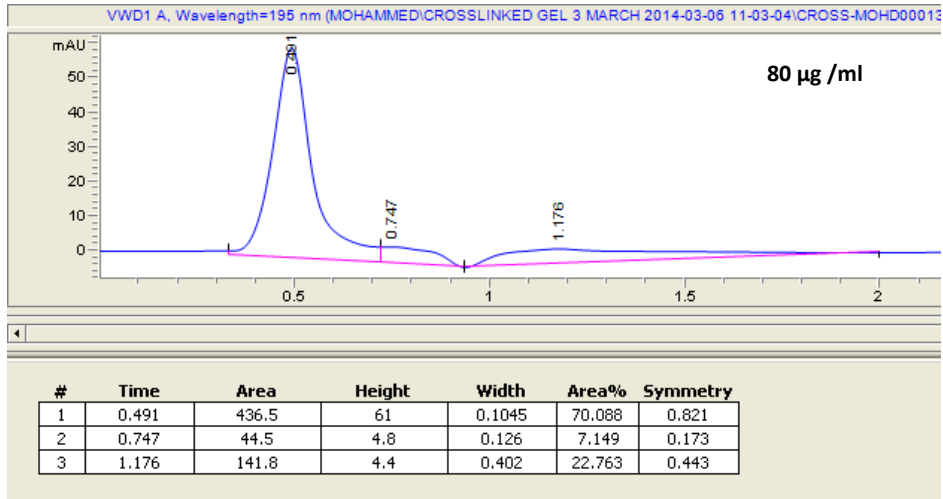
APPENDICES



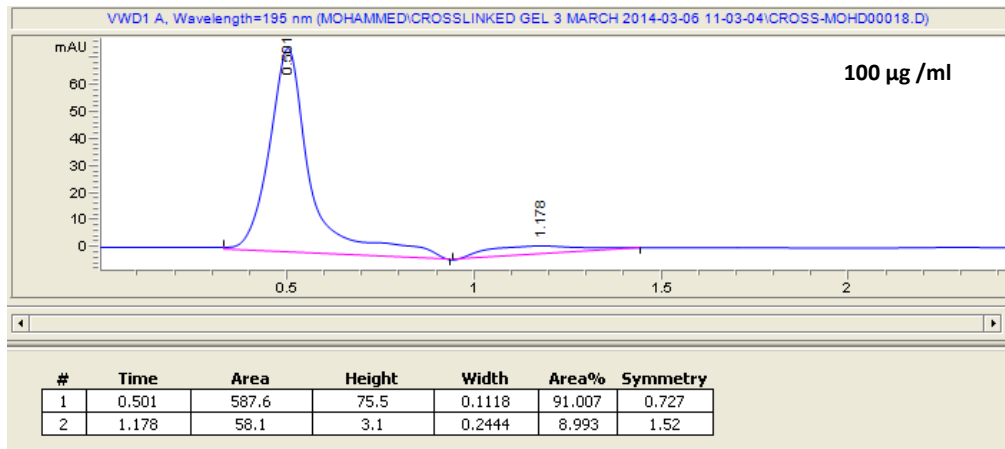
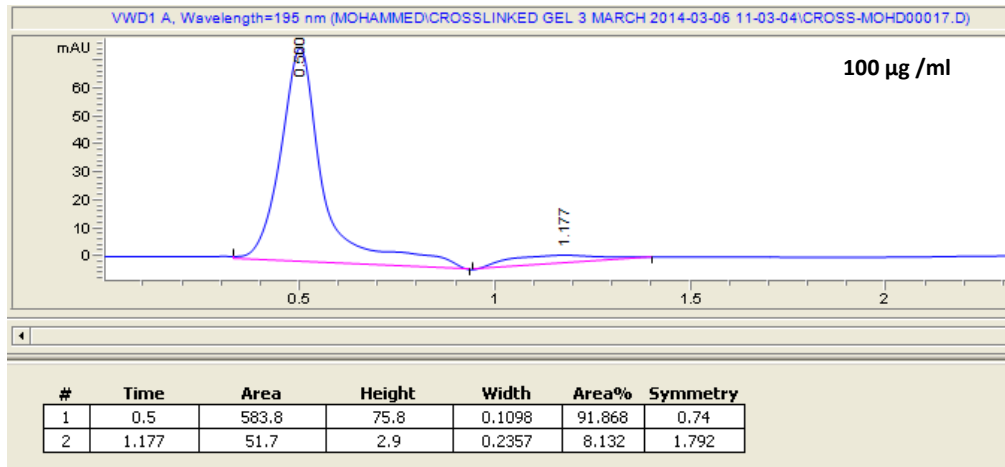
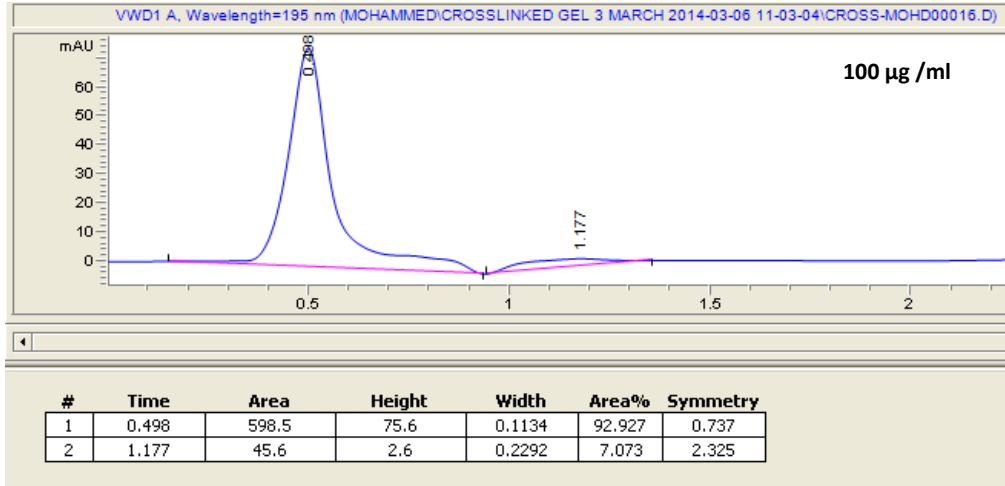
APPENDICES



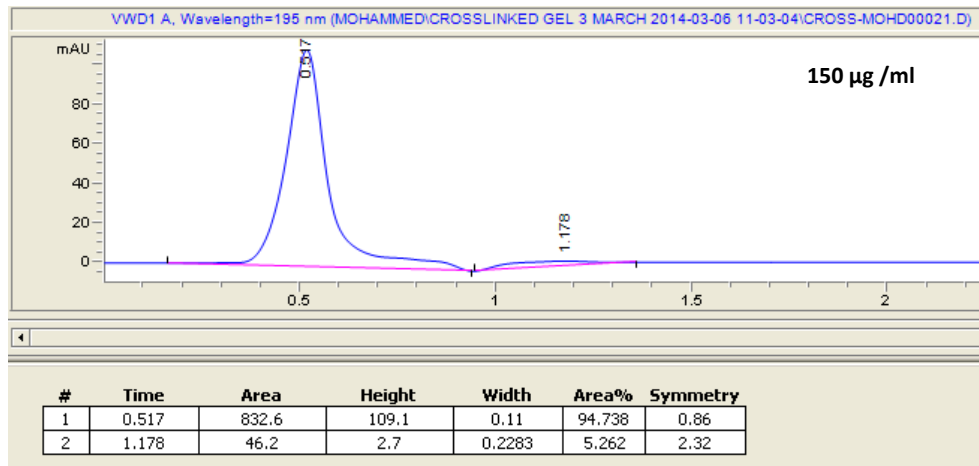
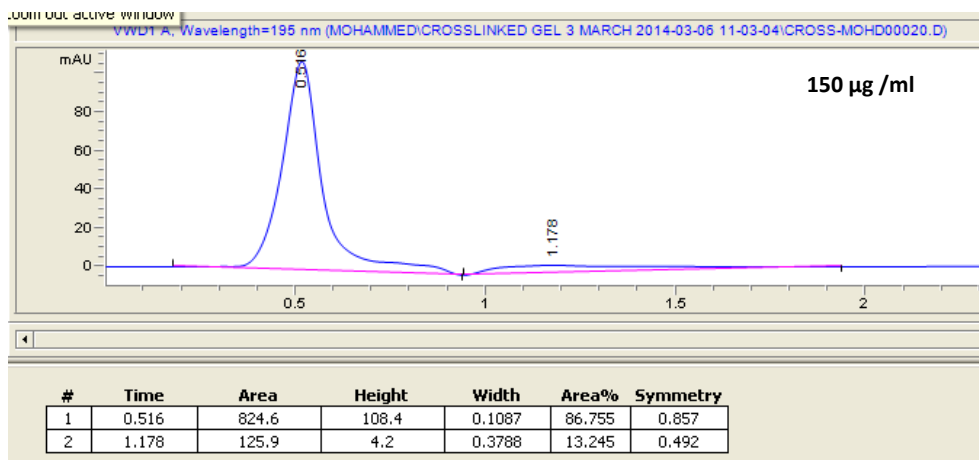
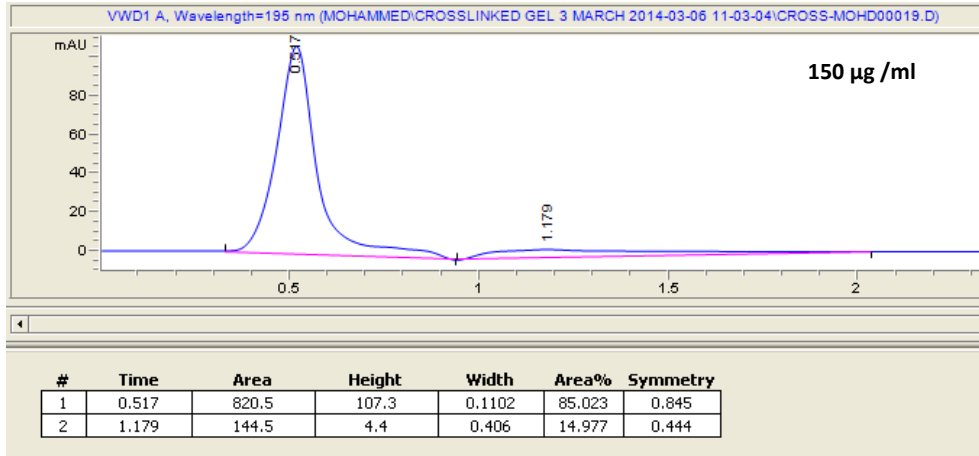
APPENDICES



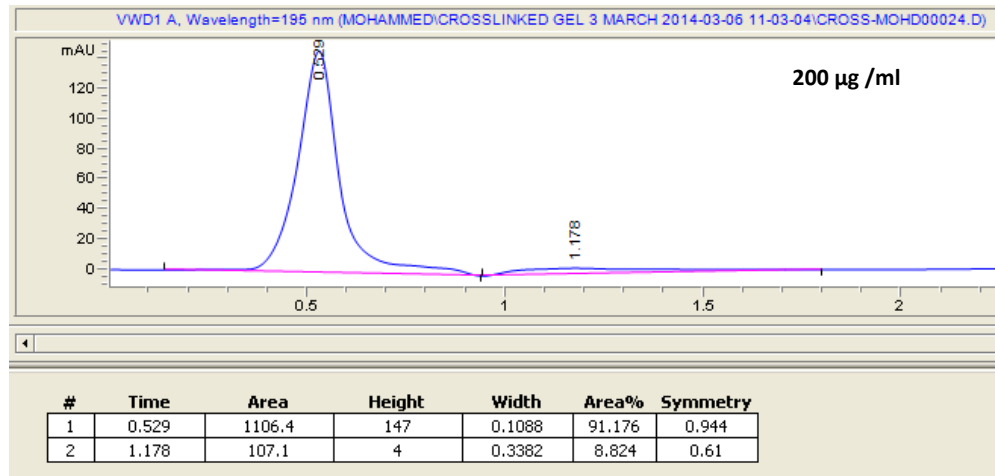
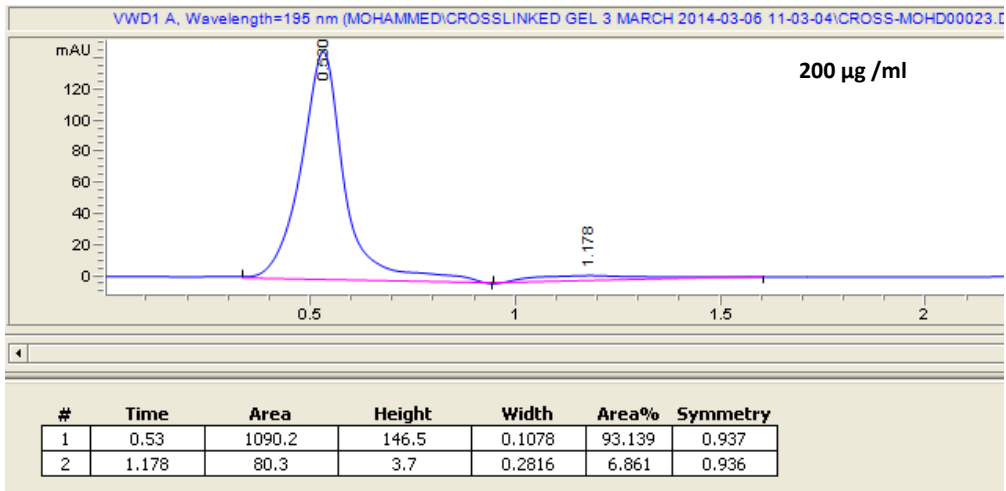
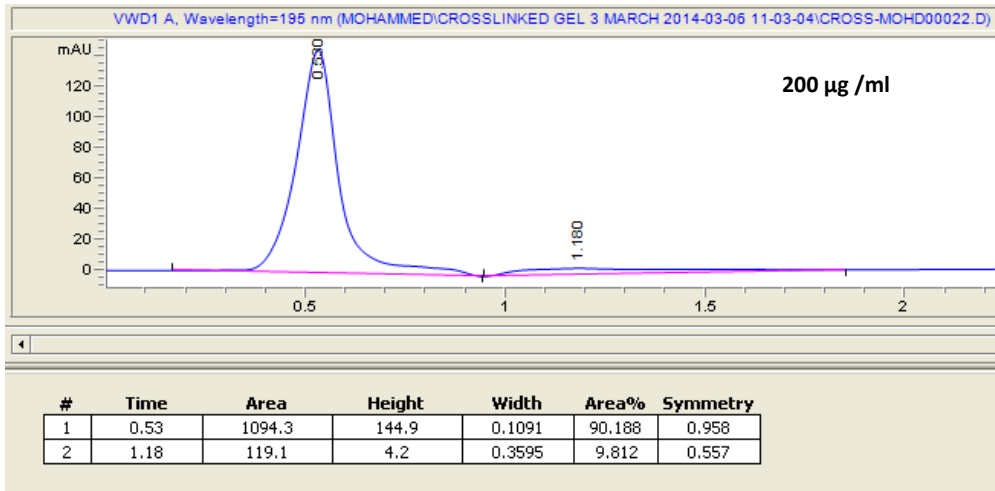
APPENDICES



APPENDICES

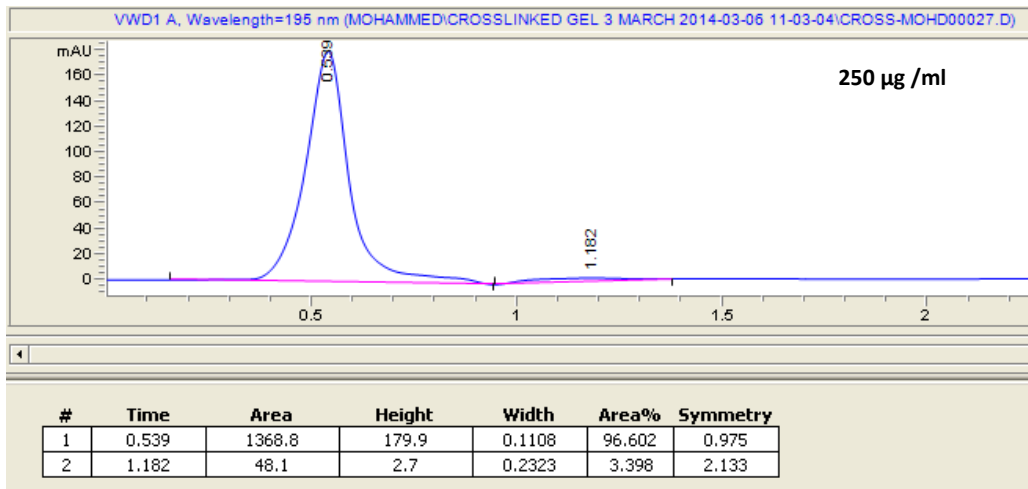
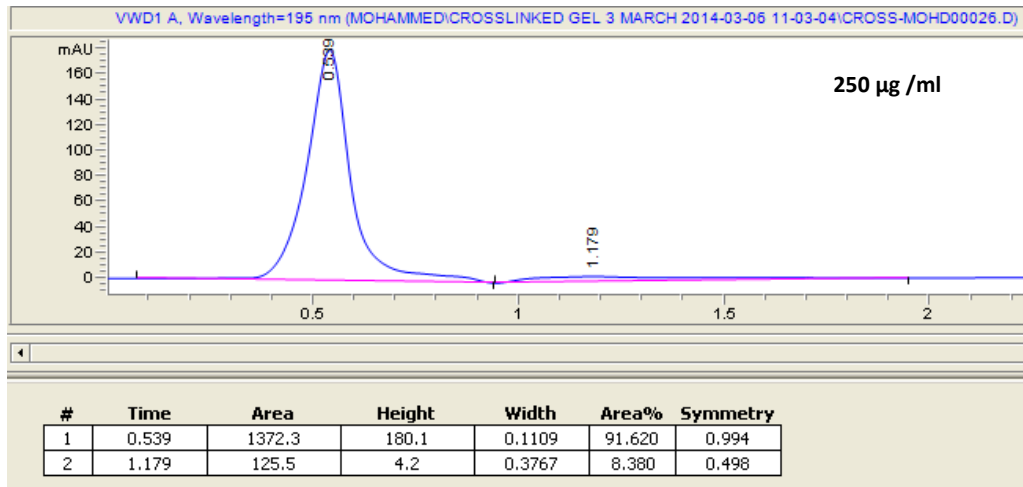
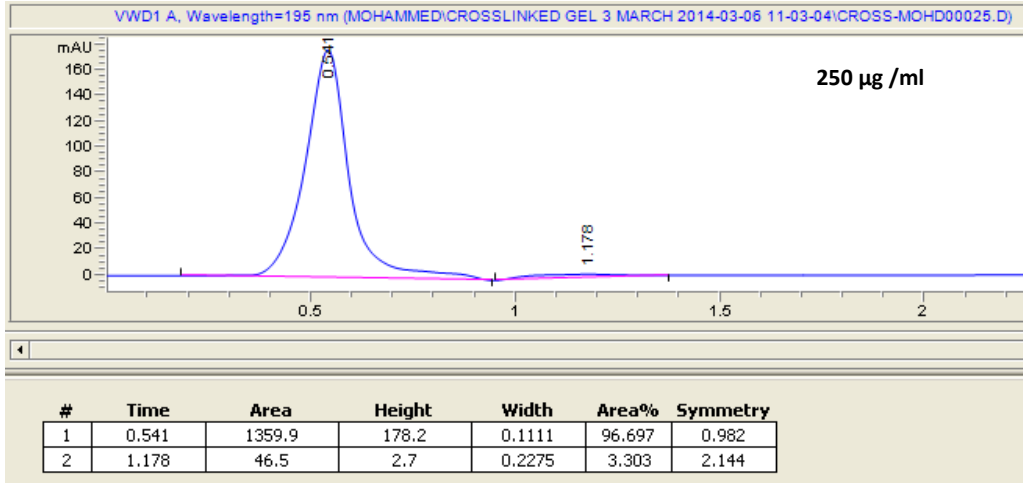


APPENDICES

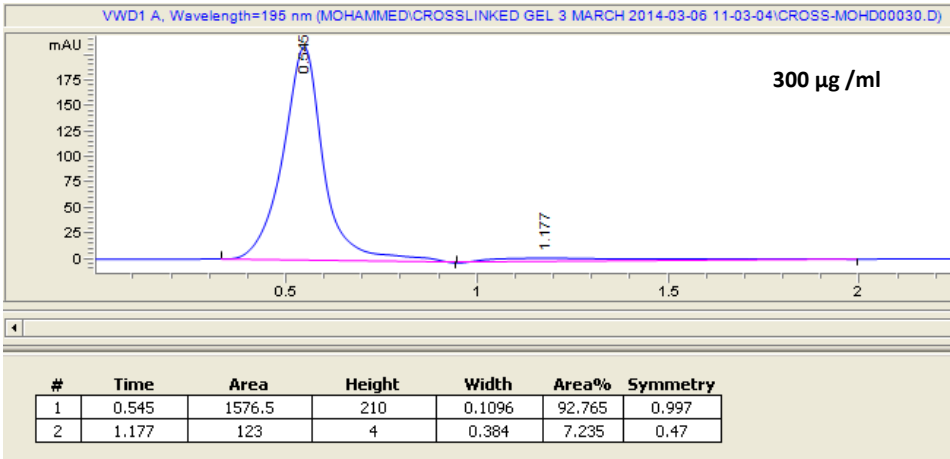
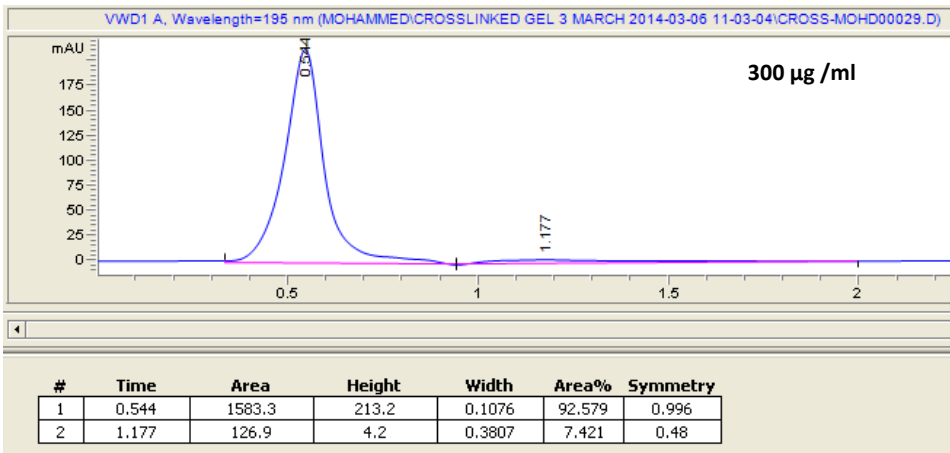
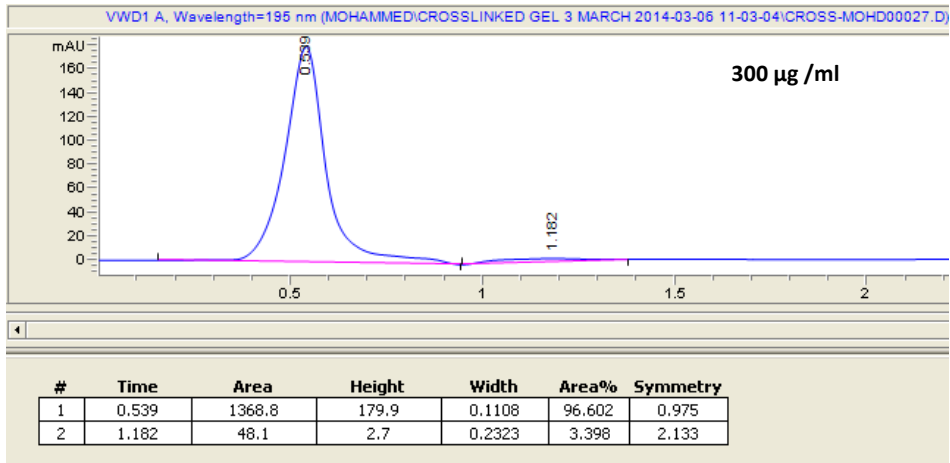




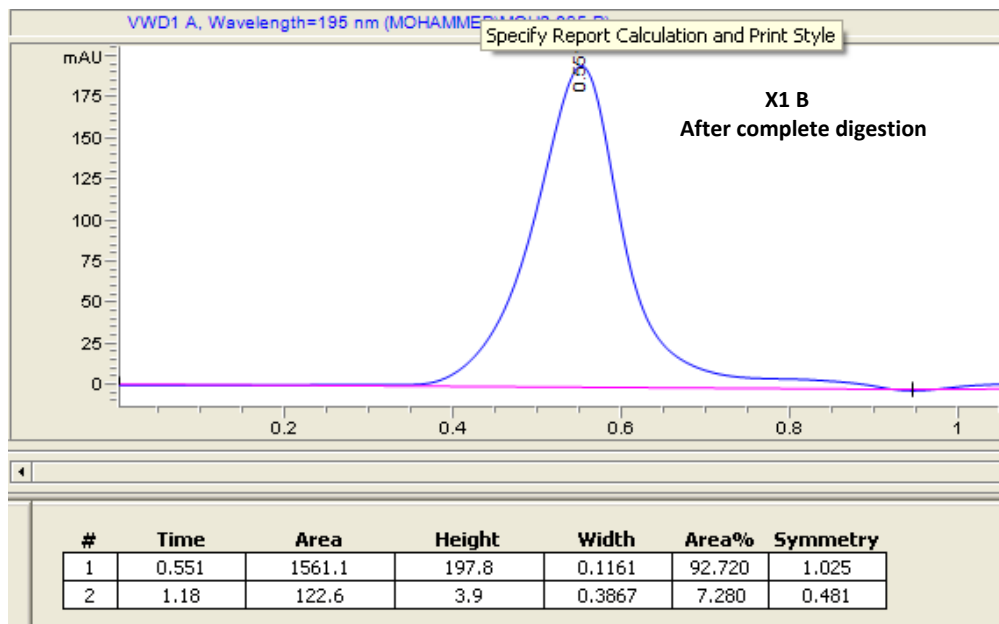
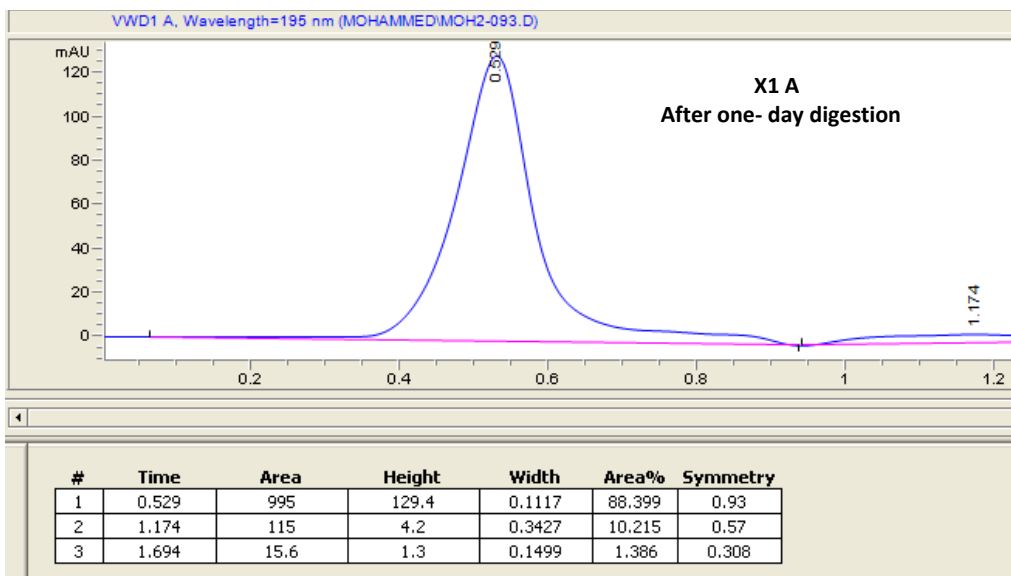
APPENDICES

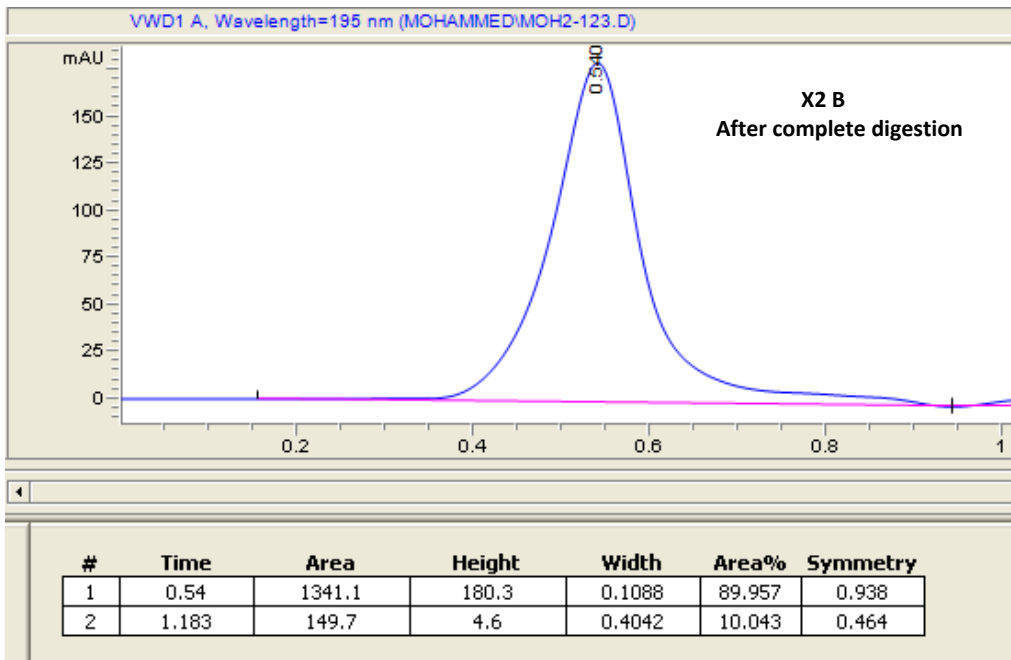
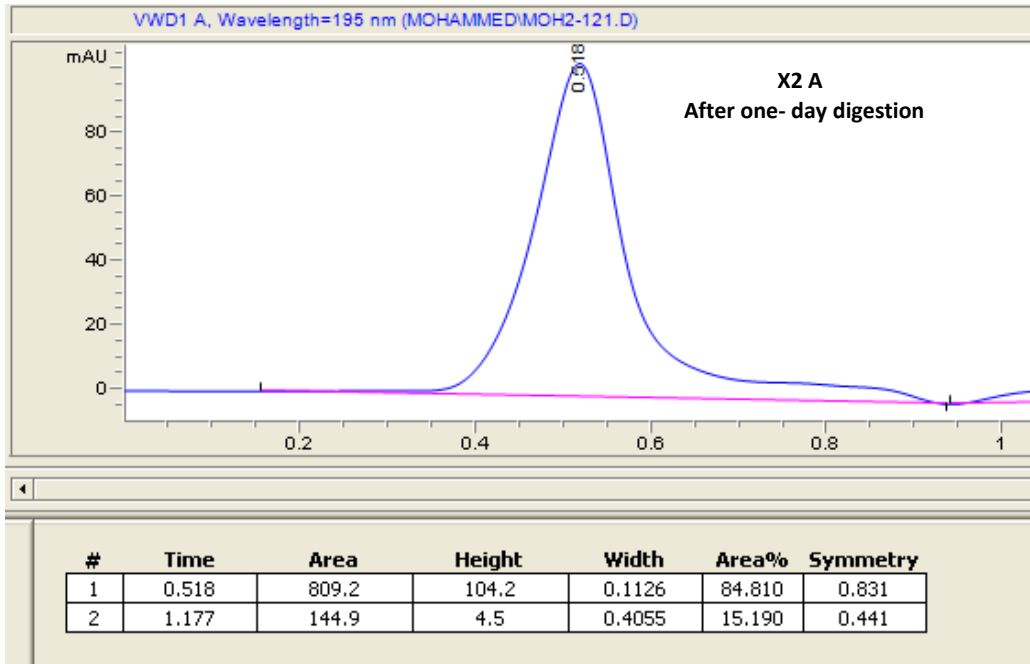


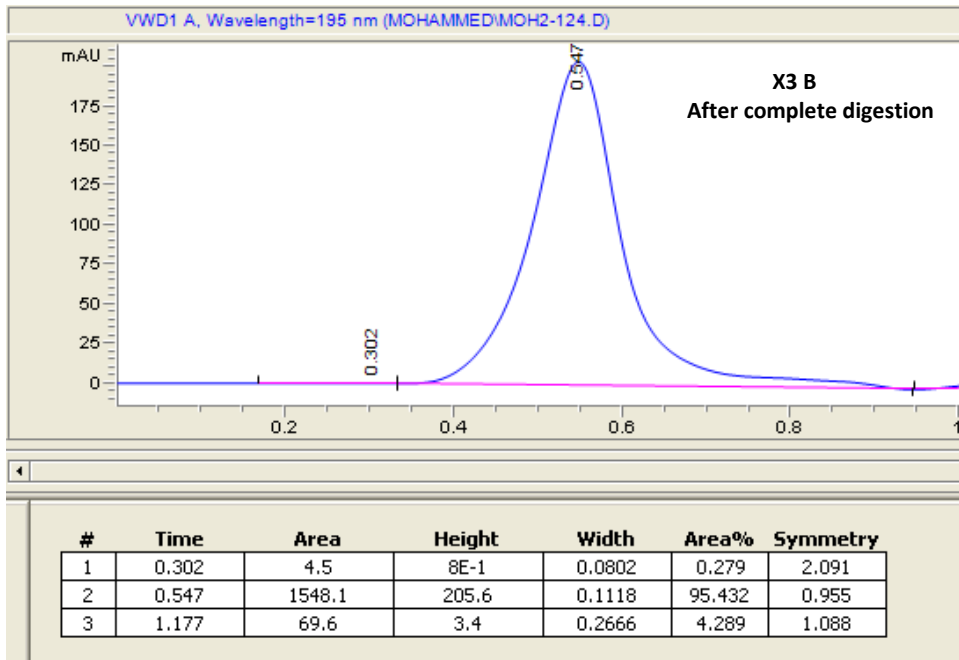
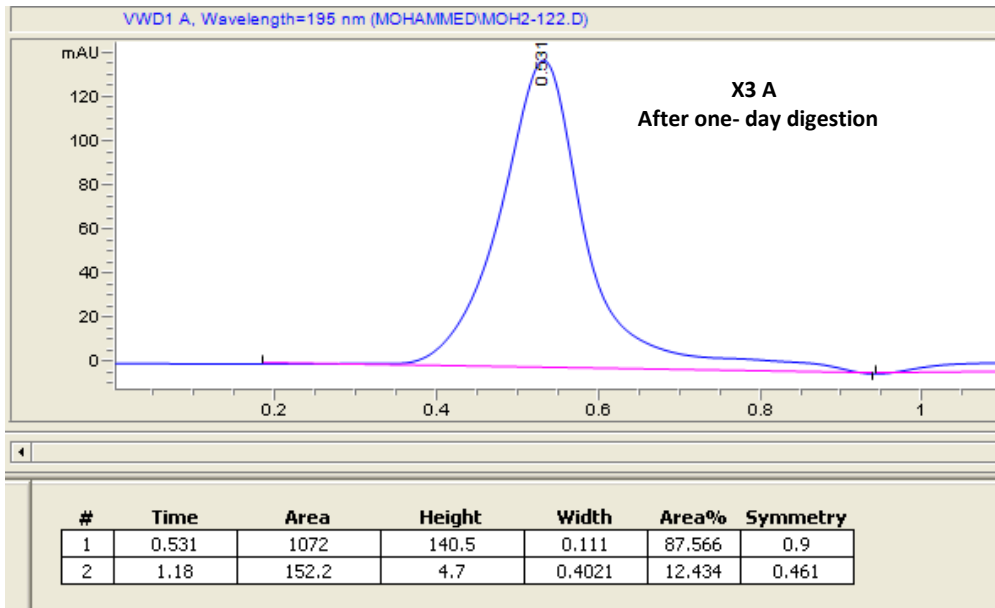
APPENDICES



### 4.2.2. Samples







### 4.2.3. Recovery

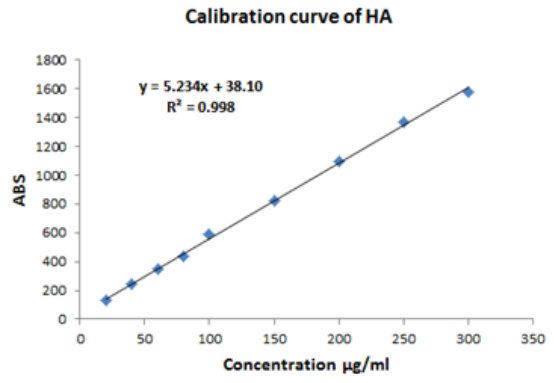
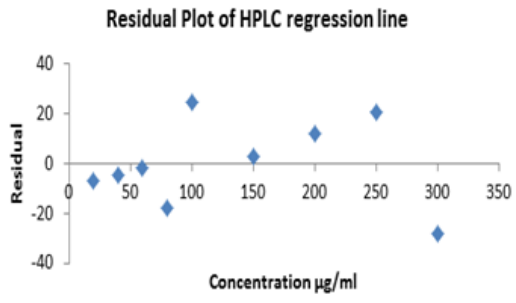
Hydrogel	Weight of swollen hydrogel	Theoretical value of HA in 5.0g sample	Actual value obtained	Recovery
X1	153	32.7 mg	29.8 mg	91.0 %
X2	144	34.7 mg	25.4 mg	73.2%
X3	139	35.9 mg	29.5 mg	82.2%

### 4.2.4. Regression

Con	AVG	min
20	135.9	0.447
40	243	0.468
60	350.2	0.48
80	438.7	0.491
100	586	0.498
150	826	0.517
200	1097	0.53
250	1367	0.541
300	1580	0.544
Native HA	6336.1	0.588
Crosslinked	1003.3	0.565

### Residual outut

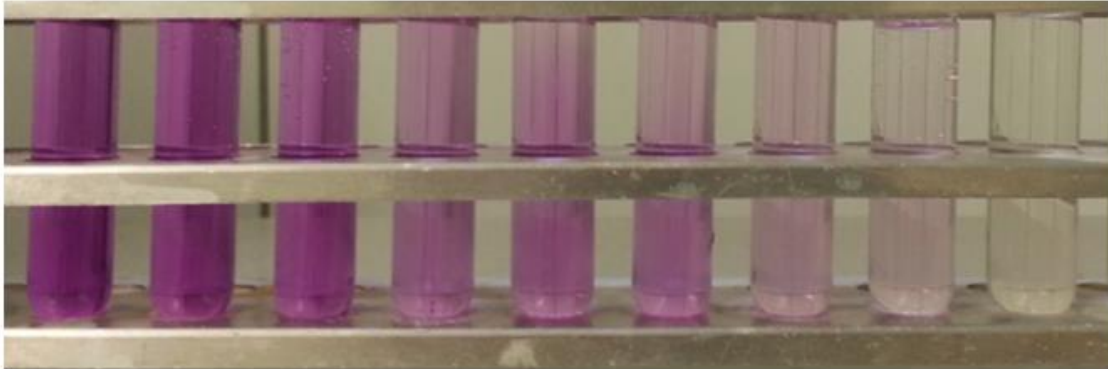
<i>Observation</i>	<i>Predicted Y</i>	<i>Residuals</i>
1	142.784242	-6.8842424
2	247.465455	-4.4654545
3	352.146667	-1.9466667
4	456.827879	-18.127879
5	561.509091	24.4909091
6	823.212121	2.78787879
7	1084.91515	12.0848485
8	1346.61818	20.3818182
9	1608.32121	-28.321212



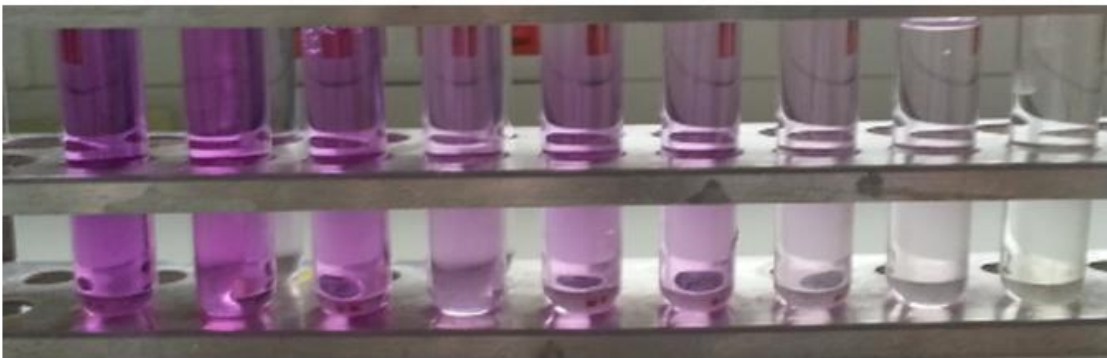
## Appendix 5: Colorimetric analysis

### 5.1. Preparation of standard solutions

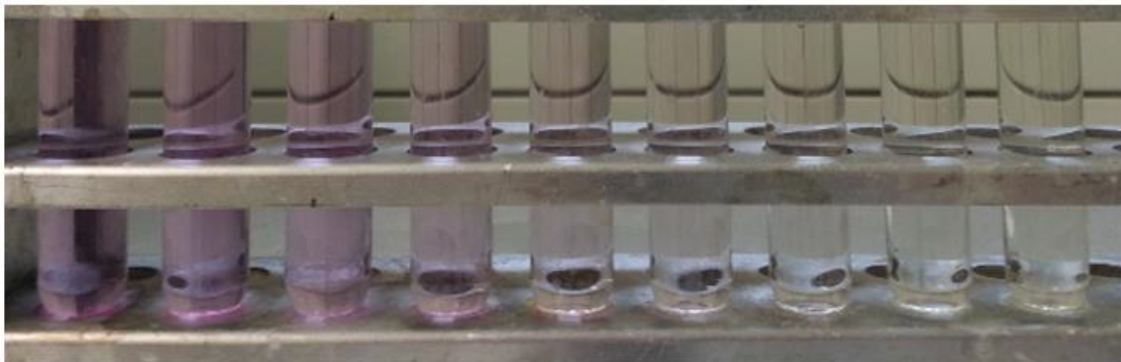
#### Range 1



#### Range 2

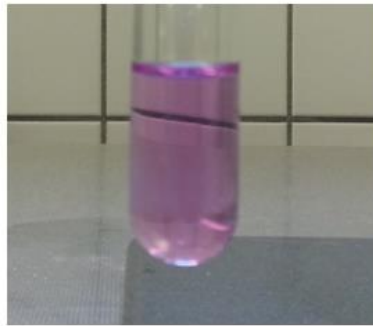


#### Range 3





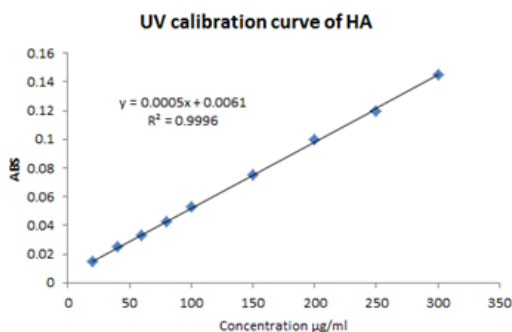
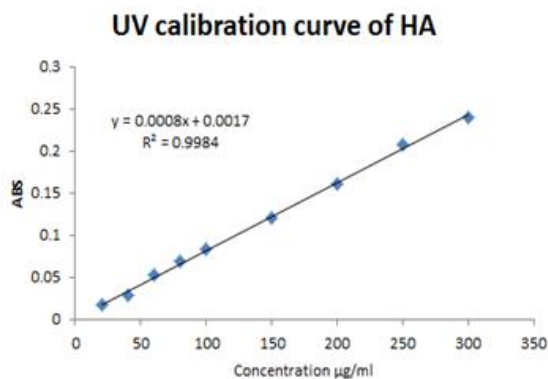
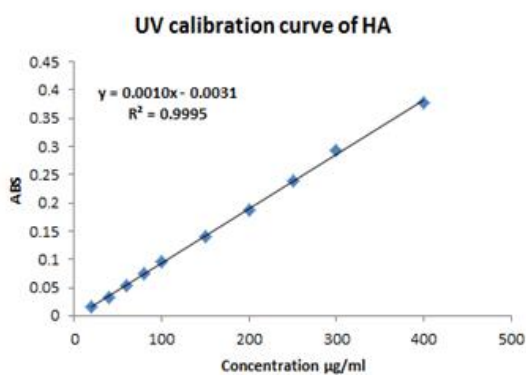
## 5.2. Samples



### 5.3. Recovery

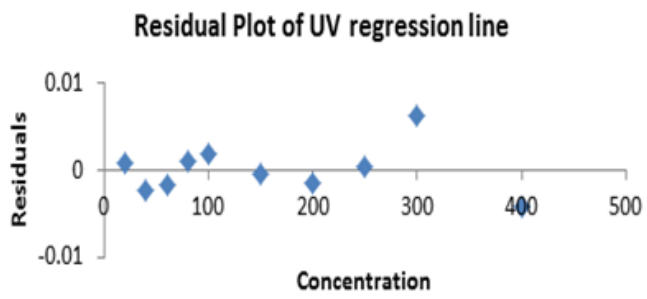
Hydrogel	Weight of swollen hydrogel	Theoretical value of HA in 5.0g sample	Actual value obtained	Recovery
X4	138	36.2 mg	27.3 mg	75.4%
X5	164	30.48 mg	28.7 mg	94.2%
X6	155	32.25 mg	25.7 mg	79.7 %

### 5.4. Regression



#### RESIDUAL OUTPUT

Observation	Predicted Y	Residuals
1	0.016173	0.000827
2	0.035434	-0.00243
3	0.054695	-0.0017
4	0.073956	0.001044
5	0.093217	0.001783
6	0.14137	-0.00037
7	0.189522	-0.00152
8	0.237674	0.000326
9	0.285827	0.006173
10	0.382132	-0.00413



Con	ABS	ABS	ABS
20	0.017	0.017	0.015
40	0.033	0.029	0.025
60	0.053	0.053	0.033
80	0.075	0.069	0.043
100	0.095	0.084	0.053
150	0.141	0.12	0.075
200	0.188	0.161	0.1
250	0.238	0.207	0.12
300	0.292	0.24	0.145

## Appendix 6: Results of the *in-vitro* degradation rate

**Appendix 6.1** Average remaining NAG (%) of BDDE-HA hydrogels prepared at different reaction time

Day	30 min	1 h	2 h	4 h	8 h	24h
0	100	100	100	100	100	100
1	49.1 ± 5.9	63.9 ± 5.1	66.7 ± 6.2	65.4 ± 4.8	62.9 ± 5.6	66.3 ± 2.4
2	28.3 ± 1.8	30.7 ± 2.7	39.7 ± 5.2	42.2 ± 4.5	40.5 ± 4.6	41.2 ± 3.9
3	18.3 ± 2.2	21.0 ± 6.6	31.3 ± 1.4	30.8 ± 6.1	28.7 ± 3.4	31.2 ± 3.1
4	8.3 ± 6.7	10.5 ± 4.5	17.3 ± 1.4	18.3 ± 3.5	16.1 ± 2	16.3 ± 1.3

**Appendix 6.2** Average remaining NAG (%) of BDDE-HA hydrogels prepared at different pH number

Day	pH 13	pH 11	pH 9	pH 3
0	100	100	100	100
1	66 ± 3.1	51.1 ± 4	46.5 ± 1.8	55.9 ± 5.3
2	40.3 ± 2.4	31.1 ± 5.9	25.4 ± 6.6	33.6 ± 6.9
3	29.6 ± 1.8	20.4 ± 2.1	14.7 ± 3.8	19.8 ± 5.2
4	18.4 ± 2.7	9.8 ± 1.8	7.1 ± 3.1	10 ± 3.3

**Appendix 6.3** Average remaining NAG (%) of BDDE-HA hydrogels prepared at different temperature

Day	25 °C	30 °C	35 °C	40 °C	45 °C	50 °C
0	100	100	100	100	100	100
1	63.6 ± 3.2	64.7 ± 1.0	65.2 ± 4.7	65.9 ± 4.6	63.3 ± 2.6	48.8 ± 5.5
2	39.8 ± 2.3	41.6 ± 2.7	42 ± 4.5	40.9 ± 0.3	39.9 ± 3.7	29.5 ± 4.7
3	29.1 ± 1.9	31.8 ± 2.9	32.6 ± 2.6	33.3 ± 1.7	32.3 ± 5.6	18.3 ± 2.1
4	19.0 ± 0.6	21.5 ± 1.9	17.9 ± 1.5	22.3 ± 3	19.5 ± 2.0	7.3 ± 2.2

**Appendix 6.4** Average remaining NAG (%) of BDDE-HA hydrogels prepared at different HA concentration.

Day	7.0 % HA	8.0 % HA	9.0 % HA	10.0 % HA
0	100	100	100	100
1	55.5± 5.7	58.9± 2.5	62.5± 3.4	68.4± 1.8
2	33.4± 1.7	35.9± 2.7	37.9± 2.0	42.9± 1.3
3	23.1± 2.8	26.9± 3.0	31.3± 4.6	34.2± 2.0
4	15.9± 5.4	18.6± 3.1	23.6± 3.8	25.1± 1.9
Day	11.0 % HA	12.0 % HA	13.0 % HA	14.0 % HA
0	100	100	100	100
1	66.6± 3.7	65.7± 6.3	64.7± 2.9	63.9± 2.0
2	41.4± 2.1	41.0± 5.5	38.9± 3.7	38.5± 3.5
3	32.5± 3.4	34.4± 4.0	30.5± 4.2	31.3± 2.1
4	22.4± 2.2	21.4± 4.9	21.9± 2.9	19.5± 2.6

**Appendix 6.5** Average remaining NAG % of native HA and cross-linked BDDE-HA hydrogels prepared at various HA molecular weight

Day	100 kDa	1000 kDa	2000 kDa
0	100	100	100
1	61 ± 7.2	66.3 ± 7.5	71.3± 3.9
2	34.1 ± 6.9	42.6 ± 4.2	46.1 ± 2.9
3	23.3 ± 5.3	33.4 ± 4.2	34.6 ± 2.0
4	13.8 ± 4.2	23.5 ± 3.0	26.5 ± 3.6

**Appendix 6.6** Average remaining NAG % of native HA and cross-linked BDDE-HA hydrogels prepared at different mixing approaches

Day	Native HA	Hydrogel 1	Hydrogel 2
0	100	100	100
1	11.7± 6.1	73.4 ± 3.5	75.6 ± 0.9
2	0.00	45.7 ± 4.6	49.0 ± 4.9
3	0.00	34.0 ± 6.0	39.2 ± 2.9
4	0.00	23.8 ± 2.9	28.5 ± 2.0

## Appendix 7: Results of the swelling ratio measurements

**Appendix 7.1** Average amounts of swelling ratios (g/g) of BDDE-HA hydrogels prepared at different reaction times

Hydrogel	Distilled water	BPS
30 min	154 ±15.5	135 ± 8.6
1 h	145 ±4.9	124 ±5.1
2 h	136 ±8.0	121 ±6.2
4 h	139 ±14.9	122± 2.2
8 h	135 ±11.7	120 ±7.2
24 h	135 ±8.7	121 ±5.7

**Appendix 7.2** Average amounts of swelling ratios (g/g) of BDDE-HA hydrogels prepared at different pH number.

Hydrogel	Distilled water	BPS
pH 13	137± 6.5	120 ± 6.2
pH 11	146 ± 6.0	137 ± 4.3
pH 9	150 ± 8.7	143± 3.8
pH 3	138± 7.9	125 ±2.5

**Appendix 7.3** Average amounts of swelling ratios (g/g) of BDDE-HA hydrogels prepared at different temperature

Hydrogel	Distilled water	BPS
25 °C	139 ± 4.9	128 ± 3.8
30 °C	138 ±1.4	125 ± 5.2
35 °C	135 ± 8.9	123 ± 5.7
40 °C	133 ±4.5	119 ± 3.8
45 °C	126 ± 6.6	117 ± 3.5
50 °C	120 ± 11.7	112± 7.5

**Appendix 7.4** Average amounts of swelling ratios (g/g) of BDDE-HA hydrogels prepared at different HA concentrations.

<b>Medium</b>	<b>7.0 % HA</b>	<b>8.0 % HA</b>	<b>9.0 % HA</b>	<b>10.0 % HA</b>
Distilled water	135 ± 6.5	134 ± 2.8	132 ± 5.1	129 ± 3.2
PBS	124 ± 4.3	122 ± 2.4	120 ± 3.8	116 ± 2.4
<b>Medium</b>	<b>11.0 % HA</b>	<b>12.0 % HA</b>	<b>13.0 % HA</b>	<b>14.0 % HA</b>
Distilled water	131 ± 6.5	132 ± 7.9	136 ± 6.2	137 ± 7.4
PBS	117 ± 1.4	119 ± 3.8	121 ± 5.0	127 ± 6.2

**Appendix 7.5** Swelling ratios (g/g) of hydrogels prepared by different HA molecular weight in distilled water and PBS

<b>Hydrogel</b>	<b>Distilled water</b>	<b>BPS</b>
100 kDa	142 ± 8.9	131 ± 6.2
1000 kDa	130 ± 6.2	119 ± 5.7
2000 kDa	133 ± 7.4	125 ± 3.7

**Appendix 7.6** Swelling ratios (g/g) of hydrogels 1 and 2 prepared by different mixing approaches in distilled water and PBS

<b>Hydrogel</b>	<b>Distilled water</b>	<b>BPS</b>
Hydrogel 1	135 ± 7.2	127 ± 10.8
Hydrogel 2	130 ± 3.8	123 ± 5.2

## Appendix 8: Excel data for the rheological measurements

Appendix 8.1: Rheological data for native HA

Angular frequency rad/s	Storage modulus Pa	Angular frequency rad/s	Loss modulus Pa	Angular frequency rad/s	Complex viscosity Pa.s
100	78.9728	100	62.9655	100	1.01002
63.0957	60.9564	63.0957	55.0833	63.0957	1.30211
39.8107	46.0454	39.8107	47.4008	39.8107	1.65994
25.1189	33.7084	25.1189	39.806	25.1189	2.07657
15.8489	23.8508	15.8489	32.6185	15.8489	2.54959
10	16.244	10	25.9175	10	3.05874
6.30957	10.6366	6.30957	20.0259	6.30957	3.59381
3.98107	6.66686	3.98107	14.9787	3.98107	4.11834
2.51189	4.01884	2.51189	10.9121	2.51189	4.62943
1.58489	2.32123	1.58489	7.75984	1.58489	5.11049
1	1.29393	1	5.37546	1	5.529
0.63096	0.7007	0.63096	3.6686	0.63096	5.91945
0.39811	0.3794	0.39811	2.49568	0.39811	6.3409
0.25119	0.20565	0.25119	1.68558	0.25119	6.76015
0.15849	0.10048	0.15849	1.14197	0.15849	7.23318
0.1	0.06155	0.1	0.71045	0.1	7.13109
0.0631	0.03365	0.0631	0.43081	0.0631	6.84865
0.03981	0.01353	0.03981	0.24275	0.03981	6.10706
0.02512	0.04187	0.02512	0.1722	0.02512	7.05516
0.01585	8.96E-03	0.01585	0.09276	0.01585	5.87997
0.01	0.01432	0.01	0.08584	0.01	8.70307



Appendix 8.2: Rheological data for BDDE-HA hydrogel prepared with 100,000 Da

Angular frequency y rad/s	Storage modulus Pa	Angular frequency y rad/s	Loss modulus Pa	Angular frequency y rad/s	Complex viscosity Pa.s
100	114.946	100	19.8767	100	1.16652
63.0957	110.293	63.0957	17.2461	63.0957	1.76926
39.8107	101.332	39.8107	14.4697	39.8107	2.57116
25.1189	97.3235	25.1189	13.7015	25.1189	3.91273
15.8489	93.9861	15.8489	12.0125	15.8489	5.97836
10	90.9413	10	10.794	10	9.15796
6.30957	88.4135	6.30957	9.72097	6.30957	14.097
3.98107	86.199	3.98107	8.45537	3.98107	21.7561
2.51189	84.1304	2.51189	8.35973	2.51189	33.6579
1.58489	82.2661	1.58489	7.61497	1.58489	52.1283
1	80.567	1	6.86371	1	80.8588
0.63096	79.2395	0.63096	6.6655	0.63096	126.03
0.39811	78.1584	0.39811	6.46093	0.39811	196.995
0.25119	77.2452	0.25119	6.18692	0.25119	308.503
0.15849	76.623	0.15849	6.11265	0.15849	484.995
0.1	75.0128	0.1	6.44047	0.1	752.888
0.0631	75.774	0.0631	5.89705	0.0631	1204.57
0.03981	77.3835	0.03981	7.72264	0.03981	1953.44
0.02512	76.8246	0.02512	9.33381	0.02512	3080.93
0.01585	79.608	0.01585	6.98886	0.01585	5042.25
0.01	104.436	0.01	10.5726	0.01	10497

Appendix 8.3: Rheological data for BDDE-HA hydrogel prepared with 1000,000 Da

Angular frequency rad/s	Storage modulus Pa	Angular frequency rad/s	Loss modulus Pa	Angular frequency rad/s	Complex viscosity Pa.s
100	166.587	100	42.787	100	1.71994
63.0957	153.982	63.0957	36.216	63.0957	2.50704
39.8107	144.649	39.8107	31.7935	39.8107	3.72014
25.1189	136.338	25.1189	28.1109	25.1189	5.54188
15.8489	129.067	15.8489	25.0909	15.8489	8.29603
10	122.519	10	22.3912	10	12.4548
6.30957	116.812	6.30957	20.1088	6.30957	18.7858
3.98107	111.677	3.98107	18.1467	3.98107	28.4199
2.51189	107.191	2.51189	16.5406	2.51189	43.1786
1.58489	102.957	1.58489	15.0931	1.58489	65.6559
1	99.0578	1	13.8947	1	100.027
0.63096	95.5287	0.63096	12.9347	0.63096	152.784
0.39811	92.3907	0.39811	12.1822	0.39811	234.084
0.25119	89.5645	0.25119	11.5739	0.25119	359.528
0.15849	87.5331	0.15849	11.4545	0.15849	557.005
0.1	85.6798	0.1	10.8647	0.1	863.659
0.0631	85.0175	0.0631	10.6636	0.0631	1357.99
0.03981	85.5784	0.03981	11.5455	0.03981	2169.11
0.02512	90.7772	0.02512	10.1599	0.02512	3636.47
0.01585	123.54	0.01585	31.5814	0.01585	8045.51
0.01	1001.2	0.01	454.56	0.01	109955

Appendix 8.4: Rheological data for BDDE-HA hydrogel prepared with 2000,000 Da

Angular frequency rad/s	Storage modulus Pa	Angular frequency rad/s	Loss modulus Pa	Angular frequency rad/s	Complex viscosity Pa.s
100	1546.87	100	469.14	100	16.1645
63.0957	1284.62	63.0957	396.15	63.0957	21.3059
39.8107	1109.66	39.8107	346.878	39.8107	29.2035
25.1189	969.521	25.1189	306.016	25.1189	40.4743
15.8489	859.521	15.8489	272.223	15.8489	56.8871
10	765.639	10	240.876	10	80.2636
6.30957	690.233	6.30957	215.4	6.30957	114.598
3.98107	624.729	3.98107	191.736	3.98107	164.149
2.51189	571.228	2.51189	170.988	2.51189	237.38
1.58489	518.583	1.58489	152.372	1.58489	341.036
1	476.179	1	135.853	1	495.179
0.63096	436.968	0.63096	122.005	0.63096	719.036
0.39811	412.687	0.39811	110.103	0.39811	1072.88
0.25119	395.964	0.25119	99.649	0.25119	1625.51
0.15849	390.304	0.15849	93.7057	0.15849	2532.63
0.1	403.494	0.1	89.9138	0.1	4133.91
0.0631	482.392	0.0631	108.508	0.0631	7836.42
0.03981	738.996	0.03981	202.586	0.03981	19247.6
0.02512	9012.51	0.02512	6992.61	0.02512	454125
0.01585	17221.7	0.01585	10188.2	0.01585	1262530
0.01	51764.1	0.01	28402.2	0.01	5904410

Appendix 8.5: Rheological data for BDDE-HA hydrogel prepared with large-batch mixing approach

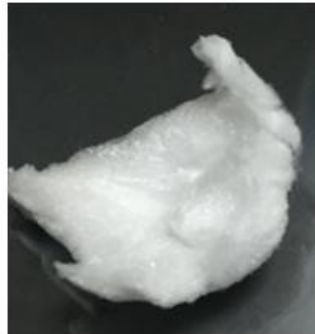
Angular frequency y rad/s	Storage modulus Pa	Angular frequency y rad/s	Loss modulus Pa	Angular frequency y rad/s	Complex viscosity Pa.s
100	3368.12	100	1132.46	100	35.534
63.0957	3032.55	63.0957	1089.86	63.0957	51.0723
39.8107	2712.22	39.8107	1037.86	39.8107	72.9456
25.1189	2412	25.1189	975.435	25.1189	103.579
15.8489	2133.94	15.8489	903.978	15.8489	146.225
10	1881.65	10	823.844	10	205.41
6.30957	1657.17	6.30957	740.795	6.30957	287.691
3.98107	1455.76	3.98107	647.427	3.98107	400.203
2.51189	1295.48	2.51189	584.015	2.51189	565.724
1.58489	1145.93	1.58489	510.113	1.58489	791.436
1	1015.28	1	438.674	1	1105.99
0.63096	907.014	0.63096	384.865	0.63096	1561.58
0.39811	822.712	0.39811	339.931	0.39811	2236.01
0.25119	749.122	0.25119	298.853	0.25119	3210.87
0.15849	694.169	0.15849	267.743	0.15849	4694.41
0.1	654.278	0.1	241.469	0.1	6974.15
0.0631	640.373	0.0631	223.357	0.0631	10748.9
0.03981	1165.01	0.03981	609.245	0.03981	33023.6
0.02512	2082.25	0.02512	1176.38	0.02512	95210.2

Appendix 8.6: Rheological data for BDDE-HA hydrogel prepared with small-batches mixing approach

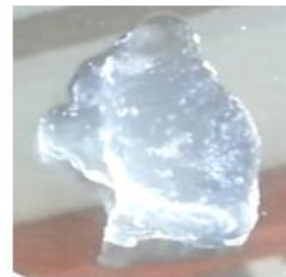
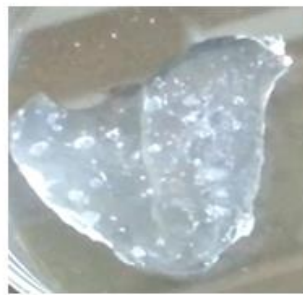
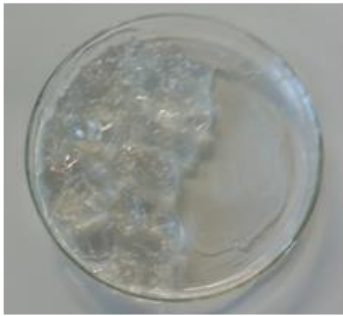
Angular frequency rad/s	Storage modulus Pa			Angular frequency rad/s	Loss modulus Pa		Angular frequency rad/s	Complex viscosity Pa.s
100	2357			100	800		100	35.534
63.0957	2137			63.0957	740		63.0957	51.0723
39.8107	1925			39.8107	670		39.8107	72.9456
25.1189	1724			25.1189	604		25.1189	103.579
15.8489	1535			15.8489	550		15.8489	146.225
10	1363			10	493		10	205.41
6.30957	1209			6.30957	447		6.30957	287.691
3.98107	1069			3.98107	394		3.98107	400.203
2.51189	958			2.51189	359		2.51189	565.724
1.58489	853			1.58489	316		1.58489	791.436
1	761			1	273		1	1105.99
0.63096	684			0.63096	241		0.63096	1561.58
0.39811	620			0.39811	213		0.39811	2236.01
0.25119	569			0.25119	190		0.25119	3210.87
0.15849	530			0.15849	172		0.15849	4694.41
0.1	503			0.1	165		0.1	6974.15
0.0631	496			0.0631	147		0.0631	10748.9
0.03981	757			0.03981	334		0.03981	33023.6
0.02512	1249			0.02512	588		0.02512	95210.2

## **Appendix 9:** Images for different hydrogel samples obtained in our work

### **9.1. Lyophilized-hydrogel appearance**

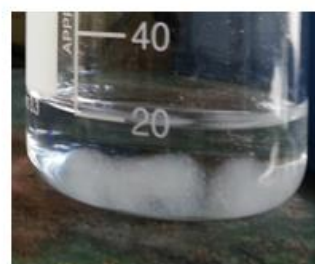
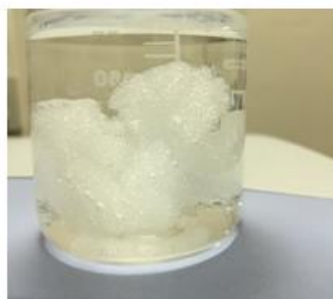
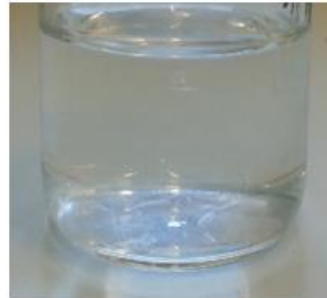


## 9.2. Open air dried-hydrogels appearance



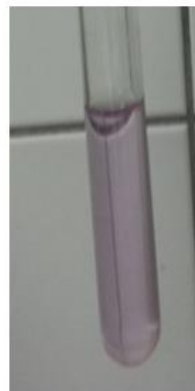


### 9.3. Swelling and purification





## 9.4 Quantity of NAG released



## ERKLÄRUNG/ DECLARATION

Hiermit erkläre ich entsprechend der Promotionsordnung der Naturwissenschaftlichen Fakultät I (Biowissenschaften) der Martin-Luther-Universität Halle-Wittenberg, dass ich die Ergebnisse der vorliegenden Dissertationsarbeit:

***Enhancement of cross-linking efficiency of hyaluronic acid-based hydrogels cross-linked with 1, 4-butanediol diglycidyl ether***

***“A comparative evaluation of different method conditions”***

am Institut für Pharmazie selbständig und ohne fremde Hilfe erarbeitet und verfasst habe und dass ich alle Informationen in dieser Arbeit und alle beschriebenen Materialien ordnungsgemäß zitiert habe. Ich habe mich zu keinem früheren Zeitpunkt um den Dokortitel an einer anderen Einrichtung beworben. Weiterhin habe ich die vorliegende Arbeit bisher keiner anderen Prüfungsbehörde vorgelegt.

I hereby certify according to the doctoral regulations of faculty 1 of Natural Science – Biological Science at Martin Luther University of Halle-Wittenberg that this dissertation:

***Enhancement of cross-linking efficiency of hyaluronic acid-based hydrogels cross-linked with 1, 4-butanediol diglycidyl ether***

***“A comparative evaluation of different method conditions”***

is entirely my own work and it was written by me without external help. All material presented in this thesis including appendices has not been taken from the work of others except the work that is cited and referenced within the text. This work also has not been previously submitted for a degree to any other University or Institution. Any contributions made by the others are acknowledged in this dissertation.

## PUBLICATIONS



### Journal of Drug Delivery Science and Technology

Volume 29, October 2015, Pages 24–30



Original research

### Evaluation of in-vitro degradation rate of hyaluronic acid-based hydrogel cross-linked with 1, 4-butanediol diglycidyl ether (BDDE) using RP-HPLC and UV–Vis spectroscopy

Mohammed Al-Sibani<sup>a</sup>, Ahmed Al-Harrasi<sup>b</sup>, Reinhard H.H. Neubert<sup>a</sup>  

European Journal of Pharmaceutical Sciences 91 (2016) 131–137



Contents lists available at ScienceDirect

### European Journal of Pharmaceutical Sciences

journal homepage: [www.elsevier.com/locate/ejps](http://www.elsevier.com/locate/ejps)



### Study of the effect of mixing approach on cross-linking efficiency of hyaluronic acid-based hydrogel cross-linked with 1,4-butanediol diglycidyl ether



Mohammed Al-Sibani<sup>a</sup>, Ahmed Al-Harrasi<sup>b</sup>, Reinhard H.H. Neubert<sup>a,c,\*</sup>

Department of Pharmaceutics and Biopharmaceutics<sup>1</sup>, Martin-Luther University Halle-Wittenberg, Germany; Chair of Oman's Medicinal Plants and Marine Natural Products<sup>2</sup>, University of Nizwa, Oman

### **Effect of (HA) initial concentration on cross-linking efficiency of hyaluronic acid –based hydrogels used in biomedical and cosmetic applications**

M. Al-Sibani<sup>1</sup>, A. Al-Harrasi<sup>2</sup>, R. Neubert<sup>1</sup>

*Accepted for publication in Die Pharmazie*

## CURRICULUM VITAE

### **Personal information**

**Name** Mohammed Abdullah AL-Sibani

**Nationality** Omani

**Date of Birth** 28.6.1971

**Marital status** Married

**Address** Nizwa, AL Dhakilia Governorate, Sultanate of Oman

### **Education**

#### **1986-1989**

General Education Diploma

Abu Abida School, Oman

#### **1989-1993**

BSC Science Education- Chemistry,

Sultan Qaboos University, Oman

#### **2007-2008**

MSc Analytical chemistry

University of Huddersfield, UK

### **Job title**

**1993-1999/** Chemistry Teacher, Ministry of Education, Oman

**2000-2009/** Chemistry curriculum Officer, Ministry of Education, Oman

**2010-Present/** Analysis and Application Technician, DARIS Centre for Scientific Research and Technology Development, University of Nizwa, Oman

## **Professional development**

**1/6-1/8/92** Petroleum analysis, Oman petroleum development company, Oman (training)

**4/6-6/8/93** Petroleum analysis, Oman petroleum development company, Oman (training)

**Oct, 1994** Conducting lab experiments from simple materials, SQU, Oman (workshop)

**Jan 2001** Learning outside school, Saudi (workshop)

**Apr, 2002** Technology and science, Kuwait (conference)

**May, 2003** Curriculum strategies, Lebanon (workshop)

**Dec, 2004** Intellectual property, Oman (workshop)

**Dec, 2005** Skills of the trainer, Oman (workshop)

**April 2005** Gaps between scientists and science teachers, Egypt (conference)

**Jun, 2006** Environmental forum, Japan (conference)

**May, 2008** Science and supervision, USA (conference)

**Mar, 2009** Science books and publishers, Germany (workshop)

**Jun , 2012** Peak Scientific- Nitrogen generator workshop, Dubai (workshop)

**Sept, 2012** Optimization of pesticide analysis by ESI LC-MS/MS, Oman (workshop)

**Oct, 2012** GC-MS installation, Oman (workshop)

**Nov, 2012** Writing peer review paper, Oman (conference)

**April, 2016** Food safety conference, Oman (conference)

**Mohammed Al-Sibani**